Aus der Klinik für Visceral-, Thorax und Gefäßchirurgie

Direktor: Prof. Dr. Detlef K. Bartsch

des Fachbereichs Medizin der Philipps-Universität Marburg

The role of MMP3 and Rac1b during the development and progression of pancreatic cancer

Inaugural-Dissertation zur Erlangung des Doktorgrades der Humanbiologie
dem Fachbereich Medizin der Philipps-Universität Marburg
vorgelegt von

Juliane Förster, aus Greiz
Marburg, Juni 2017

Angenommen vom Fachbereich Medizin der Philipps-Universität Marburg am:

Gedruckt mit Genehmigung des Fachbereichs.

Dekan: Prof. Dr. Helmut Schäfer

Referent: PD Dr. Malte Buchholz

1. Korreferent:

Abstract

Chronic pancreatitis is a major risk factor for pancreatic ductal adenocarcinoma (PDAC), one of the deadliest cancer types. During the progression to cancer the inflammatory-harmed tissue undergoes formations such as acinar to ductal metaplasia (ADM), pancreatic intraepithelial neoplasia (PanIN) and epithelial mesenchymal transition (EMT). Previously it has been shown that MMP3 and Rac1b play important roles during the progression of lung and mammary cancer and transition in different cell lines. To investigate whether MMP3 and Rac1b have an influence on the development and progression of pancreatic cancer, different cell lines for *in vitro* and two triple transgenic mouse models (rtTA-Ela1/tet-HA-MMP3/tet-KRAs and rtTA-Ela1/tet-YFP-Rac1b/tet-KRas) for *in vivo* experiments were examined. The *in vitro* results were achieved by comparing different cell lines to the amount of endogenous MMP3 and Rac1b and the growth behavior. S2-007, an invasive and epithelial cell line, and MiaPaCa, a more mesenchymal behaving cell line, were the most promising ones and used for further investigations. To examine the effects on EMT, the cells were treated with recombinant protein or adenoviral constructs to overexpress MMP3 and Rac1b and screened for EMT marker proteins by RT-qPCR. The results show an influence of MMP3 and Rac1b on EMT machinery mainly in S2-007 cells and less in MiaPaCa cells. In the same way, a higher migration potential in S2-007 cells after MMP3 overexpression was found by using a wound healing assay performed. The infection with adenoviral constructs showed different effects on EMT marker expression compared to the ectopic expression with recombinant proteins. Additionally, both kinds of treatment resulted in higher Rac1b, E-cadherin, and Vimentin expression levels on Plastic than on Matrigel.

For *in vivo* experiments mice were treated for 5 months either with NaCl or Caerulein to induce chronic pancreatitis. The transgene was activated by using a reverse tetracycline-dependent promotor. The expectation that KRas on the background of chronic pancreatitis drives forward the tissue alterations to pancreatic cancer could not be confirmed, but ADM was found, what is one of the pre-stages of PDAC.

All these findings suggested that MMP3 and Rac1b seem not to influence the EMT machinery in pancreatic tissue as much as expected, especially under *in vivo* conditions. Here additional pathways, such as TGFβ or NFκB signaling, seem to prefer Rac1b as interaction partner to promote EMT.

Keywords: Pancreatitis, PDAC, ADM, PanIN, EMT, MMP3, Rac1b, KRas

Zusammenfassung

Die chronische Pankreatitis ist der Hauptrisikofaktor für die Entstehung eines duktalen Adenokarzinoms des Pankreas (PDAC). Während der Entwicklung zum Karzinom, durchläuft das belastete Gewebe verschiedene Vorläuferstadien, wie z.B. die azinäre-duktale Metaplasie (ADM), intraepitheliale Neoplasie des Pankreas (PanIN) und die epithelial-mesenchymale Transition (EMT). Es ist bekannt, dass MMP3 und Rac1b wichtige Rollen während der Entstehung von Brust- und Lungenkrebs und der EMT in Krebszelllinien im Allgemeinen spielen. Um herauszufinden, ob MMP3 und Rac1b auch einen Einfluss auf die Entstehung und Entwicklung von Pankreaskarzinomen haben, untersuchte ich verschiedene Zelllinien und nutzte zwei dreifach transgenen Mausmodelle (rtTA-Ela1/tet-HA-MMP3/tet-KRAs and rtTA-Ela1/tet-YFP-Rac1b/tet-KRas). Für die *in vitro* Experimente wurden verschiedene Zelllinien auf ihren endogenen Gehalt von MMP3 und Rac1b und ihr Wachstumsverhalten untersucht. Dabei stellte sich heraus, dass S2-007, eine sehr invasive, epitheliale Zelllinie, und MiaPaCa, eine eher mesenchymale Zelllinie, die vielversprechendsten Zelllinien sind, um die Effekte von MMP3 und Rac1b Überexpression auf die EMT zu untersuchen. Die Überexpression wurde durch die Behandlung mit rekombinanten Proteinen oder adenoviralen Konstrukten erreicht. Anschließend wurde die Expression typischer EMT-Marker mittels RT-qPCR untersucht. Es stellte sich heraus, dass MMP3 und Rac1b hauptsächlich in S2-007 und weniger in MiaPaCa Zellen einen Einfluss auf die EMT-Maschinerie zu haben scheinen. Auch das Migrationspotenzial wurde maßgeblich in S2-007 Zellen durch die Überexpression von MMP3 erhöht. Die Infektion mit adenoviralen Konstrukten zeigte andere Effekte auf die EMT-Marker Expression als die Behandlung mit rekombinantem Protein. Außerdem zeigten sich auf Plastik für beide Behandlungsarten höhere Expressionslevel für Rac1b, E-cadherin und Vimentin als auf Matrigel. Während der *in vivo* Experimente wurden die Mäuse für 5 Monate mit Caerulein behandelt, um eine chronische Pankreatitis hervorzurufen. Die Transgenaktivierung erfolgte über einen reversen Tetracyclin abhängigen Promotor. Die Annahme, dass KRas auf einem Hintergrund der chronischen Pankreatitis, die entstehenden Gewebsveränderungen bis zum Karzinom vorantreibt, konnte nicht bestätigt werden. Jedoch konnte ich das Auftreten von ADM nachweisen, welche eine der Vorstufen des PDAC darstellt.

Die erzielten Ergebnisse deuten darauf hin, dass MMP3 und Rac1b speziell unter *in vivo* Bedingungen einen geringeren Einfluss auf die EMT-Maschinerie haben, wie erwartet. Hier scheint es, dass EMT-Signalwege, die an Rac1b gebunden sind (z.B. TGFβ und NFκB), vor MMP3-assoziierten Wegen, bevorzugt werden.

Schlagworte: Chronische Pancreatitis, PDAC, ADM, PanIN, EMT, MMP3, Rac1b

Index of Content

Index of figures and tables

Abrevations

α	-	*anti*
°C	-	degree Celsius
BSA	-	bovine serum albumin
cDNA	-	Complementary Desoxyribonucleic acid
DAPI	-	4', 6-Diamidino-2 phenylindole
dest.	-	distiled
DMEM	-	Dulbecco's modified eagle medium
dNTP	-	Desoxynukleosidtriphosphat
E-cad	-	E-Cadherin
EDTA	-	Ethylendiamintetraacetic acid
et al.	-	*et aliter*
FCS	-	fetal calf serum
GFP	-	green fluorescent protein
HRP	-	Horseradish peroxidase
IHC	-	immunohistochemistry
IFU	-	infection units
MOI	-	multiplicity of infection
PBS	-	phosphate buffered saline
qPCR	-	quantitative polymerase chain reaction
rpm	-	rounds per minute
RPMI	-	Roswell Park Memorial
RT	-	reverse transcription
S2	-	security level 2

s.d.	-	standard deviation
SMA	-	smooth muscle actin
TBS	-	Tris buffered saline
Tris	-	Tris(hydroxymethyl)aminomethane
Tween 20	-	Polyoxyethylene (20) sorbitan monolaurat
VP	-	virus particle

1. Introduction

1.1. Pancreatic Cancer

Cancer is a disease characterized by uncontrolled growth and spread of abnormal cells (American Cancer Society 2013). The prerequisite for a normal cell to become abnormal is the irreparable damage of its DNA. This can be caused by external factors such as tobacco, chemicals or radiation or by internal factors such as spontaneous mutations and stress signals (American Cancer Society 2013; Hanahan & Weinberg 2011).

Normal cells possess strict control mechanisms for cell-cycle progression, undergoing apoptosis and many others. Cancer cells can evade some of these mechanisms to become immortal and to gain growth benefits. Douglas Hanahan and Robert Weinberg have suggested how a normal cell evolves to a neoplastic state or cancer cell in a series of events referred to as "Hallmarks of cancer". These hallmarks are sustaining of proliferating signals, evading growth suppressors, resisting cell death, enabling replicative immortality, inducing angiogenesis, and activating invasion and metastasis (Hanahan & Weinberg 2011). Different types of cancer show different strategies for survival, proliferation and dissemination during tumorigenesis. To acquire these functions additional hallmarks are necessary. One the one hand, the cells need the enabling characteristics *"Tumor-promoting inflammation"* and *"Genomic instability and mutation".* On the other hand, the emerging hall marks *"Deregulating cellular energetics"* and *"Avoiding immune destruction"* are required to promote tumor progression (Hanahan & Weinberg 2011).

The most common form of pancreatic cancer, and one of the deadliest types of cancer overall, is pancreatic ductal adenocarcinoma, short PDAC. Late diagnosis in most cases leads to a high rate of advanced tumors and distant metastases at initial diagnosis. Only half of the patients at initial diagnosis represent good candidates for surgery, and in these, complete resection at surgery is achieved in only 60% of cases. Chemotherapy is conducive to prolong survival in a palliative setting, but cures less than 5% of patients (American Cancer Society 2016). The five-year survival rate is about 7% in the US and Europe, meanwhile the death rates increase. This type of cancer is a disease of the elderly and the risk increases past the age of 50 (American Cancer Society 2013). Certain risk factors increase the risk to develop pancreatic cancer. Tobacco – smoked and unsmoked – is a major risk factor, whereas there is no clear evidence for alcohol (American Cancer Society 2013). In addition obesity, diabetes and a history of chronic pancreatitis can facilitate pancreatic cancer (Berrington de Gonzalez et al. 2003; Aune et al. 2012; Stolzenberg-Solomon et al. 2005; Stocks et al. 2009; Raimondi et al. 2010; Guerra et al. 2007). In some studies it has been shown that an infection with Hepatitis B or C virus as well as the infection with *Helicobacter pylori* may also increase the risk to develop pancreatic cancer

(Hassan et al. 2008; El-Serag et al. 2009; Risch et al. 2010). Among these risk factors the personal genetic background plays an important role for the development of pancreatic cancer. If there is a familiar history of pancreatic cancer, the risk is two-fold higher than in "normal" population. This risk increases for people with one first-degree relative with pancreatic cancer. If there are more than three first-degree relatives with pancreatic cancer, the risk rises up to 32-fold (Berrington de Gonzalez et al. 2003). Some of the genetic risk factors are mutated *BRCA1* and *2* genes, mutations in the *CDKN2A* gene (associated with FAMMM), and other cancer-related syndromes (Thompson & Easton 2002; Streff et al. 2016; Hahn et al. 2003; Couch et al. 2007; Slater et al. 2010; Bartsch et al. 2002; Lynch et al. 2002). Although there are no reliable methods for the early detection of pancreatic cancer in people with a familiar history of pancreatic cancer, there is an option of early detection and intervention in case of malignancy – the diagnosis of pancreatic intraepithelial neoplasia (PanINs) and the punctual resection of a part or the entire pancreas. PanINs represent a reorganisation of the pancreatic ductal epithelium with aggregation of histologic and genetic abnormalities (Maitra et al. 2003). In addition to intraductal papillary mucinous neoplasm, PanINs are the microscopic precursor lesions of PDAC (Singh & Maitra 2007). They are classified into different stages (Figure 1). The lowest grade is PanIN-1 with either a flat (1A) or papillary (1B) structure and the absence of nuclear atypia and a normal nuclear polarity. PanIN-2 show more papillary features and evidence of nuclear atypia and infrequent mitosis. PanIN-3 is also called *carcinoma in situ*. It shows a nearly complete loss of polarity and nuclear atypia as well as frequent mitosis (Koorstra et al. 2008).

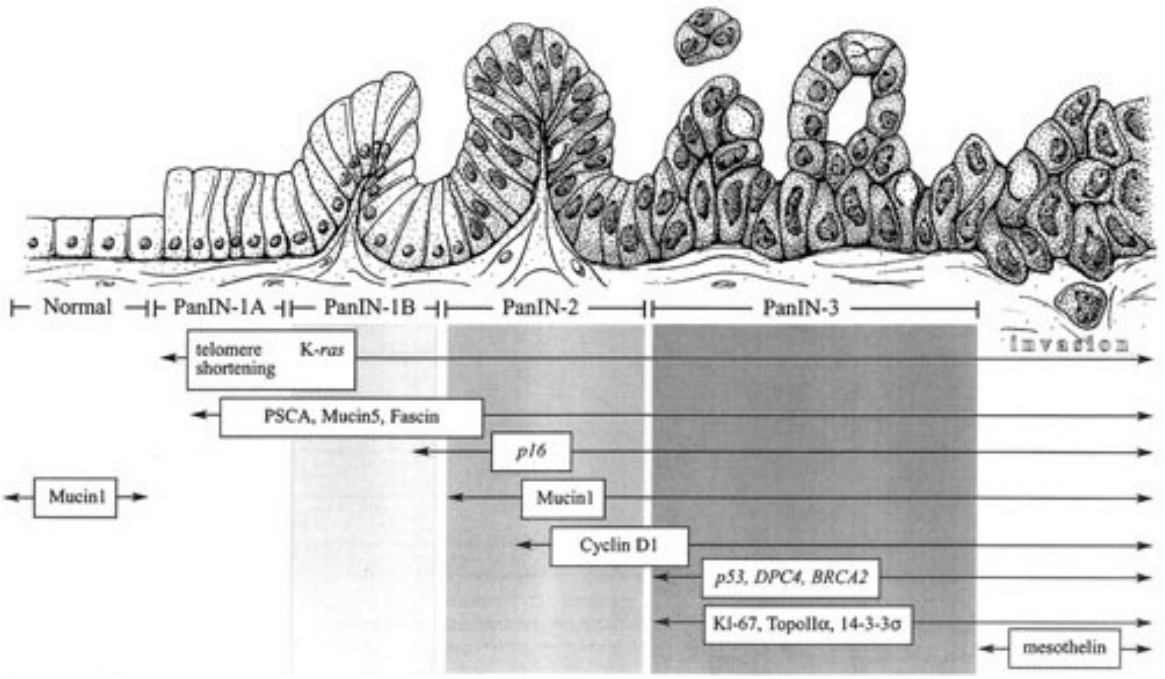

Figure 1; Pancreatic intraepithelial neoplasia (PanIN) progression and the corresponding mutations during early, intermediate and late changes of pancreatic ductal epithelium (Maitra et al. 2003)

Rudolf Virchow assumed that benign, inflammatory processes could lead to malignancy (Balkwill & Mantovani 2001). Since then, different reports confirmed Virchows assumption for different organ systems (Thun et al. 2004). Long standing inflammation of the pancreas, which is known as chronic pancreatitis (CP), is a major risk factor for PDAC, although not all CPs develop to PDACs (Lowenfels et al. 1993; Ekbom et al. 1994). Chronic pancreatitis is defined through the loss of acinar cells, the occurrence of acinar-to-ductal metaplasia (ADM), leukocyte infiltration and replacement of stroma. The period until CP becomes pancreatic cancer can last up to two decades. For a long time, the link between CP and PDAC was not clear. Both diseases show similar histological features, except that PDACs occur with carcinoma cells (Logsdon & Ji 2009). Contrary to the initial assumption that PDACs arise from ductal cells, it was shown that PDAC and CP may both arise from acinar cells (Guerra et al. 2007) that undergo a formation evoked by the genetic instability and damage during constant inflammation (Brentnall et al. 1995; Maitra & Hruban 2008). It is known that all PDACs show areas of fibrosis as does CP, and that nearly all CPs contain early PanINs which possess mutations in KRas (Logsdon & Ji 2009; Volkholz et al. 1982; Löhr et al. 2005; Deramaudt & Rustgi 2005).

It has been shown that Ras activity is upregulated in all PDACs (Almoguera et al. 1988; Ji et al. 2009). Elevated Ras activation leads to extensive senescence of acinar cells and serious inflammation and fibrosis (Ji et al. 2009). Subsequently, additional spontaneous genetic alterations may occur, which again results in CP and PanINs (Maitra & Hruban 2008). Different studies have shown not only a mutated KRas gene is responsible for the progression of CP, PanINs and finally invasive carcinoma also additional factors are necessary for the development of PDAC. Ji et al. showed that pancreatic acinar cells transform by endogenous levels of mutated KRas only in combination with displaced tumor suppressor p53 (Ji et al. 2009). Others have shown that mutations in regulatory genes (e.g. *p16*), mucins, and different inflammatory stimuli are needed in addition to mutated KRas for development of the full spectrum of CP and PanINs (Maitra et al. 2003; Guerra et al. 2007) (see also Figure 1). On the other hand, inflammatory stimuli are mediated by the combination of mutated KRas with TGF-α (Siveke et al. 2007). These findings suggest that KRas plays a key role in the progression of pancreatic cancer, but it is not the only actor during this multilayer process.

1.2. Epithelial to Mesenchymal Transition

The loss of adherent junctions and the change to a fibroblast-like morphology are typical for cancer cells. This change in cell shape and cell-cell and cell-extracellular matrix (ECM)

connections are embraced by the term epithelial to mesenchymal transition - EMT. EMT is a form of epithelial plasticity, where epithelial cells detach from their neighbors to acquire mesenchymal characteristics and become motile and invasive. Different molecular processes take part during the initiation of EMT and its completion. This includes the activation of transcription factors, the expression of certain cell-surface proteins, the reorganization and expression of cytoskeletal proteins, the production of ECM-degrading proteins, such as MMP3, and changes in the expression of certain miRNAs (Lee et al. 2012; Kalluri & Weinberg 2009).

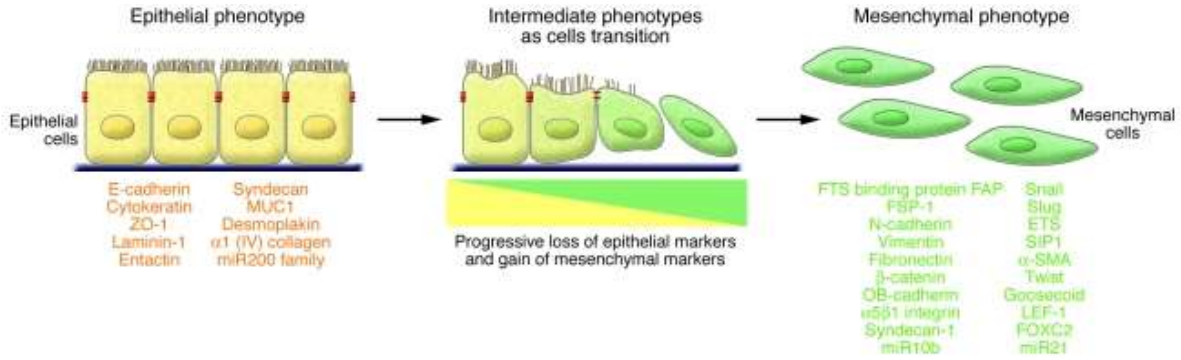

Figure 2; Overview of EMT

Polarized epithelial cells expressing typical markers such as E-cadherin, Cytokeratin, and MUC1 undergo a transition to mobile mesenchymal cells expressing ECM components such as Snail, α-SMA, and Vimentin. During this process, cell-cell junctions are dissolved, a modification of the cytoskeletal structure leads to a change in cell shape from polygonal in spindly, and the cells detach from the basement membrane or destroy these by secreting inflammatory molecules. Assumed from Kalluri (Kalluri & Weinberg 2009)

Physiologically, EMT is essential for embryonic development and enables the epithelium to form the mesoderm, the neural crest, and the heart valves (Nieto 2011). In adults EMT is needed for the branching of mammary ductal glands, wound healing, and tissue regeneration (Maier, Wirth, et al. 2010; Lee et al. 2012). However, EMT is also activated during organ fibrosis and tumor progression. Although the different types of EMT show many similarities in signaling pathways, regulators, and effector molecules, it is not clear which specific signals are responsible for the subdivision and the functional differences. Therefore, a classification into three subtypes, which was recommended by Kalluri and Weinberg in 2009 (Kalluri & Weinberg 2009), has since been widely addopted. Type I EMTs occur during the implantation of the embryo, the generation of germ layers during gastrulation, and the organ formation. This type of EMT can generate primary mesenchymal cells that can undergo MET to form secondary epithelia. The EMT associated with gastrulation is orchestrated by Wnt signaling, especially by Wnt3 and Wnt8c. A lack of Wnt3 blocks the EMT during gastrulation (Liu et al. 1999). Conversely, an ectopic expression of Wnt8c leads to the formation of multiple primitive streaks (Pöpperl et al. 1997).

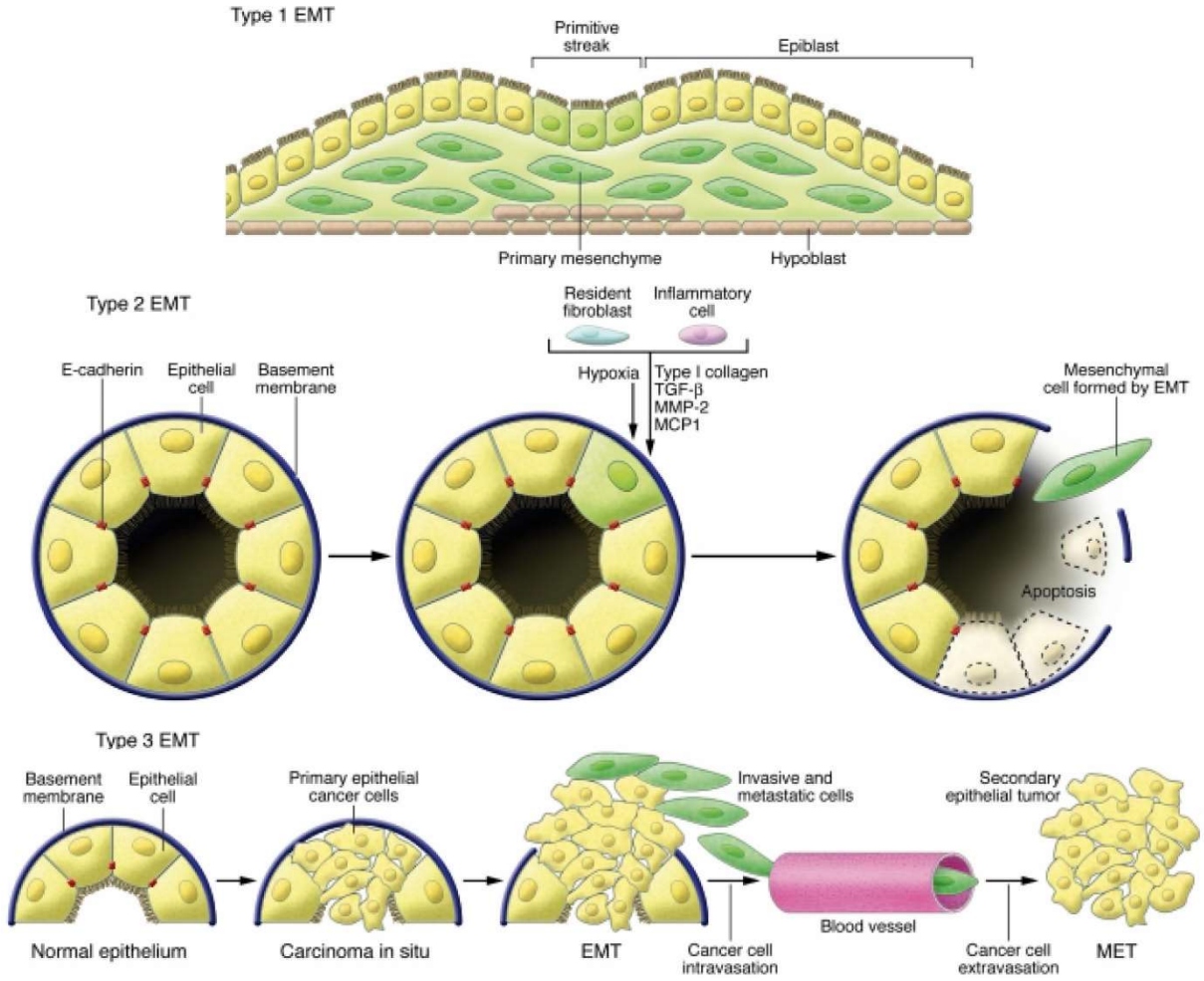

Figure 3; Different types of EMT

Type I EMT is associated with embryogenesis and forms the mesoderm, endoderm and mobilizes neural crest cells. Primary mesenchyme built via EMT can be re-induced to undergo MET.

Type II EMTs are associated with inflammation and fibrosis and can be expressed over a prolonged period. Due to inflammation, different molecules are generated by inflammatory cells and myofibroblasts (residential activated). This can lead to the degradation of the basement membrane, the loss of cell polarity, and the occurrence of either apoptosis (majority of cells) or EMT (minority).

Type III EMTs occur after normal epithelial cells lost their polarity and detached from the basement membrane. The basement membrane changes its morphology resulting in the change of cell-EC; interactions and signaling networks. Only now does EMT take place to promote intravasation and extravasation. The formation of metastases may involve MET to allow the cells to get back to an epithelial phenotype. Modified from (Kalluri & Weinberg 2009)

Type II EMTs are associated with wound healing, tissue regeneration, and organ fibrosis. The EMT program begins as a repair program that normally generates fibroblasts and other related cells to reconstruct tissues following injury. The generated fibroblasts release different inflammatory signals as well as components of ECM such as collagens, laminins, and elastin (Kalluri & Weinberg 2009). Other recruited inflammatory cells such as macrophages can trigger EMT through the release of growth factors and chemokines. The epithelial cells influenced by these signals can lose their polarity and induce the damage of basement membrane (e.g. through MMP3), which is a main characteristic of EMT. This process can end in ongoing inflammation what again leads to organ fibrosis and eventually destruction. During chronic

inflammation the cells may display both epithelial morphology and molecular markers (E-cad, Cytokeratin), and expression of mesenchymal markers like α-SMA (Kalluri & Weinberg 2009).

As described above, extensive proliferation, migration and invasion are hallmarks of cancer (Hanahan & Weinberg 2011). In different studies EMT has been suggested as a critical mechanism for these hall marks (Thiery et al. 2009). This type of EMT was termed by Kalluri and Weinberg as type III EMT. It only occurs in cells that have previously undergone genetic and epigenetic changes, which would lead to cancer progression and metastasis. Therefore it is not surprising that cells at the invasive tumor front undergo type III EMT (Thiery et al. 2009). These cells pass through the EMT program in different extents, so that some cells keep many epithelial properties and acquire just a few mesenchymal ones. Other cells lose all their epithelial behavior and become fully mesenchymal (Kalluri & Weinberg 2009). It is still unclear which specific signals induce type III EMT and which signals dictate the extent to which a cell undergoes EMT, but it is accepted that TGFβ plays a crucial role (Song 2007; Bierie & Moses 2006). Other studies have shown that metastasizing cancer cells not only undergo EMT, but also must undergo mesenchymal to epithelial transition (MET) when forming secondary tumors (termed metastasis) (Zeisberg et al. 2005).

As mentioned before, TGFβ seem to play a key role during the initiation of type III EMT and might be the most important soluble EMT-inducer (Ikushima & Miyazono 2010). TGFβ is an important regulator of tissue homeostasis and has distinct roles during tumor development and progression. For example, it was shown that in cancer cells TGFβ can induce either apoptosis or survival associated with EMT. EMT is favored when TGFβ acts on activated Ras (Barrallo-Gimeno & Nieto 2005) because of the Ras-mediated stimulation of the RAF-MAPK pathway that appears to be necessary for EMT (Janda et al. 2002). In early tumor development TGFβ acts more as a tumor suppressor because of its inhibitory effect on tumor growth by the inhibition of MYC transcription factors and the induction of cell cycle inhibitors (Giehl et al. 2000). In later stages, tumor cells can overcome this suppression by becoming resistant to the cytostatic effect (Ellenrieder et al. 2001) and TGFβ acts as a promoter. Because there are rarely mutations in the TGFβ gene itself (Maitra & Hruban 2008), other pathways that mediate the effects of TGFβ must be affected. These include the MAPK/ERK pathway (Ellenrieder et al. 2001; Maier, Schmidt-Strassburger, et al. 2010), the SMAD/STAT3 signaling (Zhao et al. 2008), and the activation of NFκB (Maier, Schmidt-Strassburger, et al. 2010). Mutations observed in the TGFβ signaling pathways are most often related to SMAD4 resulting in its inactivation in 55% of cases and poor prognosis for PDAC patients (Blackford et al. 2009). In $SMAD4^-$ PDACs other signaling pathways (e.g. NFκB signaling) must compensate for the loss of canonical TGFβ signaling.

A major point of EMT is the loss of E-cadherin and the associated loss of cell-cell contacts. Through its intracellular domains, E-cadherin is linked to many signaling pathway molecules which in turn can influence its loss (Berx & van Roy 2009; Heuberger & Birchmeier 2010). A prominent influencer is mutated KRas that leads to a loss of E-cadherin and an increase of Vimentin and ZEB1. This EMT-promoting transcription factor represses E-cadherin transcription directly through a NFκB-mediated up-regulation (Maier, Schmidt-Strassburger, et al. 2010). Therefore NFκB seem to be the most prominent factor to replace TGFβ-induced EMT in SMAD4 deficient tumors (Fujioka et al. 2003; Maier, Schmidt-Strassburger, et al. 2010). Similar to ZEB1, Snail1 represses E-cadherin by binding directly to its promoter. In contrast, Twist indirectly represses the E-cadherin transcription (Peinado et al. 2007; Yang & Weinberg 2008). Another similarity between Snail1 and ZEB1 is the induction of MMP expression that can lead to the degradation of the basement membrane. MMP3 can trigger EMT by increasing the cellular levels of reactive oxygen species (ROS) which in turn induces Snail1 expression (Radisky et al. 2005).

1.2.1. The role of Rac1b and MMP3 during EMT in pancreatic cancer

Rac1 is a Rho-GTPase family member which can regulate actin organization, formation of filopodia, lamellipodia, and stress fibers (Ridley 2001; Boettner & Van Aelst 2002; Sahai & Marshall 2002). It also influences signaling pathways controlling gene expression and cell cycle progression (Schnelzer et al. 2000; Boettner & Van Aelst 2002). Rac1 cycles between its active (GTP-bound) and its inactive (GDP-bound) form. Different studies have not found mutations of Rac1 in different cancer types and cell lines, but overexpression on RNA and protein levels of a splice variant, designated Rac1b, has been described in breast and colon carcinomas (Schnelzer et al. 2000; Singh et al. 2004). This splice variant features an in-frame insertion of 19 additional amino acids behind the switch II domain of the normal Rac1 transcript (Schnelzer et al. 2000). The Switch domains are necessary for the conformational change during GDP-GTP-cycling (Vetter & Wittinghofer 2001). Due to the insertion, Rac1b shows a reduced downstream signaling compared to Rac1 and has an increased GDP-GTP-exchange leading to constitutive activation (Fiegen et al. 2004; Singh et al. 2004). The reduced ability to bind downstream effectors is apparent because Rac1b is not able to bind p21-activated kinase (PAK) or Jun NH_2-terminal kinase (JNK) (Matos et al. 2003). Rather it can hyper phosphorylate protein kinase B (known as AKT), increase ROS levels, and it retains the potential to activate NFκB (Singh et al. 2004; Matos & Jordan 2005; Radisky et al. 2005). In mammary tumor cells Rac1b enhances the malignancy, genomic instability, MMP3-induced EMT, and motility (Radisky et al. 2005). In colon cancer cells it drives cell cycle progression (Matos & Jordan 2005). It was shown that Rac1b is expressed in vivo predominantly in pancreatic ductal epithelial cells and more in CP than in

PDAC. Rac1b expression was found in PDAC patients with a survival time over 24 months, whereas it was lacked in patients with poor outcome. (Ungefroren et al. 2014). Contrary to these findings, another study showed a specifically Rac1b expression in pancreatic tumor cells with a correlation to MMP3 expression. In the same study, distinct localization patterns were observed for Rac1b, which seem to be more associated with prognostic outcome than the expression levels (Mehner et al. 2014). Because of the ability of Rac1b to enhance motility and MMP3-induced EMT, it was questioned as to its impact on TGFβ. According to the observation that Rac1b is highly expressed in longtime survivors, it was observed that Rac1b antagonizes the TGFβ-induced cell migration through the obstruction of SMAD3 phosphorylation and therefore the suppression of SMAD4 complex activation and function that results in a non-SMAD TGFβ signaling-mediated EMT. This was true in both malignant and non-malignant pancreatic ductal epithelial cells (Ungefroren et al. 2014).

Through integrin activation, Rac1b can generate reactive oxygen species (ROS) by interaction with NADPH oxidase (NOX) (Hordijk 2006). An activation of Rac1b and therefore elevated ROS levels lead to DNA damage and genomic instability and therefore alterations in gene regulation, cellular morphogenesis, migration, and invasion (Kheradmand et al. 1998; Radisky et al. 2005). Radisky et al. found that Rac1b-associated ROS production is MMP3-dependent and leads to EMT-like morphology of SCp2 cells (Radisky et al. 2005).

Matrix metalloproteinases (MMPs) are endopeptidases which are involved in nearly all biological processes: embryo implantation, mammary gland ductal branching, bone ossification, blood vessel remodeling, menstruation, wound healing, innate immune defense, cell death, and necrosis (Alexander et al. 1996; Vu & Werb 2000; Egeblad & Werb 2002; McQuibban et al. 2002). Due to its ability to degrade nearly every component of the ECM and the basement membrane, MMP activity is associated with the release of different ECM-bound proteins like VEGF and TGFβ. They are highly associated with chronic inflammation and cancer development, especially angiogenesis and tumor spread (Nagase & Woessner 1999; Overall 2002). MMPs are overexpressed in nearly all tumor types and they are involved in many stages of tumor progression (Radisky & Bissell 2006). They play an important role during invasion and metastasis because they also facilitate the degradation of cell adhesions, remodeling of the ECM, and intravasation and extravasation. Additionally, they are more and more considered to influence EMT (Orlichenko & Radisky 2008). Moreover, it was shown that MMP3 can induce EMT-associated fibrosis and carcinogenesis in adult transgenic mice (Lochter et al. 1997) through the induction of genomic instability by disruption of the tissue homeostasis (Radisky & Bissell 2006). Notably, MMP3 is associated with the release of pro-angiogenic factors. It cleaves VEGF-binding proteins in the ECM or the VEGF-CTGF-complex (connective tissue growth factor) to release

active VEGF (Lee et al. 2005; Hashimoto et al. 2002). In endothelial cells MMP3 can cleave perlecan to detach the basic fibroblast growth factor (Whitelock et al. 1996). In vivo MMP3 can cleave and release, and therefore activate, the heparin-binding EGF-like growth factor to promote angiogenesis (Suzuki et al. 1997). On the other hand, MMP3 can cleave off the NC1 domain of collagen which leads to the release of endostatin which acts as an anti-angiogenic factor (Ferreras et al. 2000). During tumor development MMP3 positively affects invasion and metastasis by shedding of the soluble ectodomain of E-cadherin to cleave adherence junctions and therefore disrupt cell-cell contacts (Lochter et al. 1997).

As addressed previously, MMP3 can control cell division and proliferation by regulating the availability and activation/ inactivation of ECM-bound growth factors. For the release of latent TGFβ, MMP3 cleaves the TGFβ binding partner LTBP and degrades decorin (Imai et al. 1997; Maeda et al. 2002). During wound healing and tumor development, the cleavage of osteopontin is MMP3-mediated and results in enhanced cell adhesive and migratory properties (Agnihotri et al. 2001). Tumor cells have developed several mechanisms to block and evade the immune response. Some of these mechanisms are MMP-mediated and cytokines and chemokines are MMP-targeted to modulate the immunologic and inflammatory response. MMP3-cleavage of α1-proteinase inhibitor results in a reduced cytotoxic effect of natural killer cells (Kataoka et al. 1999). MMP3 can release the Fas ligand from cell surface to bind to the Fas receptor and therefore lower its pro-apoptotic potency (Tanaka et al. 1998). Also it can process IL-1β to its biologically active form (Ito et al. 1996; Schonbeck et al. 1998). Due to an overexpression and dysregulation of MMP3 all of these points are essential for tumor development and progression, cell invasion and metastasis. Epithelial-associated MMP3 overexpression occurs in about 80% of pancreatitis patients (Bramhall et al. 1996). In normal, adult tissues MMP3 is expressed by fibroblasts at low levels and rises during wound healing and tumor development (Witty et al. 1995; Stetler-Stevenson et al. 1996). Some studies showed that MMP3 overexpression is able to induce spontaneous tumor development in the lung and it is also linked to tumor development and progression in breast, colon, and cervical cancer (Stallings-Mann et al. 2012; Lochter et al. 1997; Sternlicht et al. 1999). In pancreatic cancer it was shown that MMP3 is specifically expressed in pancreatic tumor cells with an association to Rac1b expression (Mehner et al. 2014). As previously described by Mehner et al., the expression of MMP3 in different tumor stages implies a poor outcome in breast and lung cancer (Mehner et al. 2015). The same is true for pancreatic cancer and the expression of Rac1b. Here the localization in combination with the expression plays a role in the prognostic outcome. A diffuse cytoplasmic (baseline) expression and a cytoplasmic punctate polar (polar) expression show a better chance of survival than the cytoplasmic punctate apolar (apolar) expression of Rac1b. The apolar expression of Rac1b is also

associated with higher MMP3 expression levels, but seems to be independent of the tumor stage itself (Mehner et al. 2014). Transgenic mice expressing MMP3 and $KRas^{G12V}$ show increased Rac1b expression levels and a recruitment of macrophages that leads to fibrotic changes and primes a more stromal microenvironment. In pancreatic adenocarcinoma cell lines the expression of MMP3 results in a higher expression of Rac1b and activates an invasive phenotype (Mehner et al. 2014).

A main function of MMP3 is to induce EMT. In addition to the typical EMT features of downregulation of epithelial and upregulation of mesenchymal markers, the MMP3-induced EMT is accompanied by the loss of colony formation ability, increased cell spreading, and increased lamellipodia formation due to the release of growth factors as described above. Different experiments have shown that the expression of Rac1b induces cell scattering, which is necessary for cell spreading. The cell spreading is independent of the Rac1b-induced ROS production and ROS-induced EMT can also occur without cell spreading. That implicates that MMP3-induced cell spreading occurs downstream of Rac1b, but maybe parallel to the EMT mediated by ROS (Nelson et al. 2008). Because during embryonic development MMP3 expression does not result in pathological EMT, there must be some protective signals arising from the microenvironment of normal tissue. The structure of healthy tissue is softer and more balanced, fibrotic tissue shows a stiff matrix with fibroblasts and increased scattering of cells (De Rooij et al. 2005; Liu et al. 2010). A study by Lee et al. showed that cells cultured on soft substrates did not respond to MMP3 treatment, whereas MMP3 treatment on stiff substrates resulted in EMT-like effects (Lee et al. 2012). Because Rac1b is a downstream target of MMP3, they determined whether MMP3-induced Rac1b expression is dependent on substrates stiffness. The study showed that Rac1b levels were increased by MMP3 but independent of substratum rigidity. Contrariwise, the production of ROS and the Rac1b-induced cell spreading were only detected in cells cultured on stiff substrates. In soft, compliant substrates Rac1b cannot localize to the plasma membrane because of reduced β1-integrin-mediated adhesion. The expression of MMP3 can elevate this adhesion only in cells cultured on stiff substrates. Delocalization of Rac1b inhibited interaction of Rac1b and the NOX-complex component $p67^{phox}$ at the membrane resulting in decreased levels of ROS and the block of EMT-induction (Lee et al. 2012). These findings suggest that the membrane localization of Rac1b is essential for its downstream signaling and EMT induction.

The principles of EMT have been discovered in cell culture but it is not clear if the situation *in vivo* is comparable. Furthermore, EMT is a transient event and may only occur at the invasive front of tumors. Human tumor samples stained with HE fails to show an EMT-typical morphology with spindly cells or similar. Therefore, tissues are stained for established EMT markers such as

low E-cadherin expression, Vimentin expression, and a higher Snail, Twist, and ZEB1 and ZEB2 expression.

1.3. Aim of project

Previous studies have suggested that MMP3-induced phenotypic alterations are dependent on Rac1b but little is known about the molecular details of the cooperation of MMP3 and Rac1b. The goal of this thesis work was therefore to investigate whether the expression of MMP3 and Rac1b influences the EMT machinery and if an expression of MMP3 or Rac1b in context with $KRas^{G12D}$ expression drives chronic pancreatitis to PDAC.

To define the molecular characteristics of MMP3- and Rac1b-induced EMT *in vitro*, the PDAC cell lines S2-007 and MiaPaCa, cultured on standard tissue plates or on plates coated with Matrigel, were to be analyzed. Treatment with recombinant MMP3 and adenoviral MMP3 and Rac1b to achieve overexpression was to be used to further investigate the influence on the expression and localization of the typical EMT markers E-cadherin and Vimentin. In addition, recombinant or adenovirus-expressed TGFβ was to be used as control in addition to untreated or AdGFP-treated cells.

To investigate a potential effect of MMP3 and Rac1b overexpression *in vivo* on the development of KRas-dependent PanINs and PDAC in the context of chronic pancreatitis, triple transgenic mice (rtTA-Ela1/tet-HA-MMP3/tet-$KRas^{G12D}$; rtTA-Ela1/tet-YFP-Rac1b/tet-$KRas^{G12D}$) were to be used as experimental model. The mice express either MMP3 or Rac1b under the control of the Elastase-1 promotor specifically in exocrine pancreatic acinar cells which are assumed to be cells of origin of PDAC. After defined treatment regiments mouse pancreata were to be dissected and examined by microscopy for ADM, PanINs and PDAC. Additionally, EMT markers (E-cadherin, Amylase, Smooth muscle actin, Cytokeratin 19) were to be investigated by immunohistochemistry and RT-qPCR.

2. Material

2.1. Buffers

10x PBS

1.3 M	NaCl
27 mM	KCl
100 mM	Na_2HPO_4
100 mM	KH_2PO_4

Adjust pH to 7.4; autoclave

10x TBS

100 mM	Tris pH7.9
1.5 M	NaCl

1x TBS-T

10% (v/v)	10x TBS
0.5% (v/v)	Tween 20

Tris-EDTA

0.5 M	EDTA solution
10 mM	Tris pH 7.9
0.05%	Tween 20

Citrat buffer

10 mM	Citric acid
0.05%	Tween 20

Adjust pH to 6.0

2.2. Commercial Solutions und Kits

Table 1; Commercial Kits, their application and manufacturer

Kit Name	Application	Manufacturer
Invisorb DNA Extraction Kit	DNA extraction	Stratec
PeqGOLD TriFast	RNA extraction	PeqLab
RNase-free DNase Kit	RNA extraction	Quiagen
RNeasy Mini Kit	RNA extraction	Quiagen
RNA-to-cDNA Kit	cDNA synthesis	Thermo Scientific
ABgene SYBR green	RT-qPCR Mix	Thermo Scientific
AdEasy Purification Kit	Virus purification	Agilent
AdEasy Viral Titer Kit	Virus titration	Agilent

2.3. Media for Cell culture

DMEM (Dulbecos modified eagle medium)	Biochrom
RPMI (Roswell Park Memorial)	Biochrom
FCS, Penicillin-Streptomycin, Trypsin	Gibco/Invitrogen

Freezing medium

30%	FCS
10%	DMSO
60%	DMEM/ RPMI

2.4. Cell lines

Table 2; Cell lines

Name	Origin	Medium
8988T	Human pancreatic adenocarcinoma	DMEM with 10% FCS and 1% Penicillin-Streptomycin
8988S	Human pancreatic adenocarcinoma	
Capan-1	Human pancreatic ductal adenocarcinoma	RPMI with 10% FCS and 1% Penicillin-Streptomycin
HEK 293T	Human embryonic kidney	DMEM with 10% FCS and 1% Penicillin-Streptomycin

IMIM Pc1	Human ductal pancreatic adenocarcinoma	DMEM with 10% FCS and 1% Penicillin-Streptomycin
IMIM Pc2	Human ductal pancreatic adenocarcinoma	
MiaPaCa	Human pancreatic carcinoma	
Panc1	Human pancreatic carcinoma	
S2-007	Human pancreatic carcinoma	
S2-028	Human pancreatic carcinoma	

2.5. Adenoviral vectors

Table 3; Adenoviral vectors for cell line stimulation

Vector name	Virus name	Titer	MOI
CMV-eGFP	AdGFP	8 E^6 IFU/ml	10
CMV-p-TGFβ1	AdTGFβ	1.02 E^9 IFU/ml	10
CMV-r-MMP3	AdMMP3	2.7 E^9 IFU/ml	10
CMV-m-Rac1b	AdRac1b	1.02 E^9 IFU/ml	10

All constructs are predicted on a recombinant human adenovirus type 5. The adenoviral vector AdGFP expresses enhanced green fluorescent protein (eGFP) under the control of a CMV promoter. Enhanced GFP is a GFP mutant with improved fluorescence and stability. Recombinant eGFP adenovirus serves as a control for other recombinant adenoviruses to normalize the effect of adenoviral infection. CMV-p-TGFβ is the control for adenoviral protein and EMT-mediator expression.

2.6. Antibodies

Table 4; Antibodies for immunohistochemistry and immunofluorescence

Antibody	Species	For use	Company
α-E-cadherin	mouse	1:400	BD (#610181)
α-Amylase	rabbit	1:500	Santa Cruz (#sc-25562)
α-SMA	rabbit	1:1000	Abcam (#AB5694)
α-CK19	rabbit	1:400	Abcam (#AB52625)
α-Ki67	rabbit	-	Abcam (#AB15580)
α-GFP	rabbit	1:1000	Abcam (#AB6556)
α-Vimentin	goat	1:100	Abcam (#AB11256)
Alexa Fluor488 α-goat	rabbit	1:200	Thermo Fisher (#A-11078)
α-rabbit 2nd antibody	goat	1:250	
α-mouse 2nd antibody	rabbit	1:250	

2.7. Enzymes and Proteins

DNAse I (20U/µl)	PeqLab/ Qiagen
Benzonase (10ku)	Novagene, Merck Millipore
recombinant TGFβ (2µg)	R&D Systems
recombinant MMP3	kind gift from Mayo clinic

2.8. Drugs and Chemicals

Caerulein desulfated (5mg)	Bachem
NaCl 0,9%	Braun
Mounting Medium IHC	Roth
ProLong Diamond Antifade	Applied Biosystems
Mounting medium with DAPI	Thermo Fisher

2.9. Standards

BSA	AppliChem
GeneRuler DNA Ladder 50bp	Fermentas

2.10. Oligo nucleotides

All oligo nucleotides (primers) were used for PCR as well as for RT-qPCR.

Table 5; Oligonucleotides used for PCR and RT-qPCR

Primer	Sequence in 5'– 3'
HA-MMP3_rat_fwd	CTA TCC GAG GTC ATG AAG AGC TA
HA-MMP3_rat_rev	GCC TGG AAA GTT CTC AGC TAT TT
MMP3_human_fwd	CCA GGC TTT CCC AAG CAA AT
MMP3_human_rev	CAC AGC ACA GGC AGG AGA AAA
YFP_fwd	ACG ACG GCA ACT ACA AGA CC
YFP_rev	TTG TAC TCC AGC TTG TGC CC
YFP-Rac1b_fwd	TGG ACA AGA AGA TTA TGA CAG ATT GC
YFP-Rac1b_rev	CCC TGG AGG GTC TAT CTT TAC CA
Rac1b_human_fwd	TAT GAC AGA TTA CGC CCC CTA TC
Rac1b_human_rev	CTT TGC CCC GGG AGG TTA
RPLP0_human_fwd	TGT CTC TCC TCA GTG ACA TCG T
RPLP0_human_rev	TCA GGG TTG TAG ATG CTG CC
RPLP0_mouse_fwd	CCT ATA AAA GGC ACA CGC GG
RPLP0_mouse_rev	ACG TTG TCT GCT CCC ACA AT
Ecad_human_fwd	CGA GAG CTA CAC GTT CAC GG
Ecad_human_rev	GGG TGT CGA GGG AAA AAT AGG
Ecad_mouse_fwd	CAA CGA TCC TGA CCA GCA GT
Ecad_mouse_rev	TGT ATT GCT GCT TGG CCT CA
Vim_human_fwd	CTG AAC CTG AGG GAA ACT AAT C
Vim_human_rev	GCA GAA AGG CAC TTG AAA GC

Vim_mouse_fwd	GCT CCT ACG ATT CAC AGC CA
Vim_mouse_rev	CGT GTG GAC GTG GTC ACA TA
Amylase_mouse_fwd	CAG AGA CAT GGT GAC AAG GTG
Amylase_mouse_rev	ATC GTT AAA GTC CCA AGC AGA
CK19_mouse_fwd	CCT CCC GAG ATT ACA ACC ACT
CK19_mouse_rev	AGG GCT GTT CTG TCT CAA ACT
GFP_fwd	CCC CAA CGA GAA GCG CGA TCA C
GFP_rev	TTA CTT GTA CAG CTC GTC CAT
TGFβ_fwd	ACT GAG TGT CTA GGC TCC AG
TGFβ_rev	CCC TTC CTG CTC CTC ATG G

2.11. Specialized software

Time Lapse Analyzer (Huth et al. 2011)

Leica Slide Path Gateway; Leica Image Scope

Adobe Illustrator

2.12. Hardware

Autoclave	VX95; Systec
Gel documentation device	Vilber
Cell culture hood	Thermo Scientific
Centrifuges	Eppendorf, Heraeus, Beckmann, BioSan
Electrophoresis chamber	BioRad
Heating block	Dri-Block DB3A; Techne
Heating board	Heraeus
Incubator Cell culture	Sonyo
Microscope for IHC	DMIL LED; Leica
Microscope for cell imaging	Axiovert 2000M; Zeiss

“Mr. Frosty” Freezing container	Thermo Scientific
NanoDrop	ND-1000; NanoDrop Technologies
PCR Maschine	Master cycler ProS ; Eppendorf
Powersupplys	BioRad, Consort
qPCR Maschine	Applied Biosystem
Slide scanner	SCN400; Leica
Water bath	TW 20; Julabo

3. Methods

3.1. Cell line cultivation

Cell lines were cultivated at 37°C and a CO_2 concentration of 5%. For all cell lines DMEM with 10% FCS and 1% Penicillin-Streptomycin is used. The different cell lines were cultured in a monolayer at the bottom of the culture flask. Because the cells should not overgrow each other, they were splitted frequently. The ratio depends on the cell line and its behavior of growth, but normally it lies between 1:5 and 1:20.

First the cells were washed with 1x PBS and they were trypsinated afterwards for about 3 minutes at 37°C. The effect of Trypsin is stopped by the addition of DMEM. The cells were centrifuged for 3 minutes at 1200 rpm. After resuspending the cells, they were seeded in the needed ratio.

3.2. Freezing and thawing of human cell lines

For freezing cell lines, a so called “Mr. Frosty” is used. This is a container, which is filled with 100% isopropanol. It can be stored in a freezer and the temperature drops step wise to -80°C. This leads to a gentle freezing of the cells. For freezing the cells, a special medium was needed. It contains 60% DMEM, 30% FCS, and 10% DMSO.

After washing and trypsinating the cells they were centrifuged for 3 minutes at 1200 rpm. The pellet was resuspended in an appropriate volume of freezing medium and is converted in a cryotube. The tubes were placed in the freezing container, which was stored in the -80°C freezer. After 24 hours, the tubes were carried in to a storage box at -80°C.

To seed frozen cells again they were thawed quickly in a 37°C water bath. The whole number of cells was transferred into a tube filled with 10 ml DMEM (37°C). This tube was centrifuged for 3 minutes at 1200 rpm. The supernatant was discarded, and the cells were resuspended in 10 ml DMEM. The cells were seeded into a culture flask of appropriate size (e.g. 75cm²).

3.3. Treatment of human cell lines with recombinant proteins

To stimulate the cells with 50U recombinant MMP3 (rMMP3) and 2ng TGFβ (rTGFβ) respectively (gifts from Derek C. Radisky, Research Center Mayo Clinic, Jacksonville FL, USA), they were solved in protein-containing DMEM and seeded on 12-well plates at a density of $7x10^4$ cells/ml for S2-007 and $8x10^4$ cells/ml for MiaPaCa cells. The growth conditions differed from normal

culture. Instead of 10% FCS only 1% was given to DMEM. Additionally, 1% Insulin-Transferrin-Selenium-Ethanolamine (ITS-X) was included. The cells were cultured for 48hrs with the recombinant proteins bevor DMEM was changed and new rMMP3 or rTGFβ was added.
In some experiments the cells were grown on Matrigel©. This simulates cells growing *in vivo*-like. The experiments were conducted under the same conditions as described above.

3.4. Wound healing with and without treatment with recombinant protein

The growth conditions were the same as described above. The cells were seeded in a bit higher concentration 24hrs prior treatment to grow till they were confluent. With a 10µl pipette tip, a wound was drawn into the cell layer and the cells were treated with the recombinant proteins as described above. The cells were monitored for 24h using a Zeiss Axiovert 2000M inverted microscope at 10X magnification. With differential interference contrast, one picture every 10min was taken. The resulting time lapse movies (picture stacks) were analyzed using the "Time Lapse Analyzer" software (Huth et al. 2011). Time lapse recording and analysis was performed by the group of Malte Buchholz.

3.5. Purification and titration of Adenovirus

The transfection and all steps afterwards were done under S2 conditions.
One day before the transfection HEK 293T cells were seeded in a concentration of $1*10^7$cells per 145cm² dish. $2.7*10^5$ VP AdTGFβ and $1.6*10^5$ VP AdRac1b were given to the cells and they were incubated for 5 days under normal growth conditions until most of the cell were detached.
The purification was conducted with the AdEasy virus purification kit by Agilent technologies. First, the medium was transferred into a 50ml tube and centrifuged at 3 500 x g for 15min. A part of the supernatant was stored in a new tube at 4°C. The cell pellet is resuspended in 10ml of left supernatant and lysed by three freeze-and-thaw cycles. Afterwards, the suspension was centrifuged again at 3 500 x g for 15min. The supernatant was kept and added to the reserved supernatant. The DNA and RNA digestion with 12.5U Benzonase per 1ml supernatant was performed at 37°C for 30min. During this time, a tube set was attached to a 50ml syringe and the air was cast out of the syringe by drawing up and down some supernatant. The whole amount of supernatant was filtered through a 45µm filter into a sample container until 2ml were left. Nine parts of supernatant were attenuated with 1 part 10x loading buffer and the syringe was filled with it. A Sartobind unit was placed on the syringe and the supernatant was passed dropwise through it. The sample container was filled with the same volume of washing buffer

and passed through the sartobind unit until 2ml were left in the syringe. The Sartobind unit was transferred to a 10ml syringe, which was filled with 5ml elution buffer. A red solution tip was fixed at the outlet of the sartobind unit and 1ml elution buffer was passed very slowly through the unit. The supernatant is collected in a sterile 15ml tube. The left 4ml were incubated for 10min and then also passed through very slowly. Finally, some air was pushed through the sartobind unit to get out as much elution buffer as possible.

In the last step, a centrifuge concentrator was used to concentrate the virus to a suitable grade. The centrifugation at 3 000 x g is stopped when sample volume reaches 1ml. The flow through was discarded, 4ml of storage buffer were added, and the centrifugation step was repeated. The concentrated virus was resuspended, aliquoted, and stored at -80°C.

One aliquot was used to determine the viral titer with the AdEasy viral titer kit. Therefor HEK 293T cells were seeded in a 24-well plate with a concentration of $2*10^5$ cells per well. The virus was diluted in a range from 10^{-2} to 10^{-6} with DMEM and 50µl of each dilution was added dropwise to two wells each. The cells were incubated for 48hrs at 37°C. Afterwards the medium was evacuated and the cells were dried for 10min at 37°C. To fix the cells, 500µl ice cold 100% methanol were added to each well and incubated for 10min at -20°C. The methanol was aspirated and the cells were washed twice carefully with 500µl 1xPBS containing 1% BSA. The mouse anti-hexon antibody was diluted 1:500 in 1xPS with 1% BSA, 250µl were added to each well, and incubated for 1hr at 37°C. The cells were washed twice carefully with 1xPBS containing 1% BSA and 250µl of HRP-conjugated antibody – diluted in 1xPBS with 1%BSA – were added to each well. Again, the antibody was incubated for 1hr at 37°C. During this time a working solution of one part 10xDAB and 9 parts peroxide buffer was prepared. The cells were washed twice with 1xPBS containing 1% BSA and 250µl DAB working solution were added. The incubation lasts until the cells become dark brown or black. The DAB was aspired and 250µl 1xPBS were added to each well.

To calculate the titer, the well with about 10% positive stained cells was chosen and enumerated (10 fields in a 20fold magnification). The infection units (IFU) were calculated with the following formula:

$$X = \frac{Average\ number\ of\ cells\ per\ field * field\ per\ well}{Volume\ of\ diluted\ virus\ per\ well\ in\ ml * used\ dilution\ factor}$$

$$X = \frac{Average\ number\ of\ cells\ per\ field * 314\ fields\ (given\ for\ 20fold\ magnification)}{0.05\ ml * used\ dilution\ factor}$$

3.6. Treatment of human cell lines with Adenovirus

The appropriate volume of Adenovirus was added to standard-used DMEM with a MOI of 10, meaning $7*10^5$ / $8*10^5$ VP were needed for infection for a cell density of $7*10^4$ cells/ml for S2-007 and $8*10^4$ cells/ml for MiaPaCa. The cells were seeded on 12-Well plates and cultured for 48hrs at 37°C with 5% CO_2.

3.7. DNA preparation

For the DNA preparation from mouse tail the Invisorb Spin Tissue Mini Kit is used. Before the preparation was started some buffers must be set up. To the binding buffer A 21ml pure Isopropanol and to the washing buffer 105ml of pure Ethanol were added. The Proteinase K tube was conducted with 2ml of nuclease free water. All components of the kit can be stored at room temperature accept the Proteinase K, which must be stored at -20°C.

To each mice tail, 400µl Lysis Buffer G and 40 µl Proteinase K were added. The samples were mixed well and they were incubated over night at 52°C.

On the next day at first an appropriate amount of Elution buffer was heated up to 52°C. The samples were centrifuged for 2min at 11 000 x g. The lysate was transferred into a 1.5ml reaction tube and 200µl Binding Buffer A were added and the sample is mixed well. The whole sample, but not more than 700µl, was converted to the DNA spin column, incubated for 1min and centrifuged for 2min at 11 000 x g. The flow-through is discarded. For washing the column twice, 550µl Wash Buffer were added and the column was centrifuged for 1min at 11 000 x g. Both times the flow-through was discarded. To dry the column completely, the column was centrifuged for 4min at 15 000 x g. During the last preparation step, 200µl preheated Elution Buffer were added and incubated for 3 min at room temperature, and then the column is centrifuged for 1min at 11 000 x g.

3.8. RNA preparation from human cells and tissue

The preparation of RNA from human cells and mice tissue was conducted with PeqGOLD TriFast. The media was removed from the cells and an appropriate volume of PeqGOLD TriFast was given to the cells and they were detached by pipetting the solution up and down for several times.

When RNA was conducted from mice tissue the tissue was crushed with a tissue mixer. The following steps were the same for cells and tissue.

The mixture was converted in to a 1.5ml reaction tube and incubated for 5min. Afterwards, it was possible to store the samples for a few months at -80°C or to go on with preparation of RNA. For the preparation 200µl Chloroform were added to the TriFast-mixture. After shaking well, the sample was incubated for 10min at room temperature and centrifuged for 5min at 12 000 x g. The colorless upper phase was taken and transferred in to a new 1.5ml reaction tube. The left two phases can be stored at -10°C for potential protein and DNA preparation. For precipitation, 500µl Isopropanol were added and the sample was mixed well before it was incubated for 10min on ice. After a centrifugation step of 15 min at 12 000 x g the Isopropanol-supernatant was taken carefully. The left pellet was washed twice with 1ml 75% Ethanol. Therefor it was mixed and centrifuged for 10min at 12 000 x g. When the pellet was washed the second time it was dried for a few minutes, but it should not dry completely. This will downgrade the solubility of the RNA. To resolve the RNA pellet, 87.5µl preheated RNAse free water were used.

Because there can be left some DNA at the sample a DNAse treatment and a subsequent cleaning were necessary. Therefore, the RNase-free DNase Kit and the RNeasy Kit from Quiagen were used.

At first, the whole amount of the sample was given to 10µl RDD buffer which was shifted with 1µl DNAse. To get an end volume of 100µl the sample was filled up with RNase-free water and incubated at room temperature for 10min. Afterwards 350µl RLT buffer were added and the samples was mixed well. The procedure was repeated with 250µl 100% Ethanol. Then the mixture was converted into a column with 2ml collection tube and centrifuged for 15sec at 10000 x g. The flow-through was discarded, 500µl RPE buffer with Ethanol were given on the column, and the column was centrifuged for 15sec at 10 000 x g again. This washing step was repeated and after discarding the flow-through the column was transferred in to a new 2ml collection tube to centrifuge for 1min at full speed. Now the column was transferred into a 1.5ml collection tube and 40µl RNase-free water were added. Again a centrifugation step for 1min at full speed was conducted. The eluate was transferred to the column again and the centrifugation step was repeated.

The concentration of the RNA was measured with the NanoDrop. Afterwards the RNA was stored on ice for usage or at -80°C for longtime storage.

3.9. cDNA synthesis

The cDNA was synthesized from mRNA by reverse transcription using the High Capacity RNA-to-cDNA Kit from Applied Biosystems. The included RT Enzyme Mix contains Oligo dT primers and RNA-depending DNA-Polymerase (reverse transcriptase).

For the synthesis 1µg total RNA is used. The needed sample volume was calculated from the RNA measured concentration.

$$V = 1\mu g / c_{RNA}$$

The calculated sample volume was added to 10µl RT buffer and 1µl Enzyme Mix. With nuclease-free water the sample was filled up to 20µl. All components were mixed and they were spine down to eliminate any bubbles. The reaction was incubated at 37°C for 60min, then stopped by heating up to 95°C for 5min, and at least cooled to 4°C. For convenience, the incubation was performed in a thermal cycler. The synthesized cDNA was diluted 1:10 with nuclease free water before it was used for RT-qPCR or stored at -20°C.

3.10. Primer design for RT-qPCR and PCR

For the following described PCR methods, short nucleotides called primers were needed. These primers were designed by myself.

The NCBI reference number for your chosen gene was set in the NCBI primer blast tool. The product size should range between 120 and 160 base pairs and the melting temperature was set between 53°C and 63°C. The maximum temperature difference between the primer pairs was et to 1°C. The stringency of primer specificity was set to 4, 4, 4, and 9. NCBI Primer Blast gives out mostly more than one primer pair. Which one is the best was tested with two other primer design tools – Integrated DNA Technologies Oligo Analyzer and Primer3 Primer3Plus Interface. In both cases the primer sequences were supplied to the tool and different options were shown for the tested sequences. The hairpin stability, and the self and hetero dimerization were chosen as low as possible. The best fitting primer pairs were ordered by Biomers or Invitrogen.

3.11. Polymerase Chain Reaction (PCR) – genotyping of mice

First the template DNA is melted at 90 degrees. During the 30sec annealing period specific primers (see Table 5) bound to the template and be extended with the help of a Taq-Polymerase and nucleotides at the for the used primer appropriate temperature. The procedure was repeated 35 times, so that enough DNA was synthesized to show it on a 2%-agarose gel.

3.12. Real Time – quantitative Polymerase Chain Reaction (RT-qPCR)

With this method, it is possible to quantify the relative expression of a target gene in relation to a reference gene like RPLP0.

The used primers were complementary to the cDNA strand and they were designed to span exon-intron boarders so that they were specific for cDNA and not for genomic DNA, which could be still in the sample. For each sample a triplicate with respectively 6 µl cDNA were prepared. In addition, 19 µl of a master mix were added. This mix contains 1 µl of the appropriate primer pair (forward and reverse; 100 pmol/µl), 11.5 µl ABgene SYBR green PCR mix, and 8 µl double distilled water. After the activation of the hot-start polymerase for 15 min at 95°C, the PCR run through 40 cycles of denaturing (95°C), annealing (60°C), and elongation (60°C). During the denaturing, the DNA double strand melts into its two single strands and the primers can bind to the single strands (annealing). The polymerase can bind to the 3' end of the primer-DNA hybrid and can elongate it.

The quantification is possible because the PCR mix contains the dye SYBR green, which only can intercalate between double stranded DNA. After each cycle the emission of SYBR green is measured and the amount of double stranded DNA is detected. At the end of the PCR, a melting curve is monitored to investigate the specificity of the amplification products.

With the collected data, the average of the cycle threshold (C_T) from one triplet was calculated. The C_T is the PCR-cycle, of which the background fluorescence has significantly exceeded by the fluorescence of DNA-bound SYBR green. The C_T of the investigated gene (sample) was normalized with the C_T of the housekeeping gene (hkg) RPLP0.

Normalization: $\Delta C_T = C_T \text{ sample} - C_T \text{ hkg}$

Aberration of ΔC_T: $\sqrt{((\text{aberration sample})^2 + (\text{aberration hkg})^2)}$

Comparison of conditions: $\Delta\Delta C_T = \Delta C_T \text{ control} - \Delta C_T \text{ treatment}$

Relative expression: $x = 2^{\Delta\Delta CT}$

Error of relative expression: $\Delta x = \sqrt{((x * \ln 2)^2 * \text{aberration } \Delta C_T^2)}$

The final result of the RT-qPCR was shown graphically in a bar chart.

3.13. Mouse Handling

Original adult transgenic mice were a generous gift from Derek C. Radisky.

3.13.1. Mating of breading and weaning of baby mice

On a regular basis, it was controlled if the breeding mates got pups. If so, the breeding number, the birth date, and how many babies were born was documented. Three weeks later the pups were old enough to set an ear clip and to get some tail tissue for genotyping (see 3.7 and 3.11). At the same time the mice were seated into new cages. One cage contains up to six mice. Cages with male mice were named with A, C, E, etc. and cages with female mice were named with B, D, F, etc. Furthermore, the cages were labeled with the users' name, the reference number, the breeding from which the mice derived, the number of mice which were contained in the cage, if they were male or female, and the day of birth. Additionally, the clip numbers of the mice were observed and if they get chow embedded with Doxycycline (Doxy chow). Initially, all mice get Doxy chow, the final decision for or against Doxy chow was made after the genotyping and classification in to the experimental groups.

Classification

After genotyping the mice, they were classified into different experimental groups. There should be six mice in each group, three males and three females. Ideally, they were not from the same breeding.

Table 6; experimental classification of double and triple transgenic mice

Genotype	Experimental groups	
rtTA-Ela1/tet-HA-MMP3/tet-KRas	- Doxycycline; + NaCl	5 months, 5x week
	+ Doxycycline; + Caerulein	5 months, 5x week
	- Doxycycline; + Caerulein	5 months, 5x week
rtTA-Ela1/tet-YFP-Rac1b/tet-KRas	- Doxycycline; + NaCl	5 months, 5x week
	+ Doxycycline; + Caerulein	5 months, 5x week
	- Doxycycline; + Caerulein	5 months, 5x week

The grouped mice should be between 6 and 8 weeks old, the age difference should not be higher than one week.

3.13.2. Treatment with Caerulein

Before starting the experiments, the used Caerulein must be tested. Therefore, wild type mice were splattered eight times each hour (8x a day). After two days, they were killed and the pancreas was dissected out as described below. When the organ shows pancreatitis, the Caerulein flask can be used for the experiments.

As described above the experiments last 20 weeks (5 months). During this time, the mice were splattered each day on the left side with 100µl of 0.05µl Caerulein or physiological NaCl, depending on experimental group. It was important to splatter intraperitoneal and not subcutan to guaranty that the solution reaches the pancreas. By male mice it was also important not to splatter to close at the sexual organs, because than they can develop an inflammation of the penis, what can lead to death. In case of redness and hardening of the skin, it was possible to splatter with caution on the right side of the mouse.

3.13.3. Euthanizing of mice and organ removal

After 5 months of experimental time, the mice were put to death by cervical dislocation after they have been sedated with 20mg per kg body weight Ketanest. The body was opened and the pancreas was dissected. It was divided by cutting into four pieces (each two pieces of pancreatic head and tail) and one part of the head and tail were carried into paraformaldehyde for IHC the other parts was transferred in to trizol for RNA preparation. Afterwards, other organs such as liver, kidney, or lung were dissected.

3.14. Immunohistochemistry

For every immunohistochemically staining paraffin sections were used. Therefor it was important not to allow the slides to dry at any step during the staining procedure.

3.14.1. Hematoxylin Eosin staining

A standard staining procedure for paraffin sections is the Hematoxylin-Eosin (HE) staining.
For this method, the slides were deparaffinized and dehydrated for 10min in Xylene, afterwards for 5min in 100% Ethanol and then 2min each in 80% and 70% Ethanol. Then the slides were washed two times for 5min in deionized water.

3.14.2. Antibody staining

For the E-cadherin, the Amylase, the SMA and the CK 19 antibodies a protocol according to Cell Signaling was used. Ki67 was stained by Dr. Ramaswamy according to a protocol likely to the following one. The deparaffination and rehydration steps were the same as described above.
For the staining with antibodies it is necessary to unmask the epitopes which should be recognized by the current antibody.
For unmasking with 10 mM sodium citrate buffer at pH 6.0(α-Amylase, α-SMA) the slides were maintained at a sub-boiling temperature for 10 minutes in the microwave. The slides were

cooled down on ice for 20 minutes. For unmasking in 1 mM EDTA at pH 8.0(α-E-cadherin, α-CK19) the slides were boiled in the microwave for 15 minutes at a sub-boiling temperature. No cooling was necessary and the slides were left on the bench top for 20min.

The sections were washed in dH_2O three times for 5min each, followed by incubating them in 3% hydrogen peroxide for 10min. This step was necessary to block the endogenous peroxidase. Afterwards they were washed two times for 5min each in distilled water. The slides were transferred into a wet chamber and the tissue was circled with a DAKO Pen to provide a barrier to liquids applied to the sections. Each section was blocked with 200µl 10% BSA for 60min at room temperature. After removing the blocking solution, 200µl primary antibody, diluted in DAKO background reducing antibody diluent, was added to each section. They were incubated overnight at 4°C. The antibody solution was removed and the sections were washed three times in PBST for 5min each. The biotinylated secondary antibody, diluted 1:250 in PBST with 1% BSA, was added to each section and incubated for 60min at room temperature in the wet chamber. The ABC reagent was prepared 30min before use and incubated at room temperature. After removing the secondary antibody solution, the slides were washed three times with PBST for 5min each. 200µl ABC reagent was added to each section and they were incubated for 60min at room temperature in the wet chamber. The slides were washed three times in PBST for 5min each. Then, 200µl DAB were added to each section and the staining to brown is monitored closely. As soon as the sections develop, they were immersed in distilled water. The slides were counterstained in hematoxylin for 20sec and then blued in tapped water for 5min. At least the sections were dehydrated. Therefor they were incubated 2min each in 70% and 80% ethanol followed by 5min in 100% ethanol and 10min in xylene. Then they were mounted.

For the GFP antibody, a protocol given by our cooperation group at the mayo clinic was used. This protocol is executed in one day. The steps from deparaffination up to unmasking the antigen were the same as described above. Blocking the sections was done with serum-free protein block by DAKO for 5min at room temperature. The primary antibody was diluted 1:1000 in background reducing reagent and incubated for 60min at room temperature in the wet chamber. After washing the slides three times in PBST the secondary antibody (anti rabbit; 1:250) was incubated for 30min at room temperature in the wet chamber. Again, the slides were washed three times for 5min each in PBST and the ABC reagent was incubated for 30min. All remaining steps from incubating with DAB up to dehydrate and mount the sections were the same as described above.

3.14.3. Picrosirius Red staining

The slides were deparaffinized and hydrated as described above, then they were stained in Weigerts Hematoxylin solution for 4min. To get shot of dispensable dye the slides were rinsed in distilled water for 10min. They were placed in Solution A (phosphor molybdic acid) for 2min and rinsed in distilled water till the water remains clear. The slides were placed in Solution B (Picrosirius Red) for 60min and then directly in to Solution C (HCl) for 2min. At least, the slides were dehydrated and mounted.

Under polarized light the staining with Picrosirius Red shows different collagen types in different colors. The fibrils of type I were stained yellow and type III collagen is stained green.

3.15. Immunofluorescence Staining

For this staining method cells were used. They were seeded in an appropriate amount in 4-chamber slides, treated or not, and then incubated for 72h under normal growth conditions. All following steps were performed with the chamber left on the slides. First the cells were washed with PBS, and then fixed with 4% Paraformaldehyde for 10min at room temperature. To make the cell membrane more permeable, they were washed with PBS and incubated with 0.2% Triton-X on ice for 2min. After washing with PBS, a blocking step with 1µg/µl BSA in PBS was performed for 15min at room temperature. The chambers were rinsed with 0.3% Triton-X bevor the primary antibody – diluted in PBS with 1.5% BSA – was incubated for 60min at room temperature. Washing three times PBS for 10min is followed by a washing step with 0.3% Triton-X for 10min, bevor the secondary antibody was incubated for 60min at 37°C in the dark. The chamber is removed from the slide and the washing steps were repeated. The slide was mounted with ProLong Diamond Antifade Mountant, which already contains DAPI. The slides had to dry for 24hrs in the dark bevor they were monitored.

3.16. Statistics

The calculations of relative expression after RT-qPCR were performed as described in 3.12.

The analyses of wound healing experiments were performed by the group of Dr. Buchholz using the Time Lapse Analyzer software (Huth et al. 2011).

Ki67 positive cells were counted by hand vie Leica Image Scope Software.

All statistical analysis was performed with Microsoft Office Excel 2016.

4. Results

4.1. *In vitro* experiments with PDA cell lines

4.1.1. Endogenous expression of Rac1b differs in PDAC cell lines

To determine which PDAC cell lines were the most promising for further experiments, the endogenous expression of Rac1b and MMP3 was investigated by RT-qPCR. All cell lines used had an expression for MMP3 of not detectable (data not shown). Rac1b expression varied between cell lines, with the highest expression (8988S) measuring approximately 7fold higher than in the lowest expressing cell line (IMIM Pc2) (Figure 4). Cell lines marked with an arrow (S2-007, S2-028 and MiaPaCa) were chosen for further experiments based on high expression of Rac1b, and their growth characteristics. Although 8988S cells showed the highest Rac1b expression they were excluded due to a slow and unsteady growth under regular culture conditions. Instead of them, S2-028 cells were chosen because they represent a less invasive clone of the originally Suit2 cell line. Oppositional to the high invasive clone S2-007 it would be interesting which behavior both cell lines would show after a potential EMT-induction.

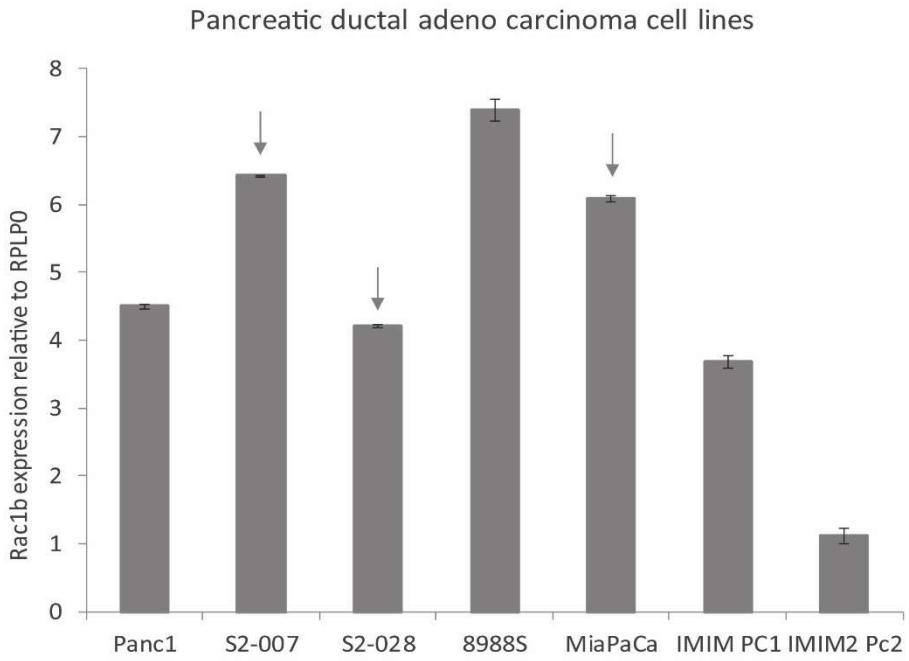

Figure 4; Expression of Rac1b compared to RPLP0 in pancreatic ductal adenocarcinoma (PDAC) cell lines
In Panc1, S2-007, S2-028, 8988S, MiaPaCa, IMIM-Pc1, and IMIM-Pc2 cells the endogenic expression of Rac1b was investigated by RT-qPCR and was normalized to the housekeeping gene RPLP0. Cell lines marked with arrows were used for further experiments.

4.1.2. Treatment with recombinant MMP3 elevates wound healing rate in S2-007 cells

The wound healing experiments were performed in cooperation with the group of Dr. Malte Buchholz. For the above outlined reasons, S2-007 and S2-028 cells were cultured on standard tissue culture plates and were either treated with 50U rMMP3 or not. After screening for 24hrs with a Zeiss Axiovert 2000M microscope the data were analyzed with the TimeLapseAnalyzer (Huth et al. 2011) and the wound healing rate of untreated cells was compared to treated ones. In S2-007 cells the wound healing rate increased after treatment with rMMP3 (Figure 5A), whereas in S2-028 cells the wound healing rate was nearly the same in both conditions (Figure 5B). This is most likely due to the higher invasiveness of S2-007 cells compared to S2-028 cells. The S2-028 cells show congenitally low replication and migration rates, which seems to be unaffected by the potentially MMP3-mediated EMT activation. Therefore, the following experiments were performed only with MiaPaCa and S2-007.

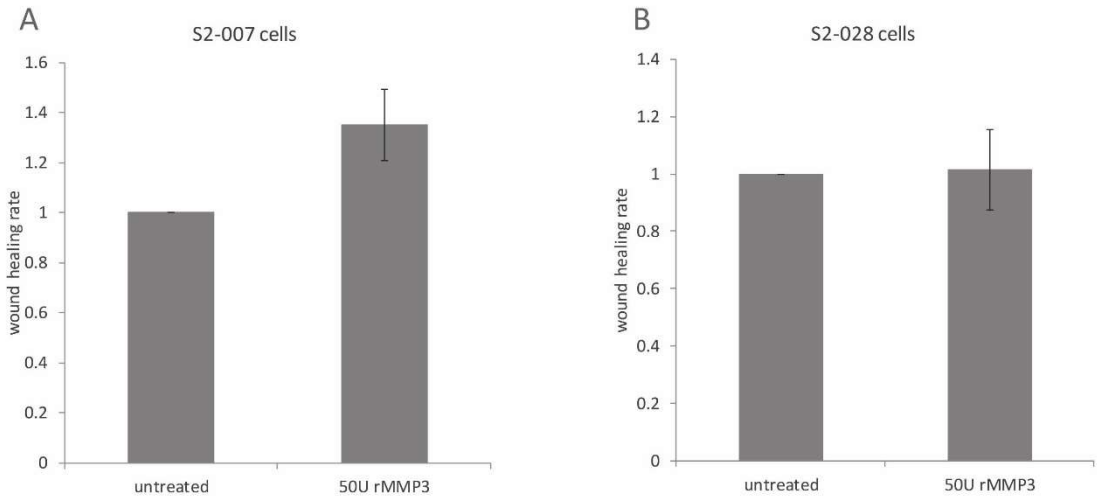

Figure 5; Rate of wounding in S2-007 and S2-028 cells after treatment with recombinant MMP3

A) S2-007 cells were cultured on standard tissue culture plates and treated with 50U rMMP3.

B) S2-028 cells were cultured on standard tissue culture plates and treated with 50U rMMP3.

Untreated cells were used as control. The replication and migration of cells were screened for 24hrs with the Zeiss Axiovert 2000M and the analysis was performed with TimeLapseAnalyzer (Huth et al. 2011) in cooperation with the group of Dr. Malte Buchholz.

4.1.3. Cells change their growth characteristics when cultured on Matrigel

S2-007 and MiaPaCa cells were cultured under two different substrate conditions. On the one hand, they were cultured on standard tissue culture plates (Plastic) and on the other hand they were cultured on Matrigel-coated tissue culture plates (Matrigel). Under both conditions, they were either treated with recombinant proteins (Figure 6) or with adenoviral constructs (Figure

7). AdGFP was used as a control for a potential effect of adenoviral treatment. TGFβ was used as an EMT-inducing control.

Untreated S2-007 and MiaPaCa cells cultured on plastic showed typical mesenchymal growth characteristics with a spindle-like shape of the cells, a development of a cell monolayer without developing cell-cell contacts, and limited migration potential. On Matrigel, which mimics the extracellular environment and the basement membrane, S2-007 developed more epithelial growth characteristics. The cells lose the spindle-like appearance, show more branching, and grew in a net-like manner. Treated with rTGFβ or rMMP3, the cells seem to grow denser than I untreated cells, due to a higher proliferation and migration rate (Figure 6 left side). MiaPaCa cells did not show a net-like growth behavior when cultured on Matrigel. The cells became more rounded, but they did not show branching, they grew from doublets to clusters instead, which does not correlate to the classical epithelial growth behavior (Figure 6 right side). In untreated MiaPaCa cells the clusters were smaller and more doublets were observed than in protein-treated ones, where MiaPaCa cells treated with rMMP3 grew in larger clusters than after rTGFβ treatment.

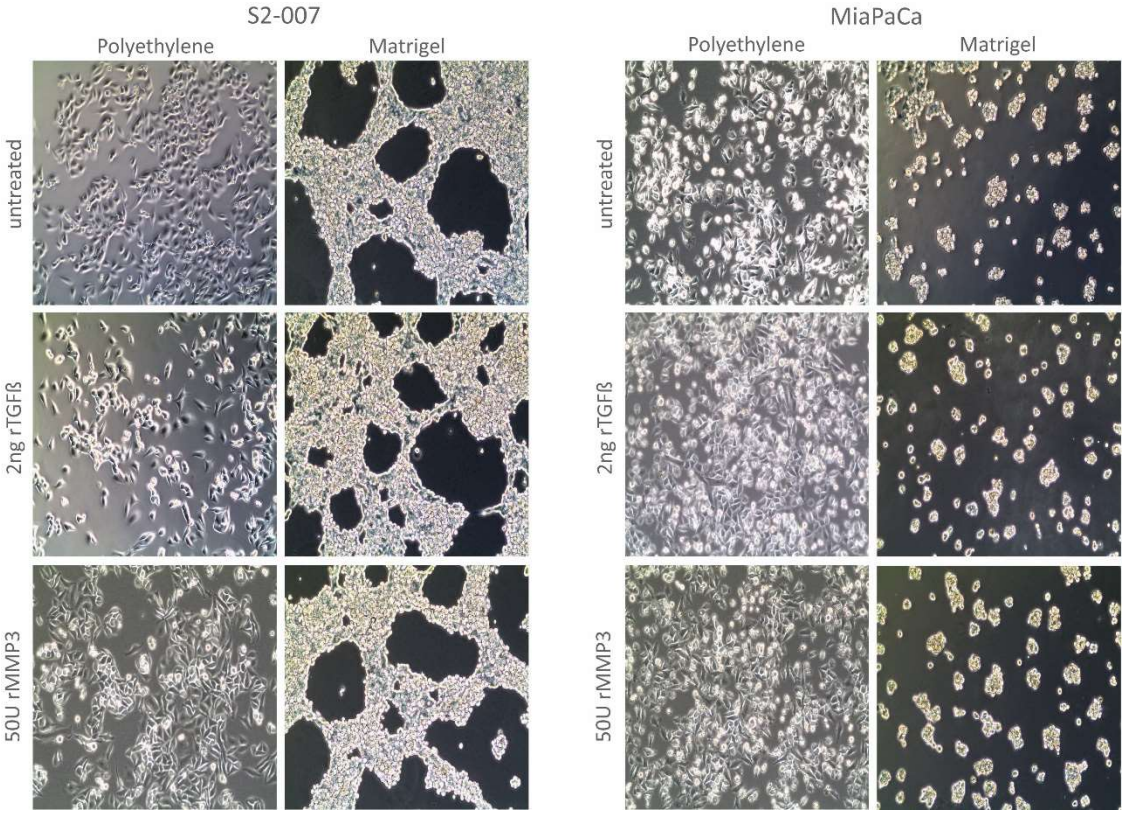

Figure 6; Morphological changes in S2-007 and MiaPaCa cells after treatment with recombinant proteins on Plastic and Matrigel

S2-007 and MiaPaCa cells were cultured on plastic and on Matrigel-coated tissue culture plates. They were treated with 2ng rTGFβ and 50U rMMP3 for 48hrs, untreated cells were used as controls and rTGFβ was used as an EMT-inducing control.

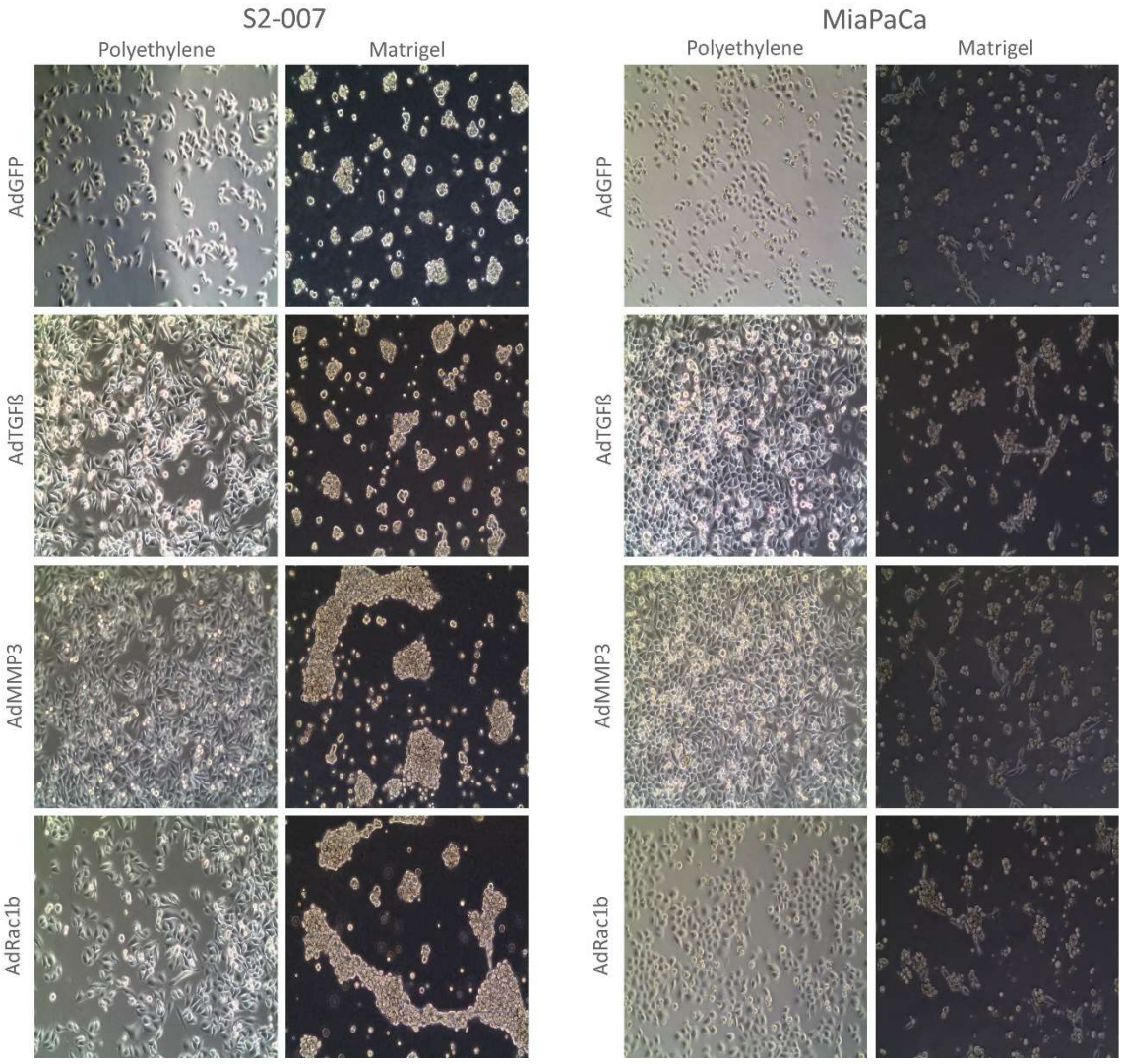

Figure 7; Morphological changes in S2-007 and MiaPaCa cells after treatment with adenoviral constructs on Plastic and Matrigel

S2-007 and MiaPaCa cells were cultured on plastic and on Matrigel-coated tissue culture plates and treated with AdGFP, AdTGFβ, AdMMP3, and AdRac1b for 48hrs with an MOI of 10. Cells treated with AdGFP were used as controls and AdTGFβ was used as an EMT-inducing control.

When S2-007 cells were grown on Matrigel and treated with adenoviral constructs, the cells became more rounded and the net-like growth pattern changed to clusters. The clusters in AdTGFβ treated S2-007 cells were larger than in AdGFP, and even larger in AdMMP3 and AdRac1b treated cells, whereas there were no visible differences between AdMMP3 and AdRac1b treatment (Figure 7 left side). When MiaPaCa cells were cultured on Matrigel and treated with adenoviral constructs they did not change their growth behavior and formed clusters again. In cells treated with AdGFP the clusters were the smallest compared to those with AdTGFβ, AdMMP3, and AdRac1b. Under these conditions the cells did not show visible differences in growth behavior (Figure 7 right side). Because Matrigel mimics the basement membrane, it is comprehensible that cells cultured on Matrigel show an epithelial growth behavior like they would do *in vivo*. Further experiments will be conducted to investigate

whether the molecular machinery is influenced by the treatment with recombinant protein or adenoviral constructs, and if there are evidences for an induction of EMT.

4.1.4. Adenoviral treatment elevates expression levels of GFP, TGFβ, MMP3, and Rac1b

Adenoviral treatment is a reliable method to induce overexpression of a particular protein. The adenoviral constructs used for TGFβ, MMP3, and Rac1b were provided by Prof. Derek C. Radisky (Mayo clinic, Florida; Lee et al. 2012) and the construct for GFP was obtained from Vector BioLabs (see 2.5). AdGFP is a non-targeting vector for the normalization of adenoviral effects and AdTGFβ is the control for EMT-inducing pathways.

To confirm that the adenoviral constructs used were working effectively, the relative expression of the related protein was investigated by RT-qPCR. S2-007 and MiaPaCa cells were cultured on standard and on Matrigel-coated tissue culture plates and treated with AdGFP, AdTGFβ, AdMMP3, and AdRac1b with a MOI of 10. For S2-007 cells, the expression of GFP after AdGFP-treatment on plastic was elevated about 60fold compared to the treatment with AdTGFβ, whereas the elevation of GFP expression after treatment on Matrigel was much weaker (Figure 8; Activation of GFP, TGFβ, MMP3 and Rac1b overexpression in S2-007 cells after treatment with the related adenoviral construct on Plastic and MatrigelFigure 8A). The expression of TGFβ after adenoviral treatment on Plastic and Matrigel gained, but showed the same pattern as it was

found for GFP. The expression after treatment on Matrigel was much weaker (

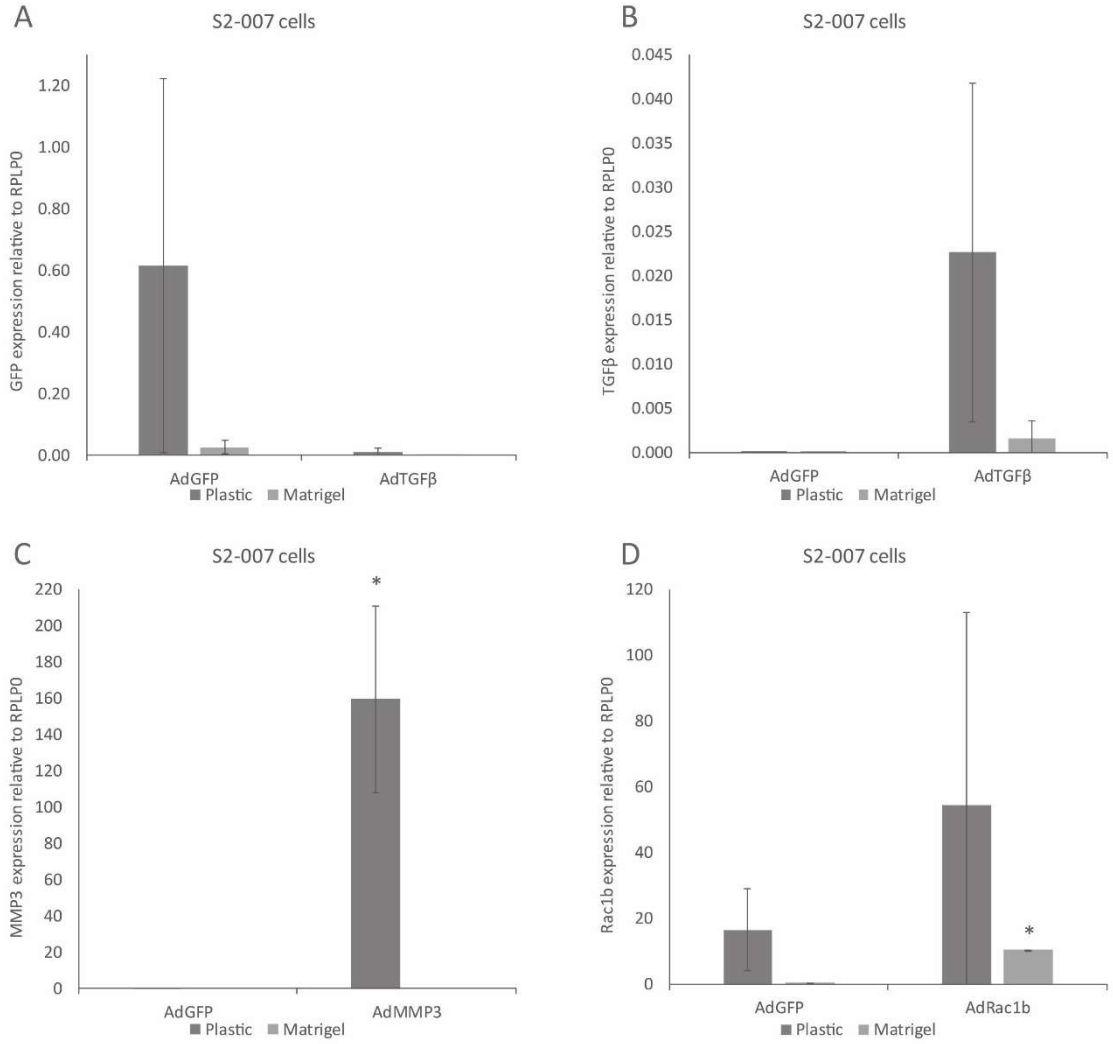

Figure 8B). The same is true for the activation of MMP3 and Rac1b over expression. After treatment on Plastic the expression of MMP3 and Rac1b was clearly elevated (Figure 8C and D), even significantly for MMP3, but after treatment on Matrigel there was just a slightly elevation of MMP3 expression (Figure 8C). An exception was the expression of Rac1b after treatment on Matrigel, here the expression was significantly elevated compared to the treatment with AdGFP (Figure 8D). But it must be pointed out that the treatment with AdGFP resulted in an elevation of Rac1b expression in both cell lines, but even more for S2-007 (Figure 8D and Figure 9D).

Also for MiaPaCa cells it become apparent that treatment with adenoviral constructs on Plastic caused a clear elevation of the related proteins, even significantly for MMP3 again (Figure 9C), whereas the adenoviral treatment on Matrigel did only lead to a slightly elevation of expression (Figure 9).

Though the results were fluctuating, they were reproducible and they show that the infection with AdGFP, AdTGF, AdMMP3, and AdRac1b results in overexpression of the related protein in

S2-007 and MiaPaCa cells on Plastic. Although adenoviral GFP, TGFβ, MMP3, and Rac1b treatment on Matrigel was not that efficient, all constructs were used under both culturing conditions to investigate, if an overexpression of MMP3 and Rac1b influences the expression of the typical EMT markers E-cadherin and Vimentin.

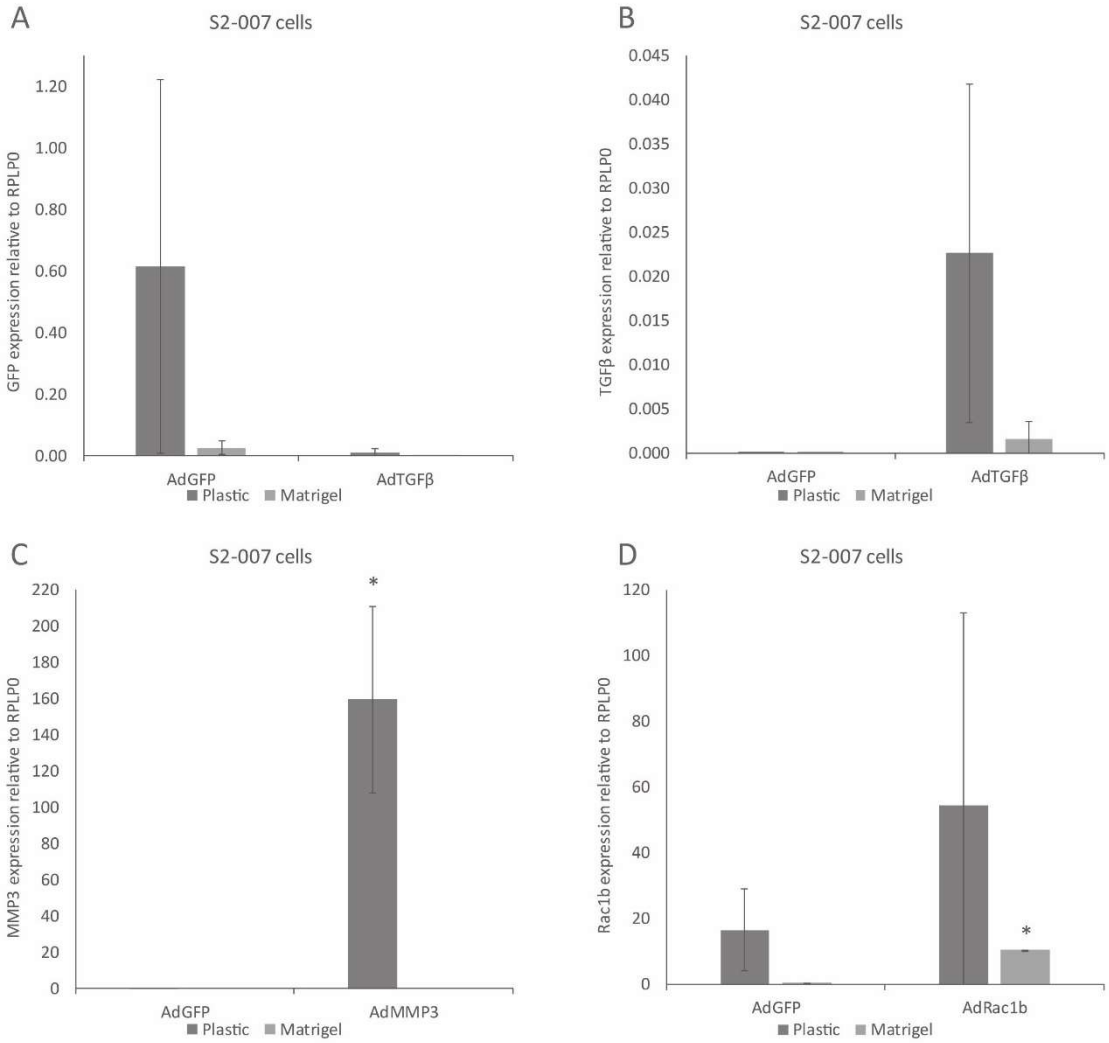

Figure 8; Activation of GFP, TGFβ, MMP3 and Rac1b overexpression in S2-007 cells after treatment with the related adenoviral construct on Plastic and Matrigel

S2-007 cells were cultured on standard and Matrigel-coated tissue culture plates and treated with adenoviral GFP, TGFβ, MMP3 and Rac1b. The expression of the respective protein was investigated by RTq-PCR and the expression was normalized to RPLP0.

A) After AdGFP treatment the expression of GFP was investigated compared to treatment with AdTGFβ.
B) After AdTGFβ treatment the expression of TGFβ was investigated compared to treatment with AdGFP.
C) After AdMMP3 treatment the expression of MMP3 was investigated compared to treatment with AdGFP.
D) After AdRac1b treatment the expression of Rac1b was investigated compared to treatment with AdGFP.

* Symbolizes significance ($p \leq 0.05$)

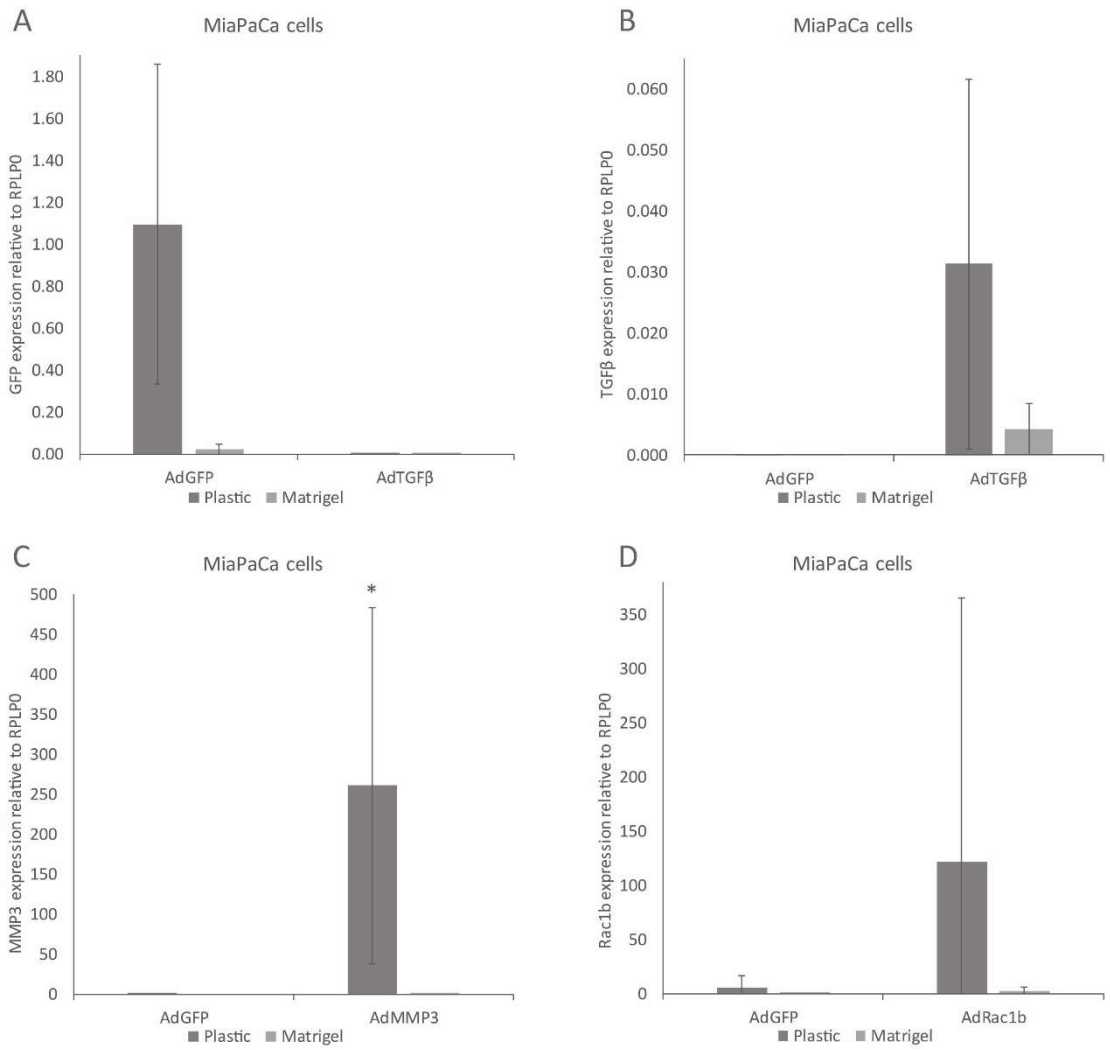

Figure 9; Activation of GFP, TGFβ, MMP3 and Rac1b overexpression in MiaPaCa cells after treatment with the related adenoviral construct on Plastic and Matrigel

MiaPaCa cells were cultured on standard and Matrigel-coated tissue culture plates and treated with adenoviral GFP, TGFβ, MMP3 and Rac1b. The expression of the respective protein was investigated by RTq-PCR and the expression was normalized to RPLP0.

A) After AdGFP treatment the expression of GFP was investigated compared to treatment with AdTGFβ.
B) After AdTGFβ treatment the expression of TGFβ was investigated compared to treatment with AdGFP.
C) After AdMMP3 treatment the expression of MMP3 was investigated compared to treatment with AdGFP.
D) After AdRac1b treatment the expression of Rac1b was investigated compared to treatment with AdGFP.

* Symbolizes significance ($p \leq 0.05$)

4.1.5. Overexpression of MMP3 influences endogenous Rac1b expression

Before investigating the expression levels of E-cadherin and Vimentin as representative EMT markers, it was of interest to analyze the influence of MMP3 overexpression on endogenous Rac1b expression levels.

The expression of Rac1b was slightly influenced by treatment with recombinant MMP3. Compared to the expression in untreated cells, Rac1b levels rose about 2fold after rMMP3 treatment, whereas the expression of Rac1b drops after treatment with the EMT-inducing control, rTGFβ (Figure 10A). After treatment on Matrigel, the expression of Rac1b drops again in rTGFβ- and was nearly doubled in rMMP3-treated cells (Figure 10B). The treatment with adenoviral constructs seem to have a contrary effect on the expression of Rac1b. Both, after treatment with AdTGFβ and AdMMP3 the expression of Rac1b seem to drop about 3fold on Plastic and even more on Matrigel (Figure 10C and D). It must be pointed out, that AdGFP treatment, what should have no effect on Rac1b expression, elevates the expression especially on Plastic.

Similar results were obtained in MiaPaCa cells. The treatment with recombinant TGFβ and the treatment with AdTGFβ and AdMMP3 lowers the expression of Rac1b as it was seen for S2-007 cells before (Figure 11). Other than in S2-007 cells the treatment of MiaPaCa cells with rMMP3 also led to a drop of Rac1b expression compared to untreated cells (Figure 11A and B).

The exogenous overexpression of Rac1b did elevate the endogenous MMP3 expression about 25fold in S2-007 and in MiaPaCa cells compared to untreated cells, when cultured on Plastic. The results could not be confirmed for Matrigel and the treatment with adenoviral constructs (Figure 11C and D). The results indicate that there might have been a problem with the TGFβ control. Nevertheless, all the collected data seem to verify that Rac1b is a downstream target of MMP3 as described in literature (Nelson et al. 2008; Lee et al. 2012).

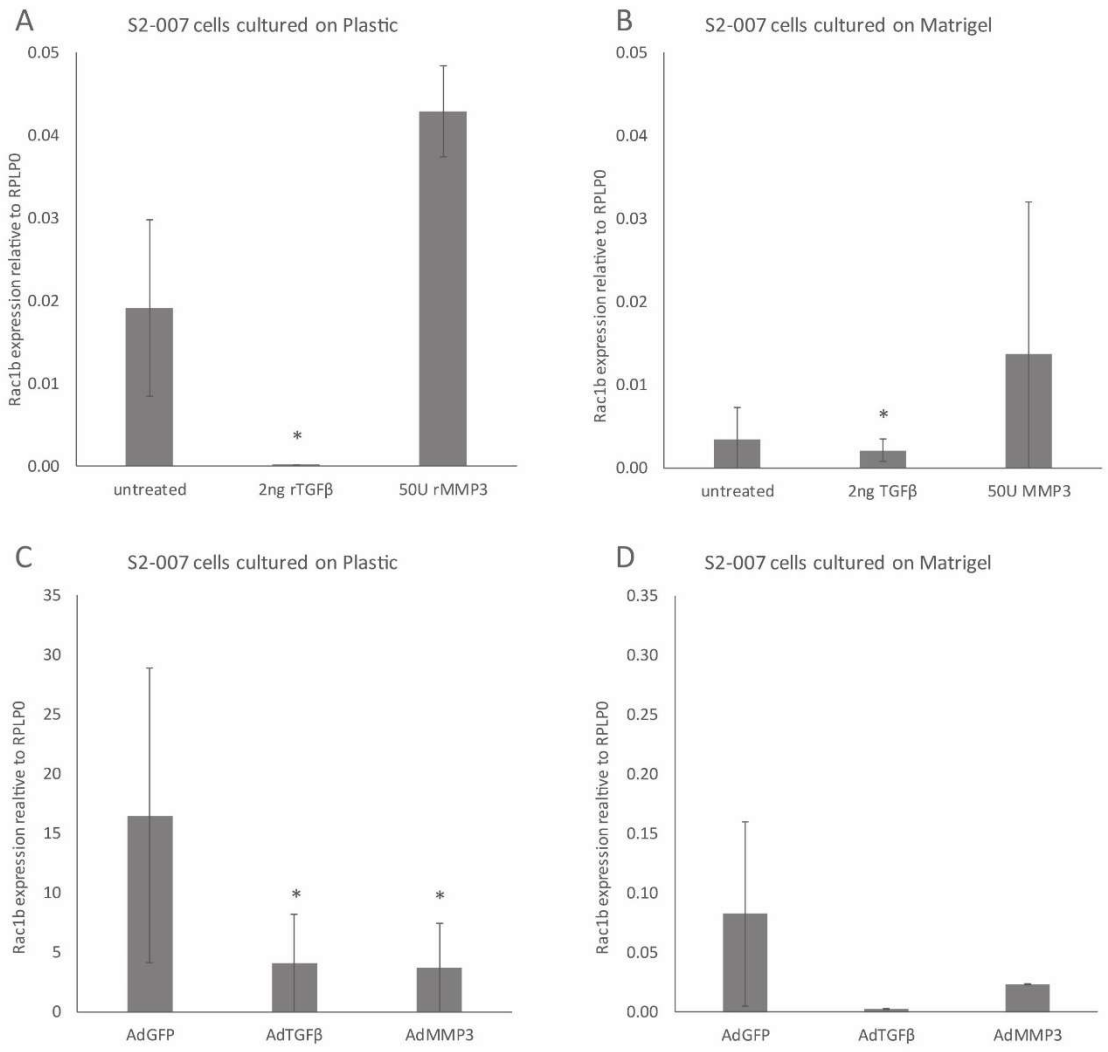

Figure 10; Expression of Rac1b in S2-007 cells after treatment with recombinant protein and adenoviral constructs

A) S2-007 cells were cultured on standard tissue culture plates and treated with 2ng rTGFβ and 50U rMMP3.

B) S2-007 cells were cultured on Matrigel-coated tissue culture plates and treated with 2ng rTGFβ and 50U rMMP3.

C) S2-007 cells were cultured on standard tissue culture plates and treated with AdGFP, AdTGFβ, and AdMMP3 (MOI=10).

D) S2-007 cells were cultured on Matrigel-coated tissue culture plates and treated with AdGFP, AdTGFβ, and AdMMP3 (MOI=10).

Untreated cells and AdGFP treated cells were used as controls, respectively. The expression of Rac1b was normalized to the expression of RPLP0. * Symbolizes significance ($p \leq 0.05$)

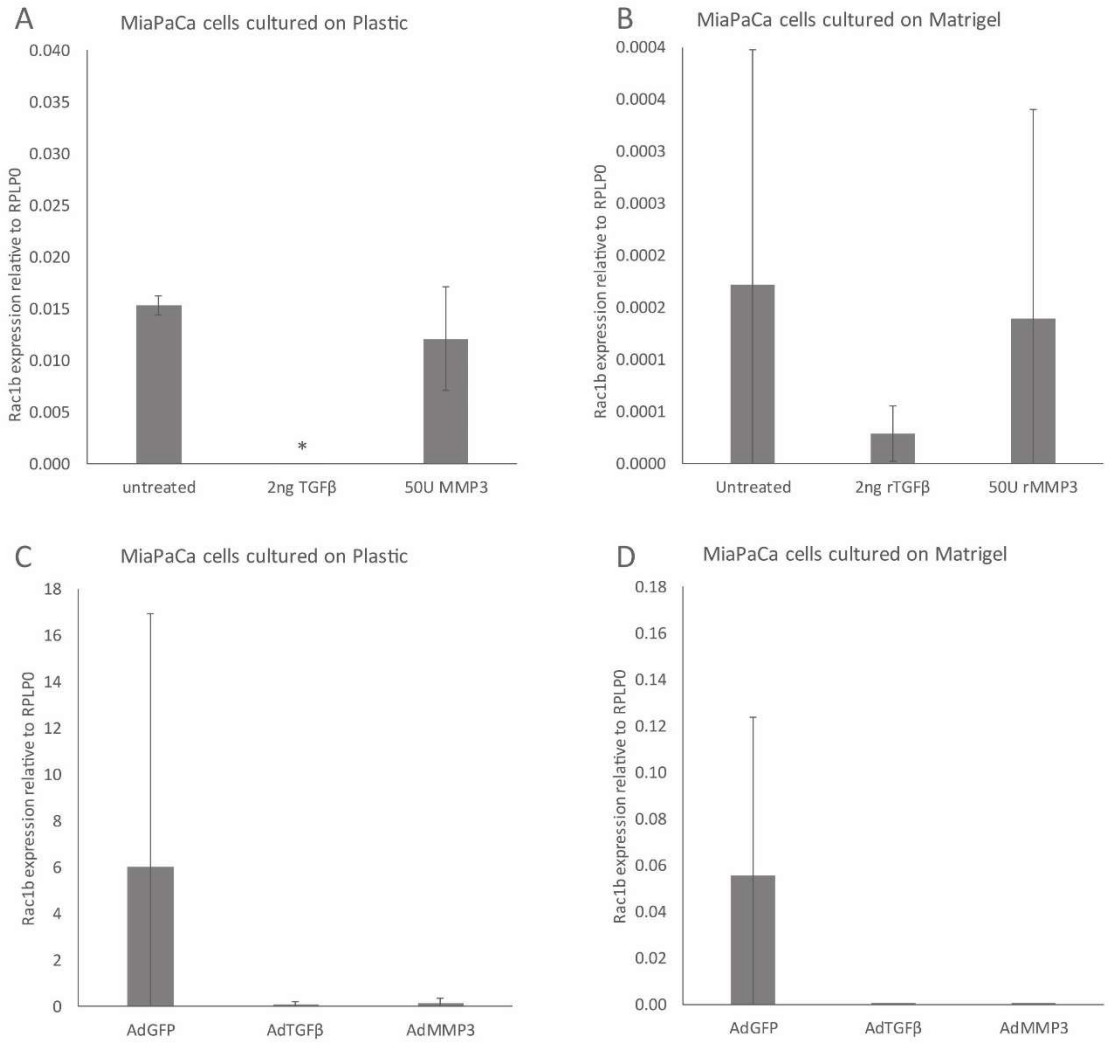

Figure 11; Expression of Rac1b in MiaPaCa cells after treatment with recombinant protein and adenoviral constructs

A) MiaPaCa cells were cultured on standard tissue culture plates and treated with 2ng rTGFβ and 50U rMMP3.
B) MiaPaCa cells were cultured on Matrigel-coated tissue culture plates and treated with 2ng rTGFβ and 50U rMMP3.
C) MiaPaCa cells were cultured on standard tissue culture plates and treated with AdGFP, AdTGFβ, and AdMMP3 (MOI=10).
D) MiaPaCa cells were cultured on Matrigel-coated tissue culture plates and treated with AdGFP, AdTGFβ, and AdMMP3 (MOI=10).

Untreated cells and AdGFP treated cells respectively, were used as control. The expression of Rac1b was normalized to the expression of RPLP0. * Symbolizes significance ($p \leq 0.05$)

4.1.6. EMT induction depends on the used cell lines and the way of protein expression

To find out whether the treatment with recombinant or adenoviral MMP3 and Rac1b and/or the matrix dependent morphological changes influenced the expression of EMT markers, S2-007 and MiaPaCa cells were treated with both recombinant proteins and adenoviral constructs on plastic and on Matrigel. The expression of E-cadherin and Vimentin was examined by RT-qPCR and normalized to RPLP0. When S2-007 cells were treated with recombinant proteins, there seem to be no effect on the EMT-machinery. The treatment on Plastic as well as on Matrigel results in all cases in a higher E-cadherin than Vimentin expression (Figure 12), what indicates an epithelial cell behavior. The growth pattern seen under the microscope was convenient to this (Figure 6 and Figure 7; left side).

Adenoviral treatment on Plastic and on Matrigel showed elevated Vimentin and lowered E-cadherin expression levels for AdTGFβ, AdMMP3, and AdRac1b compared to the treatment with AdGFP (Figure 12C and D). Although, under standard culturing conditions (Plastic), all three constructs showed an elevation of E-cadherin expression compared to AdGFP treatment, the Vimentin expression was even more elevated, whereat the treatment with AdRac1b showed the highest effect. Here the Vimentin expression was elevated about 2000fold compared to AdGFP treatment (AdTGFβ: 19fold; AdMMP3: 323fold). After treatment on Matrigel the E-cadherin expression was only elevated after AdRac1b treatment, compared to AdGFP (Figure 12D). Nevertheless, the Vimentin expression was higher after treatment with AdTGFβ, AdMMP3, and AdRac1b, compared to treatment with AdGFP. The highest Vimentin expression (277 500fold) was found after AdRac1b treatment again. AdTGFβ showed an elevation of 4.5fold and AdMMP3 showed an elevation of Vimentin expression of 37fold. These results indicate that Rac1b seem to play a crucial role during EMT-induction, but it also seems not to be influenced by MMP3 and TGFβ as much as supposed.

The same experiments as described above were performed for MiaPaCa cells. In this cell line the expression of E-cadherin and Vimentin was affected when cells were cultured on Plastic and treated with recombinant proteins (Figure 13A). Both, after rTGFβ and rMMP3 treatment the expression of E-cadherin was doubled compared to the expression in untreated cells but also the Vimentin expression was elevated 1.3fold for rTGFβ and 3.3fold for rMMP3, compared to untreated cells (Figure 13A). When the cells were cultured on Matrigel and treated with rTGFβ the E-cadherin expression was elevated about 6fold, whereas the E-cadherin expression after rMMP3 treatment was nearly the same, compared to untreated cells (Figure 13B). The Vimentin expression was highest in untreated cells and was about the half after treatment with recombinant protein. The treatment of MiaPaCa cells with adenoviral constructs showed the highest Vimentin expression levels after AdRac1b treatment (1 300fold and 27fold, compared

to AdGFP), as seen in S2-007 cells too (Figure 13C and D). Exception were the treatment with AdTGFβ and AdMMP3 on Plastic, here the Vimentin expression levels were lower than the E-cadherin expression levels (Figure 13C). Nevertheless, in most cases of treatment (recombinant protein and adenovirus, Plastic and Matrigel) the Vimentin expression was higher than the E-cadherin expression, what indicates that MiaPaCa cells show a naturally mesenchymal growth behavior, what might explain about the untypically growth pattern shown by MiaPaCa cells under the microscope (Figure 6 and Figure 7; right side).

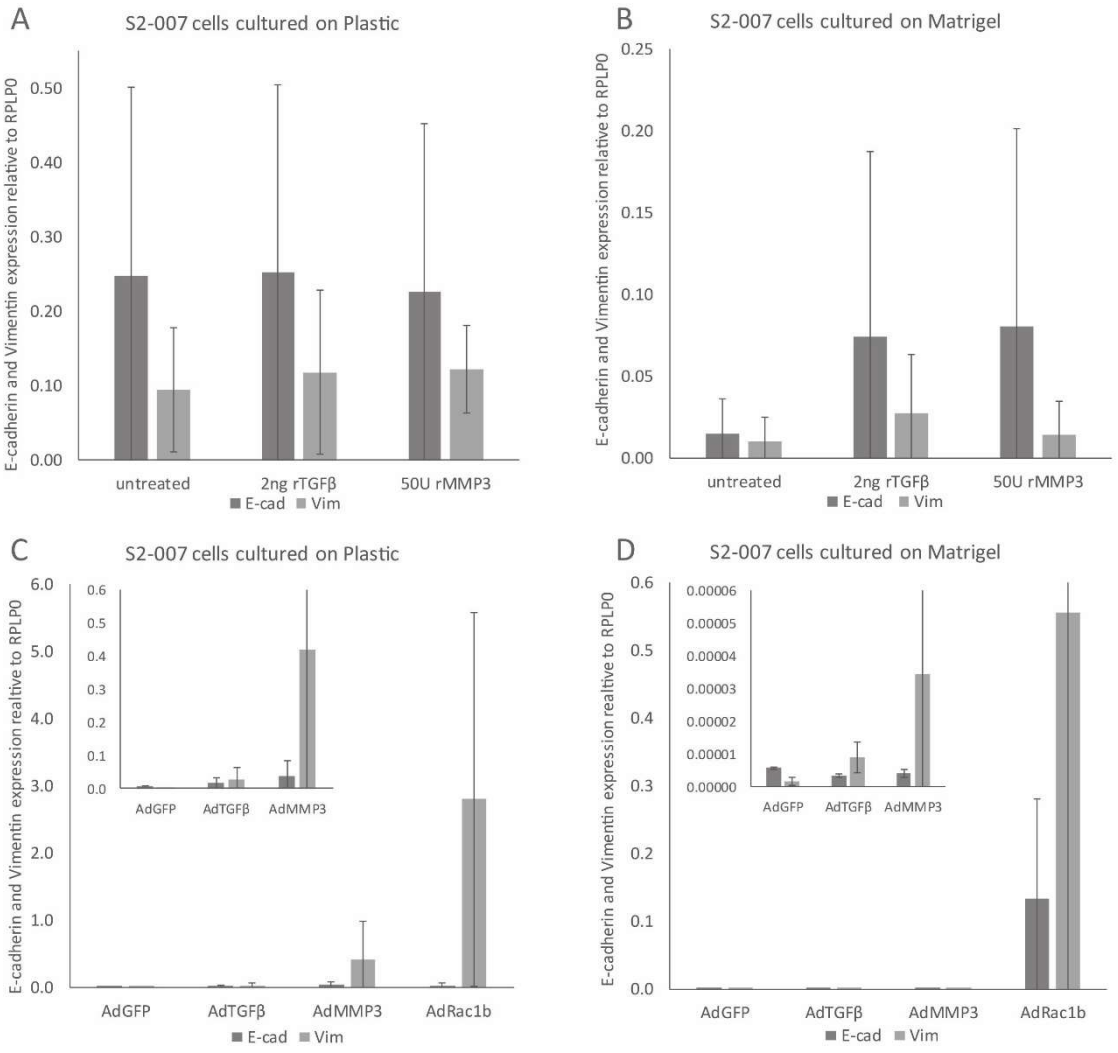

Figure 12; Expression of E-cadherin and Vimentin in S2-007 cells after treatment with recombinant proteins and adenoviral constructs

A) S2-007 cells were cultured on standard tissue culture plates and treated with 2ng rTGFβ and 50U rMMP3.
B) S2-007 cells were cultured on Matrigel-coated tissue culture plates and treated with 2ng rTGFβ and 50U rMMP3.
C) S2-007 cells were cultured on standard tissue culture plates and treated with AdGFP, AdTGFβ, AdMMP3, and AdRac1b (MOI=10).
D) S2-007 cells were cultured on Matrigel-coated tissue culture plates and treated with AdGFP, AdTGFβ, AdMMP3, and AdRac1b (MOI=10).

Small inserted graphs are detailed views of the lower bars, which do not appear well in the normal graph.
Untreated and AdGFP treated cells respectively were used as controls. The expression of E-cadherin and Vimentin was normalized to the expression of RPLP0. * Symbolizes significance ($p \leq 0.05$)

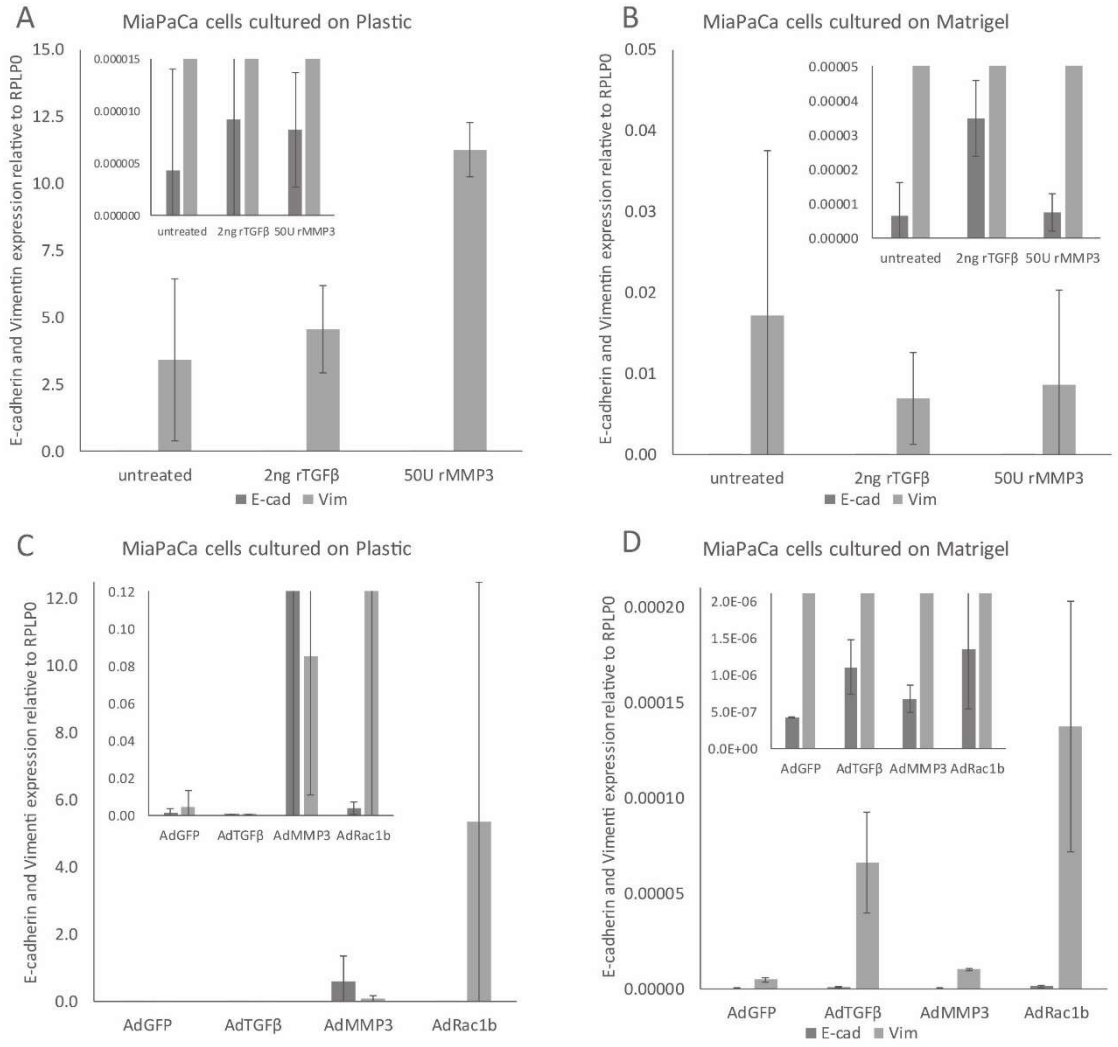

Figure 13; Expression of E-cadherin and Vimentin in MiaPaCa cells after treatment with recombinant proteins and adenoviral constructs

A) MiaPaCa cells were cultured on standard tissue culture plates and treated with 2ng rTGFβ and 50U rMMP3.
B) MiaPaCa cells were cultured on Matrigel-coated tissue culture plates and treated with 2ng rTGFβ and 50U rMMP3.
C) MiaPaCa cells were cultured on standard tissue culture plates and treated with AdGFP, AdTGFβ, AdMMP3, and AdRac1b (MOI=10).
D) MiaPaCa cells were cultured on Matrigel-coated tissue culture plates and treated with AdGFP, AdTGFβ, AdMMP3, and AdRac1b (MOI=10).

Small inserted graphs are detailed views of the lower bars, which do not appear well in the normal graph.
Untreated and AdGFP treated cells respectively were used as controls. The expression of E-cadherin and Vimentin was normalized to the expression of RPLP0. * Symbolizes significance ($p \leq 0.05$)

Summarized it appears, other than expected, that the elevated expression of Rac1b mediated by recombinant MMP3 did not result in increased EMT in S2-007 cells, the Vimentin expression stays nearly the same as in untreated cells. After adenoviral treatment, when Rac1b expression seemed to be dropped by AdTGFβ and AdMMP3 treatment (Figure 10), the Vimentin expression rose. However, MiaPaCa cells showed mesenchymal expression patterns in all cases of treatment, but once higher Vimentin expression after treatment with rMMP3 on Plastic, what goes along with a lower Rac1b expression. After adenoviral treatment, the same observations

were made for MiaPaCa as in S2-007 cells. These results, compared with the earlier ones (4.1.5.), confirm the assumption, that MMP3 might be a downstream target of MMP3 but that there must be some other mechanism and environmental impact (e.g. matrix compliance) to drive forward EMT (Nelson et al. 2008; Lee et al. 2012; Ungefroren et al. 2014).

4.2. *In vivo* experiments in triple transgenic mice

Two triple transgenic mouse models were generated by mating tet-HA-MMP3, tet-YFP-Rac1b, tet-KRas, and rtTA-Ela1 mice, which were a kind gift from Derek C. Radisky. Because a defect in both alleles is lethal, the mice were mated first with FvB wild type mice to accrue an appropriate number of mice for mating to generate double transgenic rtTA-Ela1/tet-HA-MMP3, rtTA-Ela1/tet-YFP-Rac1b, and rtTA-Ela1/tet-KRas mice. These mice were used for similar experiments as described in this work (data not show; dissertations N Voss and A Martin) and for mating to generate rtTA-Ela1/tet-HA-MMP3/tet-KRas and rtTA-Ela1/tet-YFP-Rac1b/tet-KRas mice. With these triple transgenic mice, the progression of pancreatic carcinoma following chronic pancreatitis with development of PanINs should be investigated.

It was expected that the expression of KRas in addition to MMP3 and Rac1b would drive the development from chronic inflammation caused by Caerulein treatment to pancreatic cancer. Therefore, the mice were treated daily with 5µg/ml Caerulein or NaCl by intraperitoneal injection. They were fed without Doxycycline to express either MMP3 or Rac1b under the control of the elastase-1 promoter. This expression occurs specifically in exocrine pancreatic acinar cells that are presumed to be the cells of origin of PDAC. After 5 months, the mice were sacrificed and the pancreata were examined for PanINs and fibrosis. The expression levels of HA-MMP3 and YFP-Rac1b were determined by RT-qPCR. Additionally, the EMT-markers E-cadherin, Smooth muscle actin (SMA), Amylase, and Cytokeratin 19 were investigated by immunohistochemistry and RT-qPCR.

Previous experiments with double transgenic mice did not show a development of PanINs as expected. It just became apparent that the proliferation and the ADM under Caerulein treatment was increased (unpublished data). Therefore, it would be interesting to determine whether or not the presence of KRas would lead to PanIN and tumor development.

4.2.1. The lack of Doxycycline activates tetracycline-controlled transgene

Using a reverse tetracycline-controlled trans activator (rtTA) the transgene (MMP3, Rac1b) should be activated when Doxycycline, which is a tetracycline derivate, is absent. To assure that the transgene activation was put into effect, it was investigated, if the relative expression of HA-MMP3 and YFP (Rac1b) was increased in transgenic mice fed without Doxycycline (-Doxy) compared to wildtype mice. Exemplary for this investigation the Rac1b results are shown in Figure 14 and Figure 15 (results for MMP3 were not representative). The activation of YFP in rtTA-Ela1/tet-YFP-Rac1b/tet-KRas mice in the absence of Doxycycline could be confirmed. In both experimental groups -Doxy/+Caerulein and -Doxy/-Caerulein YFP-Rac1b was detectable by immunohistochemistry. In mice treated with Caerulein the expression level of YFP-Rac1b

appeared to be lower (Figure 14 middle) than in mice treated without Caerulein (Figure 14 right) and Rac1b was localized around or in the nucleus, whereas it was cytoplasmic in Caerulein-untreated tissue. The expression of YFP-Rac1b was increased 661fold in Caerulein-treated (Figure 15A) and nearly 50 000fold in Caerulein-untreated mice fed without Doxycycline (Figure 15B).

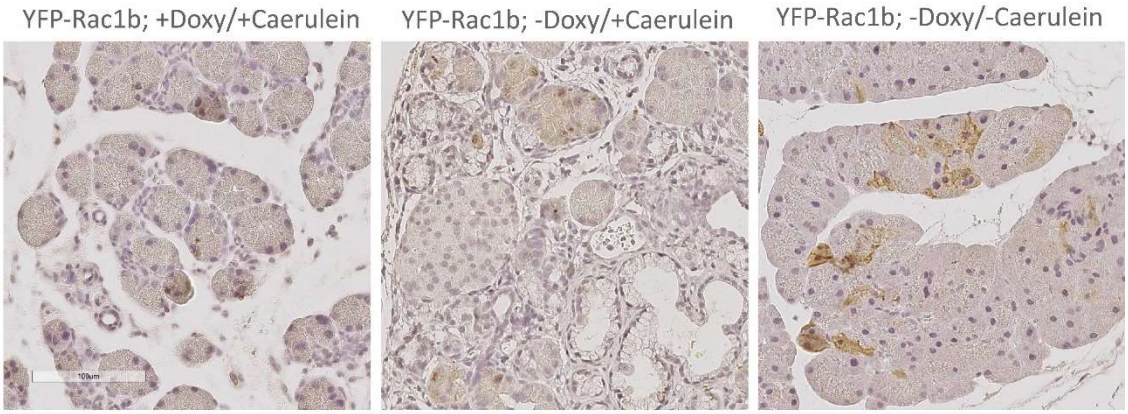

Figure 14; Histological staining for YFP tag of Rac1b in mice fed without Doxycycline
Representative images of pancreatic tissue from rtTA-ela1/tet-YFP/tet-KRas mice. The YFP tag of Rac1b is very similar to the protein GFP. Therefore, it was stained with a rabbit antibody against GFP according to the described protocol (see 3.14.2). Doxycycline treated rtTA-Ela1/tet-YFP-Rac1b/tet-KRas mice served as control. Scale represents 100µm.

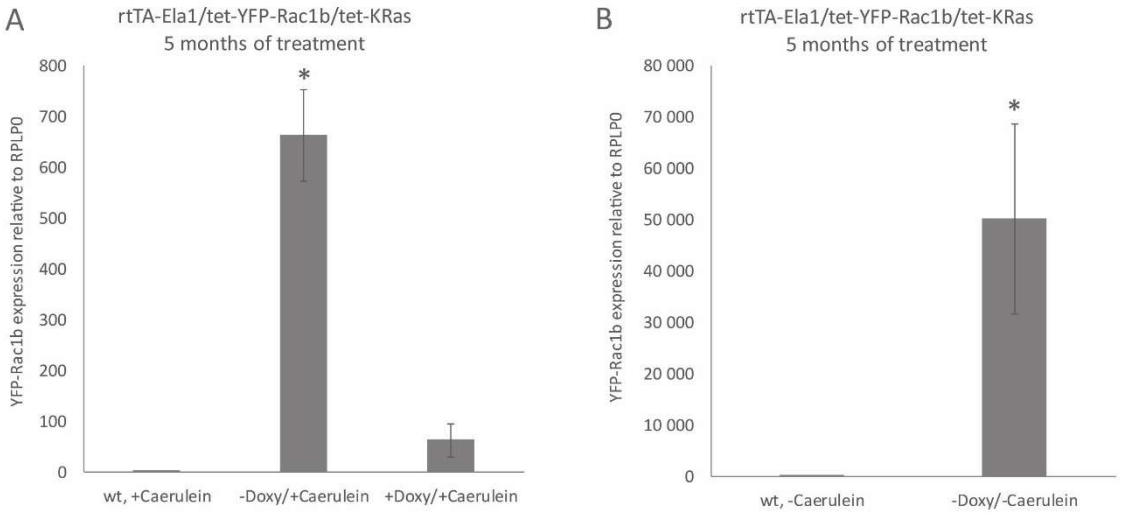

Figure 15; Expression of YFP-Rac1b in rtTA-Ela1/tet-YFP-Rac1b/tet-KRas mice after 5 months of treatment

A) The expression of YFP-Rac1b was investigated in rtTA-Ela1/tet-YFP-Rac1b/tet-KRas mice treated with Caerulein for 5 months. One experimental group was fed without Doxycycline to activate the transgene. Wild type mice treated with Caerulein were used as control group.

B) The expression of YFP-Rac1b was investigated in untreated rtTA-Ela1/tet-YFP-Rac1b/tet-KRas mice (-Doxy/-Caerulein). Wild type mice treated without Caerulein were used as control group.

The expression of YFP-Rac1b was normalized to RPLP0. * symbolizes significance ($p \leq 0.05$)

4.2.2. Caerulein treatment after transgene activation results in distinct pancreatitis

First, a HE staining was performed to investigate whether the tissue displayed chronic pancreatitis, ADM or evidence for PanINs or tumor development.

Mice without Caerulein treatment had normal pancreatic tissue (Figure 16 left). When the transgene was inactivated, but the mice were treated with Caerulein, they developed mild chronic pancreatitis (Figure 16 middle), whereas Caerulein-treated mice with activated MMP3 or Rac1b showed a more distinct pancreatitis (Figure 16 right). In this process the chronic pancreatitis developed stronger in rtTA-Ela1/tet-YFP-Rac1b/tet-KRas than in rtTA-Ela1/tet-HA-MMP3/tet-KRas mice. Both mouse models showed ADM after Caerulein treatment, but they did not develop PanINs or PDAC.

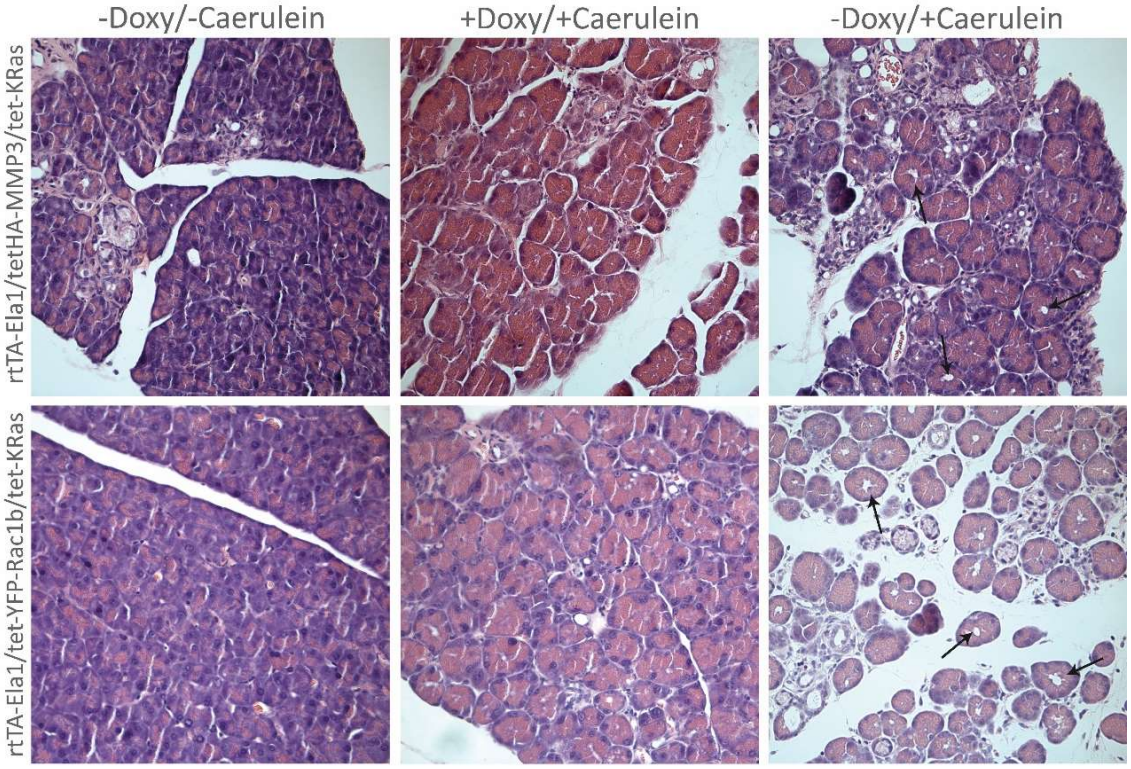

Figure 16; Development of chronic pancreatitis after 5 months of Caerulein treatment in triple transgenic mice
Representative images of the development of chronic pancreatitis after Caerulein treatment in rtTA-Ela1/tet-HA-MMP3/tet-KRas and rtTA-Ela1/tet-YFP-rac1b/tet-KRas mice depends on the absence or presence of Doxycycline and the accompanied transgene activation or inactivation. When either MMP3 or Rac1b are activated, the pancreatitis was more distinct and appeared with ADM.

4.2.3. Variable ADM occurrence after activation of MMP3 and Rac1b overexpression

Acinar to ductal metaplasia (ADM) is an indicator for EMT-independent transformation of epithelial tissue. To quantify the amount of ADM occurrences the ratio between Amylase and CK19 was calculated. A higher quotient indicates a high Amylase expression, which is an indicator for existence of acini. A lower quotient signifies a high CK19 expression and represents

the formation to ductal cells and therefor the presence of ADM. Mice with activated transgene but without chronic pancreatitis (-Doxy/-Caerulein) were used as reference for mice with chronic inflammation (+Caerulein).

From the statistics of expression levels, it was found that rtTA-Ela1/tet-HA-MMP3/tet-KRas mice with chronic pancreatitis but inactivated transgene showed the greatest extent of ADM (Figure 19). For HA-MMP3 mice fed without Doxycycline the ratio was higher (ratio = 0.0127) than in the same transgenic mice fed with Doxycycline (ratio = 0.0012). This could be confirmed histologically. HA-MMP3 mice with activated transgene seem did not show such a strong CK19 staining like the mice with inactivated transgene. Additionally, both showed a strong Amylase staining, too (Figure 17 middle and right). This is reflected in a higher ratio of expression of Amylase and CK19 in mica with activated transgene (Figure 19A).

For rtTA-Ela1/tet-YFP-Rac1b/tet-KRas mice the data implicate a higher ADM occurrence in mice with activated transgene (ratio = 0.0094) (Figure 19B). This coincides with the histological staining where the CK19 staining was strongest and the Amylase staining was weaker than in YFP-Rac1b mice with inactive Rac1b (Figure 18 middle and right). Taken together these results implicate a higher ADM occurrence after inducing chronic pancreatitis for both transgenes and additionally for overexpression of YFP-Rac1b.

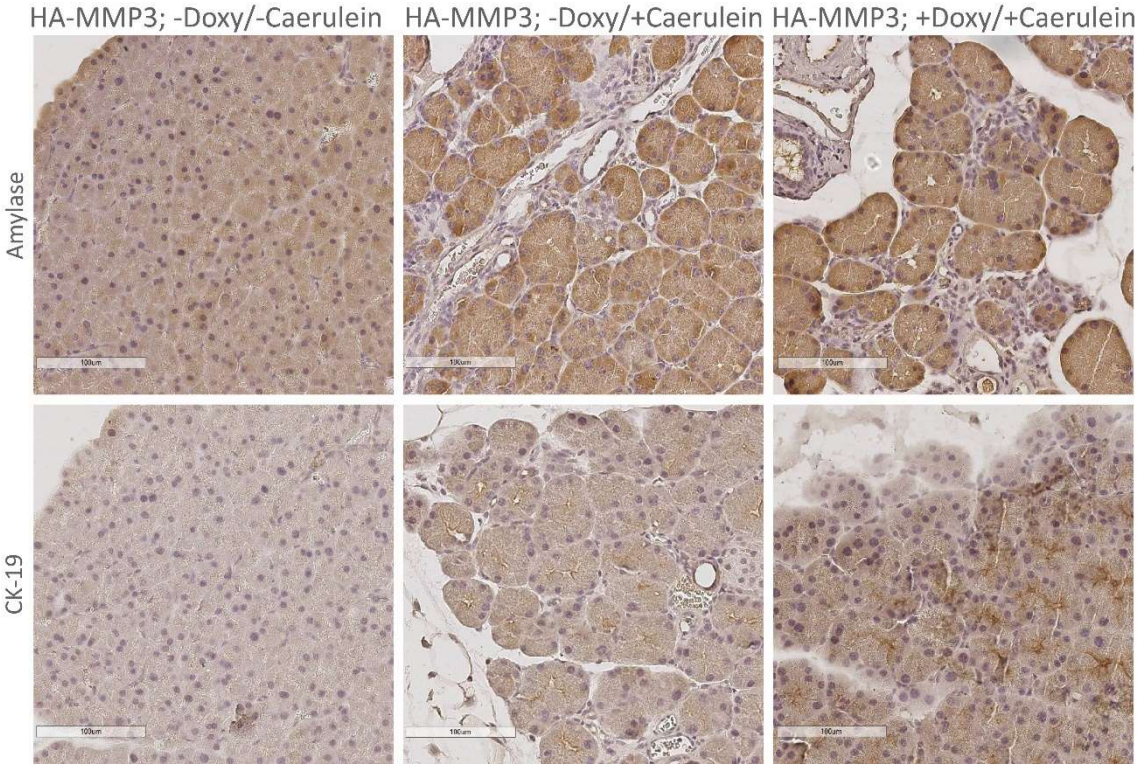

Figure 17; Amylase and CK19 in rtTA-Ela1/tet-HA-MMP3/tet-KRas mice after 5 months of treatment
Representative images of Amylase and CK19 staining in tissue from HA-MMP3 mice. Scale bar represents 100µm.

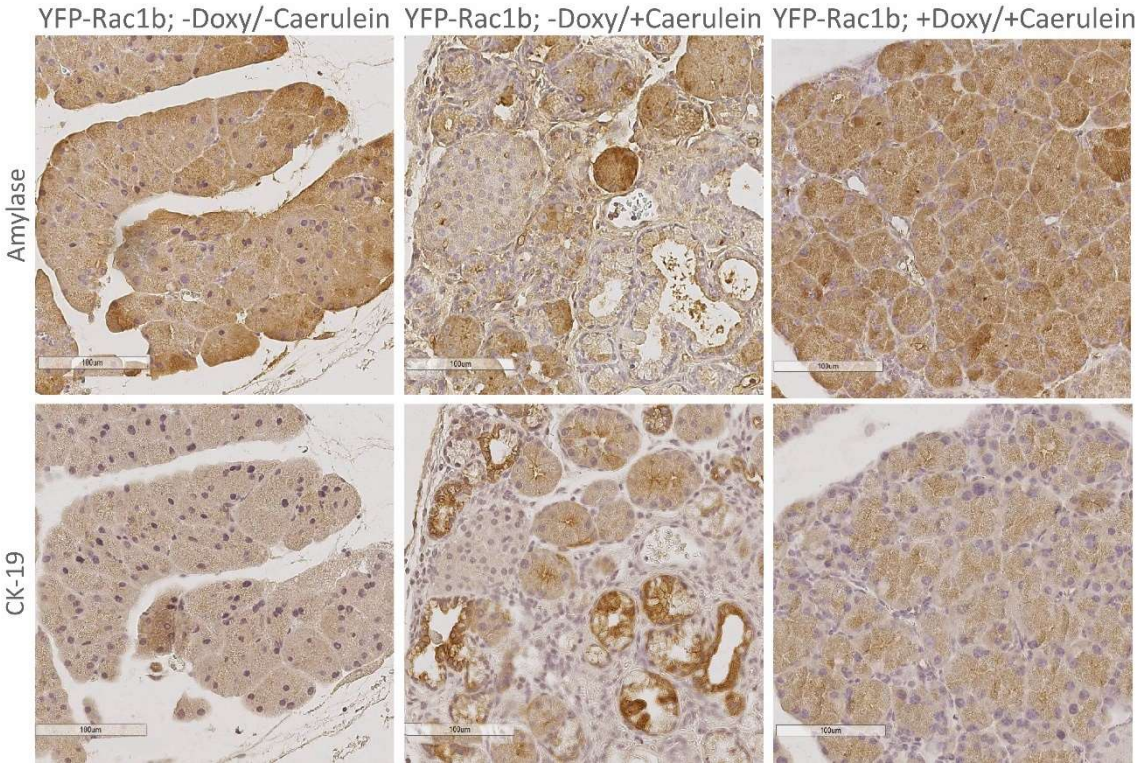

Figure 18; Amylase and CK19 in rtTA-Ela1/tet-YFP-Rac1b/tet-KRas mice after 5 months of treatment
Representative images of Amylase and CK19 staining in tissue from YFP-Rac1b mice. Scale bar represents 100µm.

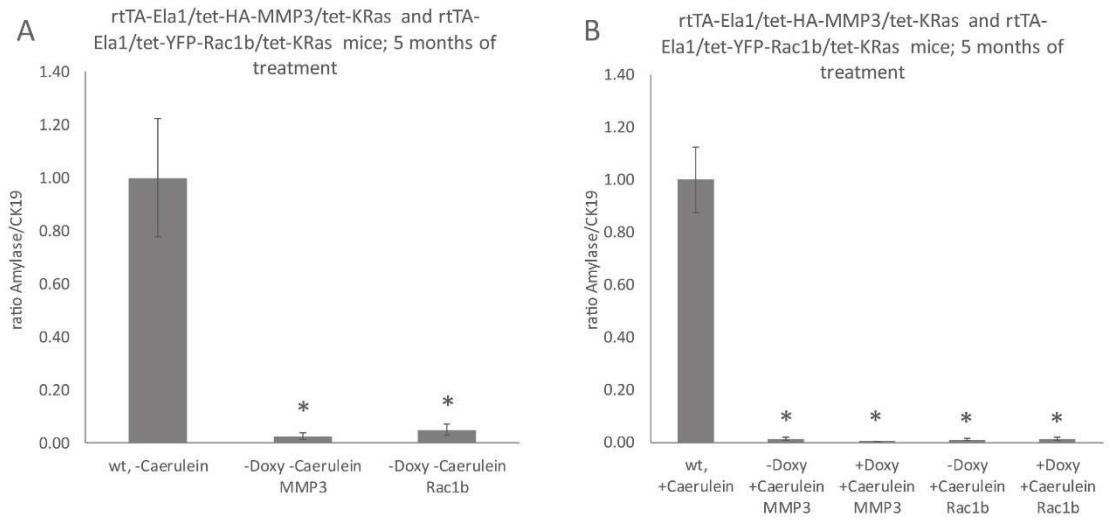

Figure 19; Ratio of Amylase to CK19 in rtTA-Ela1/tet-HA-MMP3/tet-KRas and rtTA-Ela1/tet-YFP-Rac1b/tet-KRas mice after 5 months of treatment

A) rtTA-Ela1/tet-HA-MMP3/tet-KRas and rtTA-Ela1/tet-YFP-Rac1b/tet-KRas mice were treated without Caerulein and fed without Doxycycline. Wild type mice treated without Caerulein were used as control group.

B) rtTA-Ela1/tet-HA-MMP3/tet-KRas and rtTA-Ela1/tet-YFP-Rac1b/tet-KRas mice were treated with Caerulein and fed with Doxycycline. Wild type mice treated without Caerulein were used as control group.

The expression of Amylase and CK19 was normalized to RPLP0 and the ratio from both expression levels was generated. * symbolizes significance ($p \leq 0.05$)

4.2.4. Proliferation potential depends on inflammation and transgene activation

Ki67 is nuclear protein that is well known as a proliferation marker. Due to its association with active cell cycle phases (G_1, S, G_2, M phase) (Gerdes et al. 1983) its nuclear localization varies during the cell cycle in a phosphorylation status-dependent manner (MacCallum & Hall 1999). The Ki67 staining was performed by Dr. Ramaswamy (Institute of Pathology; Universitätsklinikum Marburg). Positively stained cells or nuclei, respectively, were scored in proportion to all hematoxylin-stained nuclei.

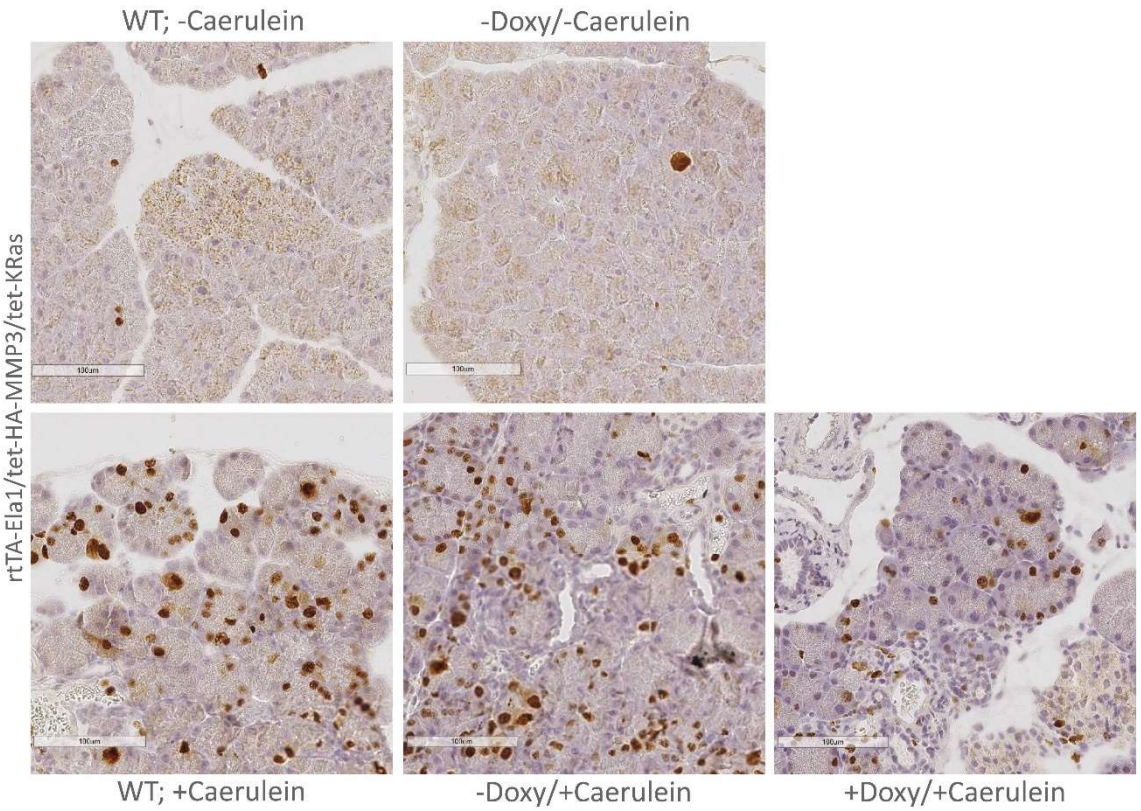

Figure 20; Ki67 staining in rtTA-Ela1/tet-HA-MMP3/tet-KRas mice after 5 months of treatment
Representative staining of Ki67 in pancreatic tissue from rtTA-Ela1/tet-HA-MMP3/tet-KRas mice after 5 months of treatment with or without Caerulein and Doxycycline. Scale bar represents 100µm.

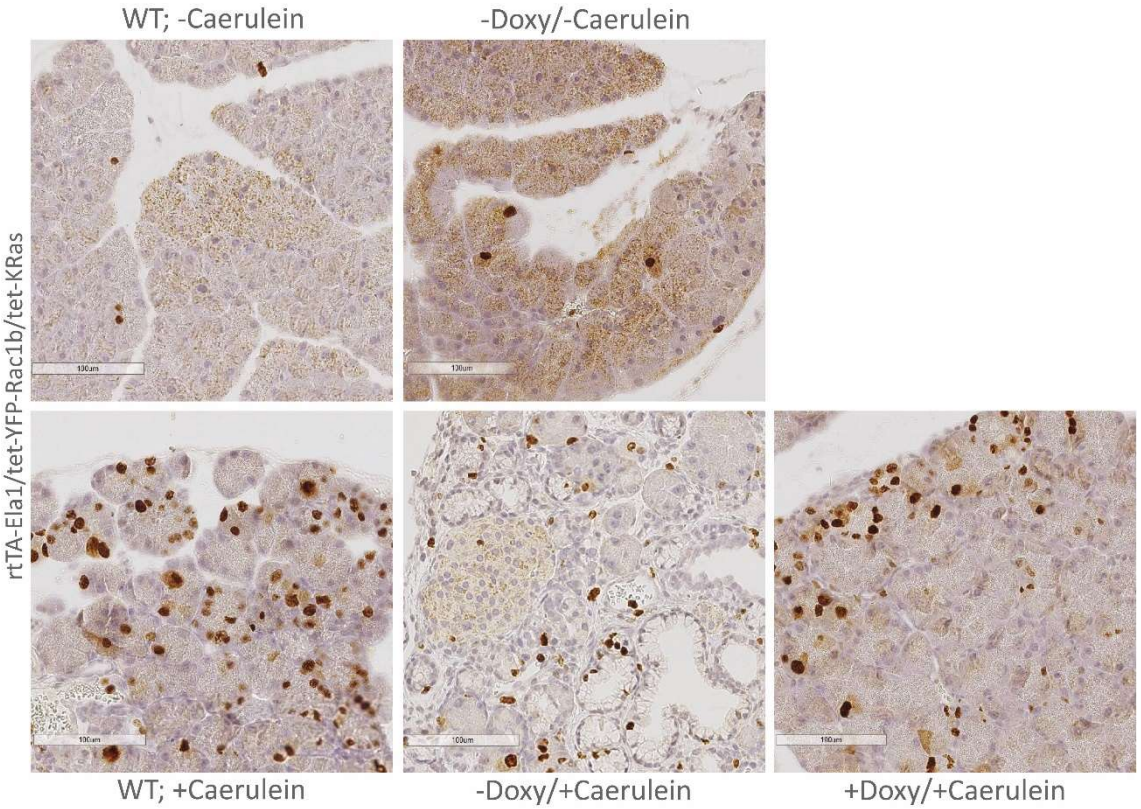

Figure 21; Ki67 staining in rtTA-Ela1/tet-YFP-Rac1b/tet-KRas mice after 5 months of treatment
Representative staining of Ki67 in pancreatic tissue from rtTA-Ela1/tet-YFP-Rac1b/tet-KRas mice after 5 months of treatment with or without Caerulein and Doxycycline. Scale bar represents 100µm.

In pancreatic tissue from rtTa-Ela1/tet-HA-MMP3/tet-KRas (Figure 22A) and rtTa-Ela1/tet-YFP-Rac1b/tet-KRas (Figure 22B) mice treated without Doxycycline and without Caerulein, more Ki67 positive cells (2.16% and 2.12%) were found than in tissue from untreated wild type mice (0.61%). The Ki67 staining in mice with activated transgene, but without chronic inflammation was found mainly at the nucleus, but also punctually located in the cytoplasm. This pattern was found also in wild type mice (Figure 20 and Figure 21 upper panel). In wild type mice treated with Caerulein, the ratio of Ki67 positive cells was elevated up to 25.39% and Ki67 was located at the nucleus (Figure 20 and Figure 21 lower panel, left). Transgenic mice treated without Doxycycline and with Caerulein (activated transgene, chronic pancreatitis) showed with 28.65% (HA-MMP3; Figure 22A) and 22.26% (YFP-Rac1b; Figure 22B) the highest percentage of Ki67 positive cells, and Ki67 was localized at the nucleus (Figure 20 and Figure 21). The same localization was found in tissue from mice treated with Doxycycline and Caerulein (inactivated transgene, chronic pancreatitis). In rtTa-Ela1/tet-HA-MMP3/tet-KRas mice (Figure 22A) the number of positive cells was calculated to be 16.56% and in rtTa-Ela1/tet-YFP-Rac1b/tet-KRas mice (Figure 22B) the percentage of Ki67 positive cells was 12.68%. In summary, these results show that the number of Ki67 positive cells mainly depends on the existence of chronic pancreatitis and is only partially influenced by MMP3 or Rac1b overexpression. The number of

proliferating and therefore Ki67 expressing cells seem to be more affected by MMP3 overexpression than by Rac1b overexpression. The localization of Ki67 only depends on the inflammatory status of surrounding tissue and not on the activation of MMP3 or Rac1b overexpression.

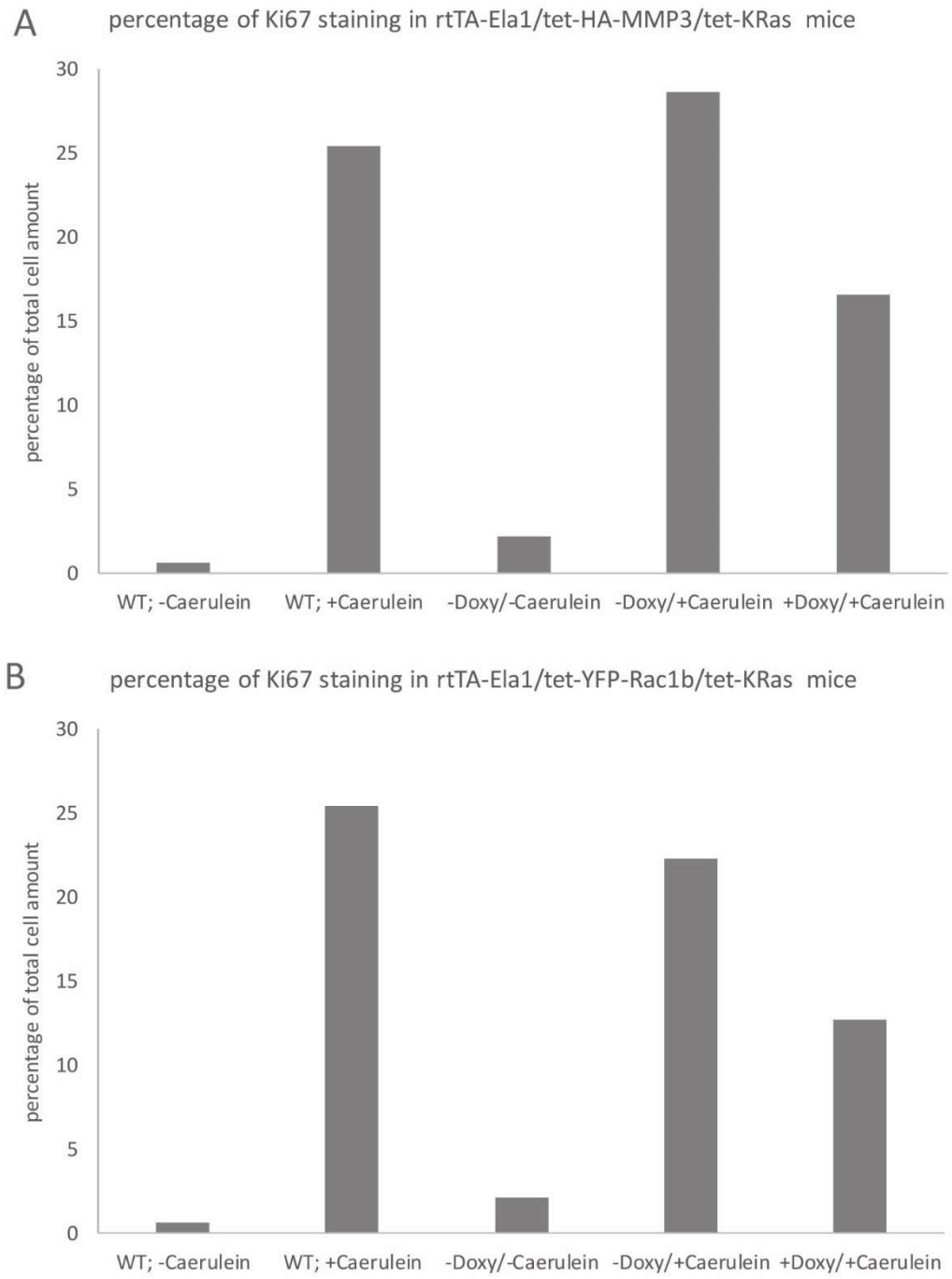

Figure 22; Percentage of Ki67 positive cells in triple transgenic mice

Pancreatic tissue from rtTA-Ela1/tet-HA-MMP3/tet-KRas and rtTA-Ela1/tet-YFP-Rac1b/tet-KRas mice was stained for Ki67. The positive cells were counted per field of view and their percentage of all pancreatic cells was calculated.

4.2.5. MMP3 activation did not show an influence on EMT markers whereas Rac1b does

For the investigation of typical EMT markers histological staining and RT-qPCR were performed. Staining of E-cadherin as a typical epithelial marker and of SMA as typical mesenchymal marker were performed as described under 3.14.2.

The pancreata of wild type mice treated without Caerulein (WT; -Caerulein) showed the regular structure of healthy pancreatic tissue and E-cadherin could be found along all cell-cell contacts. Compared to the staining of blood vessels, SMA was weaklier stained in pancreatic cells (Figure 23 and Figure 24). A different staining pattern was found in wild type mice treated with Caerulein (WT; +Caerulein). The homogenous structure of the pancreas was lost and replaced by ducts and connective tissue. Here, E-cadherin was found in only a few cells and at the inner cell-cell-contacts of the ducts. SMA staining was much weaker in pancreatic tissue than in blood vessels (Figure 23 and Figure 24). In untreated rtTA-Ela1/tet-HA-MMP3/tet-KRas mice fed without Doxycycline (-/-) the staining pattern of E-cadherin and SMA mimics the staining pattern in wild type mice without Caerulein treatment (Figure 23). This implies that the activation of MMP3 had no influence on the expression of typical EMT markers when there is no inflammatory background. The same seems to be true when chronic pancreatitis is present. The staining pattern of E-cadherin and SMA in tissue from HA-MMP3 mice with or without activated MMP3 and treated with Caerulein (-/+ and +/+) did not differ from Caerulein-treated wild type mice (Figure 23). Only the degree of chronic pancreatitis was influenced as described before. Therefore, the SMA staining was a bit higher in HA-MMP3 mice with inactivated MMP3 that also show a more distinct pancreatitis (Figure 23). The E-cadherin staining in rtTA-Ela1/tet-YFP-Rac1b/tet-KRas mice fed without Doxycycline and without Caerulein (-/-), was found along all cell-cell contacts as it was seen in untreated wild type mice. The SMA staining was comparable to that of blood vessels found in this section (Figure 24). YFP-Rac1b mice fed without Doxycycline and treated with Caerulein (-/+) presented a stronger chronic pancreatitis than YFP-Rac1b mice with inactivated Rac1b (+/+). In addition, E-cadherin was found in -/+ Rac1b mice at the inner cell-cell-contacts of the ducts, whereas +/+ Rac1b mice showed an E-cadherin staining pattern similar to wild type mice. The ducts of these mice presented a SMA staining at the outer borders (Figure 24). This is evidence for the occurrence of EMT in the pancreatic tissue of YFP-Rac1b mice with activated transgene on the background of chronic inflammation and ADM. The SMA staining in +/+ Rac1b mice was as weak as in wild type mice treated with Caerulein. In summary, the results show that MMP3 seems not to influence the EMT machinery, whereas Rac1b activation on the background of inflammation influences the expression of typical EMT markers in cells undergoing ADM.

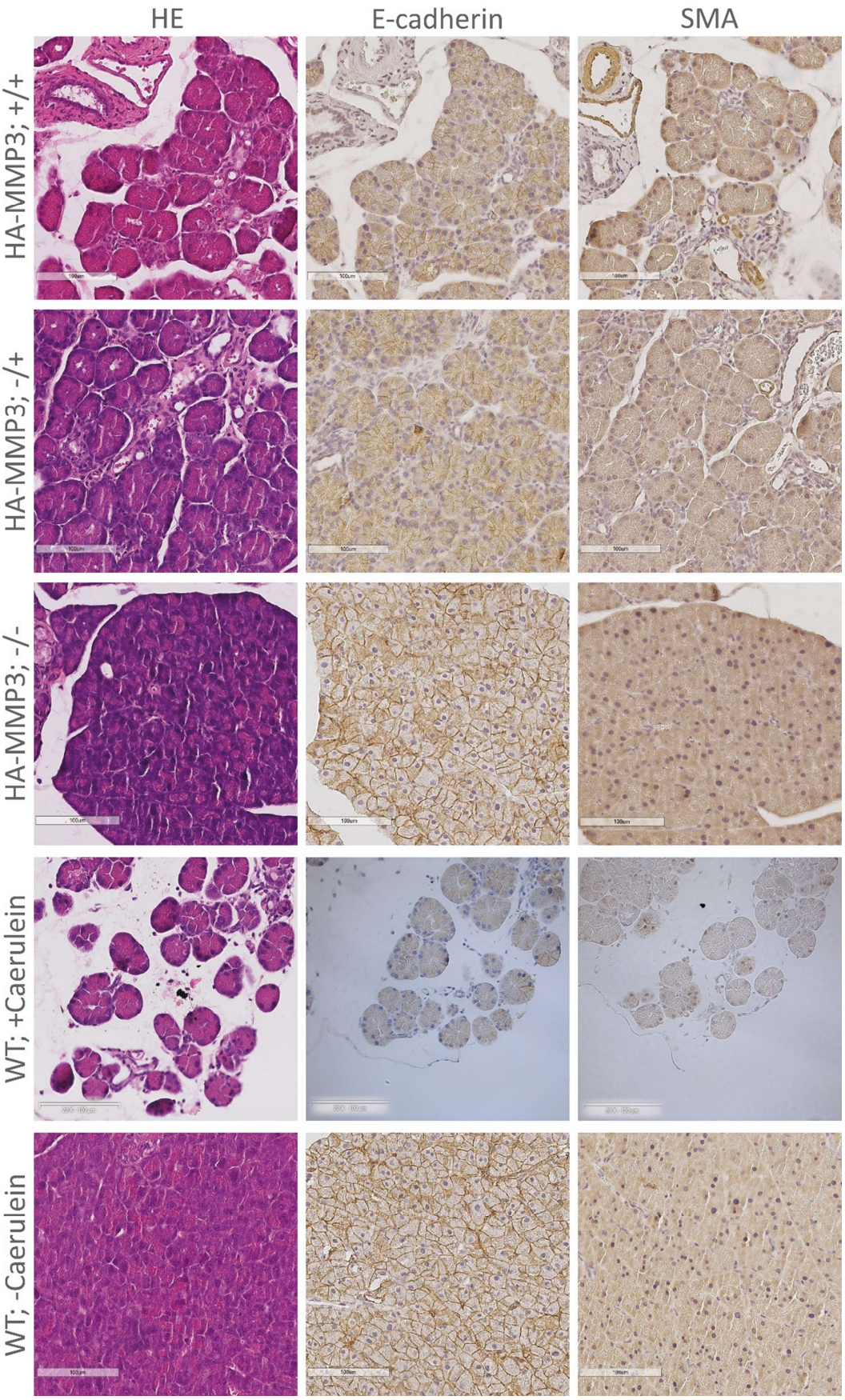

Figure 23; E-cadherin and SMA staining in rtTA-Ela/tet-HA-MMP3/tet-KRas mice after 5 months of treatment
Representative images of pancreatic tissue from rtTA-Ela1/tet-HA-MMP3/tet-KRas mice after 5 months of treatment with or without Caerulein and Doxycycline. Tissue sections were stained with HE and for E-cadherin and SMA according to described protocols. Scale bar represents 100µm.

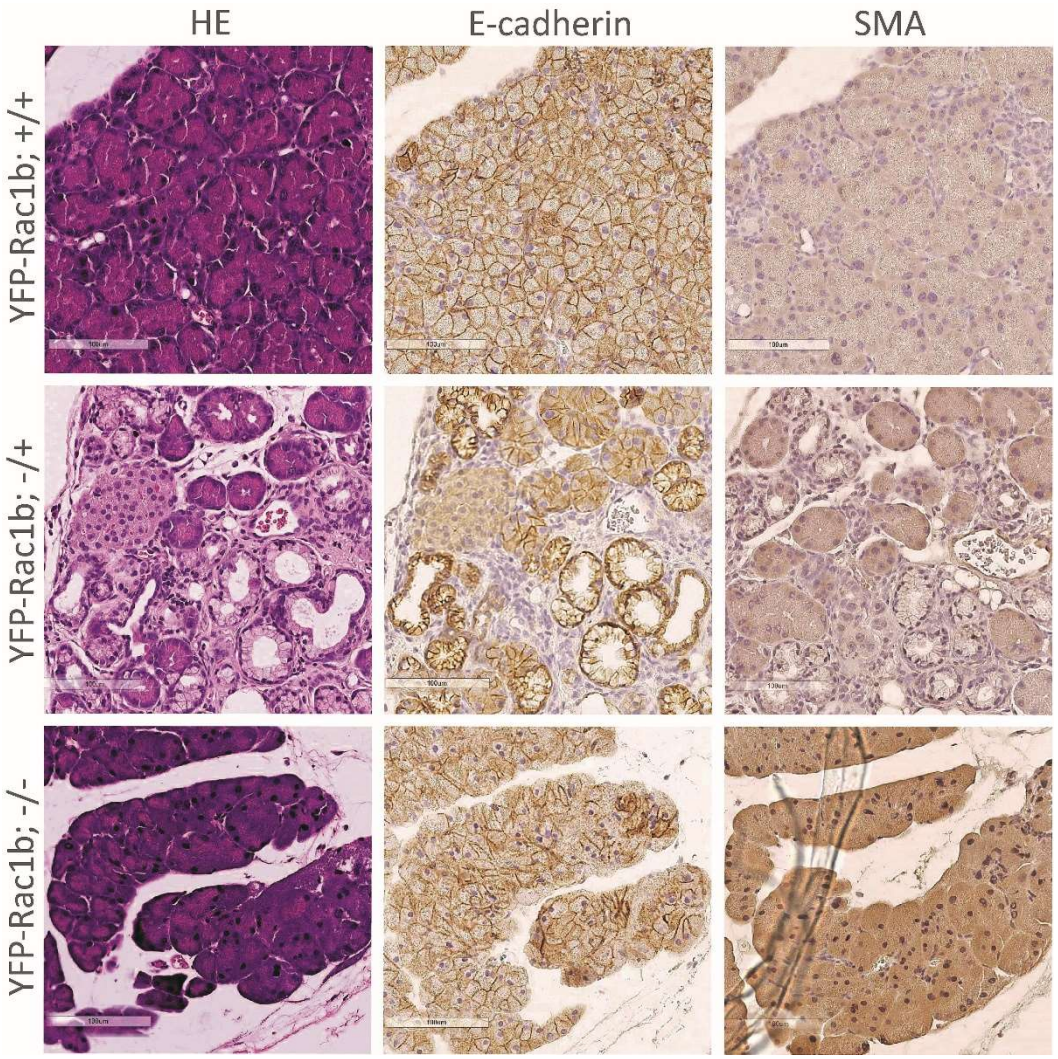

Figure 24; E-cadherin and SMA staining in rtTA-Ela/tet-YFP-Rac1b/tet-KRas mice after 5 months of treatment
Representative images of pancreatic tissue from rtTA-Ela1/tet-YFP-Rac1b/tet-KRas mice after 5 months of treatment with or without Caerulein and Doxycycline. The same wild type stainings as show in Figure 25 can be used as control. Tissue sections were stained with HE and for E-cadherin and SMA according to described protocols. Scale bar represents 100µm.

4.2.6. Transgene activation influences EMT marker expression other than expected

Although we had problems by providing the evidence for activation of HA-MMP3, we could prove the activation of YFP-Rac1b expression and the induction of chronic pancreatitis by Caerulein. Therefore, the expression levels of E-cadherin and Vimentin were investigated by RT-qPCR to determine if their levels were influenced by the potential activation of HA-MMP3 and YFP-Rac1b.

The expression levels of E-cadherin and Vimentin in rtTA-Ela1/tet-HA-MMP3/tet-KRas mice fed without Doxycycline, but without chronic pancreatitis (- Caerulein), showed a typical epithelial pattern. The level of E-cadherin was doubled compared to wild type mice, whereas that of

Vimentin was decreased (Figure 25A). When the mice were treated with Caerulein and developed chronic pancreatitis (Figure 25B), the expression levels of E-cadherin were elevated by 5.5-fold and 2-fold compared to wild type mice treated with Caerulein. Again, the expression of Vimentin was very low (0.02 and 0.01) and it seemed to be independent of the transgene. These results go along with the potentially missing transgene activation.

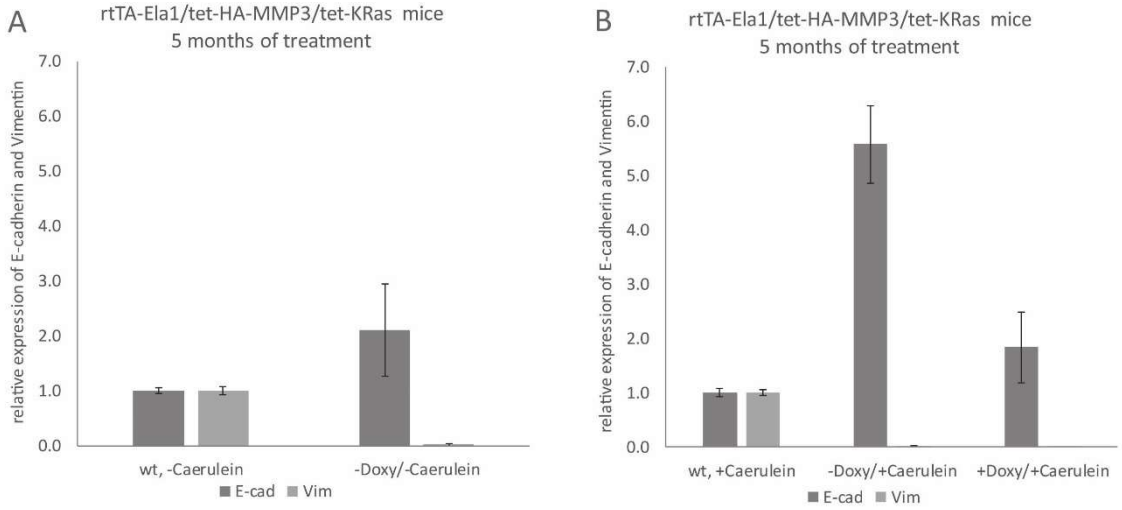

Figure 25; Expression of E-cadherin and Vimentin in rtTA-Ela1/tet-HA-MMP3/tet-KRas mice after 5 months of treatment

A) rtTA-Ela1/tet-HA-MMP3/tet-KRas mice were treated with Caerulein and fed without Doxycycline. Wild type mice treated without Caerulein were used as control group.

B) rtTA-Ela1/tet-HA-MMP3/tet-KRas mice were not treated with Caerulein and fed without Doxycycline. Wild type mice treated without Caerulein were used as control group.

The expression of E-cadherin and Vimentin was normalized to RPLP0.

The expression of E-cadherin and Vimentin in rtTA-Ela1/tet-YFP-Rac1b/tet-KRas mice is shown in Figure 26. In summary, the results were the same as in rtTA-Ela1/tet-HA-MMP3/tet-KRas mice. The E-cadherin expression was elevated independent of chronic pancreatitis and YFP-Rac1b activation. Just the level of elevation differs from 4fold (-Doxy/+Caerulein) over 5.5fold (-Doxy/-Caerulein) to 7.3fold (+Doxy/+Caerulein). The Vimentin expression is low in all three cases, which indicates that no EMT had taken place after YFP-Rac1b activation. In summary, the results show that EMT is independent of the activation of HA-MMP3 or YFP-Rac1b and the

presence or absence of chronic pancreatitis and PanINs. Other than expected, EMT seems to take place only in cancer and not in transforming tissue.

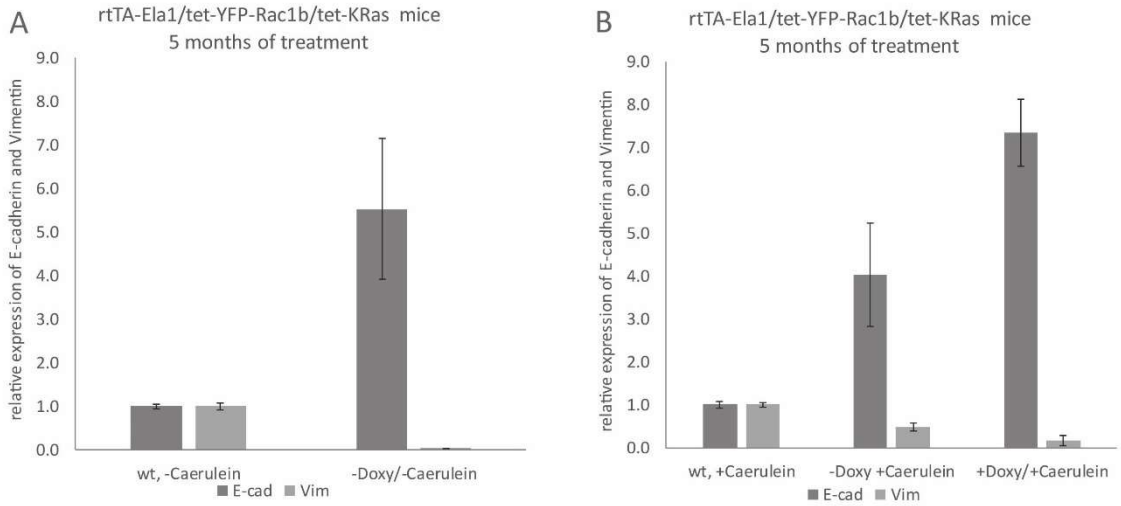

Figure 26; Expression of E-cadherin and Vimentin in rtTA-Ela1/tet-YFP-Rac1b/tet-KRas mice after 5 months of treatment

A) rtTA-Ela1/tet-YFP-Rac1b/tet-KRas mice were treated with Caerulein and fed without Doxycycline. Wild type mice treated without Caerulein were used as control group.

B) rtTA-Ela1/tet-YFP-Rac1b/tet-KRas mice were not treated with Caerulein and fed without Doxycycline. Wild type mice treated without Caerulein were used as control group.

The expression of E-cadherin and Vimentin was investigated by RT-qPCR and normalized to RPLP0.

5. Discussion

The activation of the EMT program has been proposed to be a critical mechanism during the multiple stages of tumor progression for the acquisition of malignant phenotypes that are associated with cell migration and invasiveness (Thiery 2002; Huber et al. 2005). It has been shown that cells undergoing EMT are mainly seen at the invasive tumor front and these are the cells entering the invasion-metastasis cascade, i.e. intravasation and transport through the circulation (Thiery 2002; Thiery et al. 2009). The reverse process, MET, is necessary for cells to form secondary tumors after extravasation (Zeisberg et al. 2005). Although the full spectrum of signaling agents contributing to EMT remain unclear, it is known that signals transmitted from tumor stroma, such as TGFβ, appear to be responsible for the induction of EMT-inducing transcription factors (Thiery 2002; Song 2007). TGFβ seems to be the most important soluble EMT-inducer, but it depends on a complex network of other pathways, such as the SMAD4/STAT3 (Zhao et al. 2008) and the MAPK/ERK (Ellenrieder et al. 2001; Maier, Wirth, et al. 2010) signaling pathways. Additionally, there is evidence that TGFβ-induced EMT requires the activation of NFκB (Maier, Schmidt-Strassburger, et al. 2010). In contrast to other studies, which showed Rac1b to promote EMT (Radisky et al. 2005; Stallings-Mann et al. 2012; Waldmann et al. n.d.) Ungefroren et. al. showed that Rac1b antagonizes TGFβ1 induced cell migration by suppressing the phosphorylation, and therefore, the function of SMAD3. A suppression of SMAD3 not only results in a reduced migration potential, but also may cause a disruption of SMAD4-mediated EMT signaling (Ungefroren et al. 2014).

Based on gene array data, it was found that MMP3 was not detectable in pancreatic cancer cells (Tjomsland et al. 2016), a fact that could be confirmed with the pancreatic cancer cell lines that were used for this thesis. However, it was shown that the treatment of mouse cells in culture and pancreatic cell lines (8988T, Panc1) with MMP3 is directly responsible for the induction of EMT (Lochter et al. 1997; Mehner et al. 2014) and that in mammary epithelial cells treated with MMP3 this induction is associated with the loss of E-cadherin (Radisky et al. 2005). Additionally, it was shown that MMP3 induces EMT through a cascade that involves the activation of Rac1b and the production of ROS (Radisky et al. 2005). We found that the treatment with recombinant MMP3 elevated the expression of Rac1b in the pancreatic cancer cell line S2-007, whereas MiaPaCa cells showed a slightly reduction of Rac1b expression after treatment with recombinant MMP3. Also, the inhomogeneous results for EMT marker expression in S2-007 and MiaPaCa cells showed that the investigation of EMT is heavily depending on the experimental context.

It was described that tissue stiffness has positive effects on EMT induction and that microenvironment with physiological normal compliance, as found with Matrigel, acts in a protective manner on EMT-induction by MMP3, whereas the TGFβ-mediated EMT is not

affected by substratum rigidity (Lee et al. 2012). We could not confirm that AdRac1b induces EMT on stiff (plastic), but not on soft (Matrigel) substrates as described by Lee et al. in 2012. Rather the AdRac1b treatment of S2-007 cells cultured on Matrigel resulted in a highly-elevated expression of Vimentin compared to AdGFP-treated cells. Although the results did show a high fluctuation, AdRac1b treatment resulted in 10fold (Plastic) and 10 000fold higher expression compared to the treatment with AdTGFβ or AdMMP3. Other studies showed that, to produce ROS, a localization of Rac1b at the membrane is essential. At the cell membrane, it can interact with components of the membrane-associated enzyme NADPH oxidase to promote ROS production and EMT. The intracellular localization of Rac1b depends on α5-integrin and on α6-integrin that is expressed in cells growing on laminin rich ECM, such as Matrigel (Chen et al. 2013). On soft, laminin rich substrates α6-integrin can keep Rac1b localized in the cytoplasm and there it delocalizes to the cell periphery and the membrane ruffles. This means, that Rac1b is not able to interact with components of the NADPH enzyme complex to produce Ros and to induce EMT (Lee et al. 2012). It is possible that the overexpression of Rac1b, mediated by adenoviral treatment, might overcome the effect of α6-integrin in cells cultured on Matrigel because of a remarkably high number of molecules and therefore, Rac1b can bind at the membrane and induce the EMT machinery, which results in a high Vimentin and a lower E-cadherin expression. Both integrins, α5 and α6, are also responsible for the EMT induction by MMP3. The mechanisms are not completely understood, but it was shown that α6-integrin transmits signals from laminin rich ECM to block EMT, but is not sufficient to inhibit EMT in general. On the other side α5-integrin is necessary for the MMP3-induced EMT in standard conditions (Chen et al. 2013).

The lower induction of EMT after AdMMP3 treatment can be explained by the fact that EMT induction depends on cell spreading which is a consequence of MMP3-mediated Rac1b induction (Nelson et al. 2008). Induction of EMT by MMP3/Rac1b depends on the density in which cells were cultured. It might be possible that especially S2-007 cells have overgrown, which means that the ability to change cell shape was limited, but it is required for the MMP3-induced EMT and seem to be important for EMT promotion by ROS production (Nelson et al. 2008). Again, the investigations seem to be prone to highly constant experimental settings, such as cell density, matrix, and the kind of overexpressed protein. This might influence the occurrence of EMT during different experiments and result in inhomogeneous findings. It is suspected that cancer cells do not undergo EMT completely, but only partially, thereby acquiring new mesenchymal characteristics while maintaining some epithelial characteristics (Hanahan & Weinberg 2011). In the case of MiaPaCa cells, which was defined as a poorly differentiated cell line having lost the ability to form cell-cell contacts (Sipos et al. 2003), a naturally mesenchymal

behavior influences the results in a EMT-positive manner. This means that the S2-007 cells might exhibit epithelial-specific morphology and expression of epithelial markers, such as CK19 and E-cadherin, but also show expression of mesenchymal markers, such as Vimentin or α-SMA. These cells represent the intermediate stages of EMT (Kalluri & Weinberg 2009), whereas MiaPaCa cells represent a mesenchymal cell line with unmutated SMAD4 (Sipos et al. 2003) and therefore functional TGFβ signaling.

It is not clear in which way the different localization patterns of Vimentin influences the occurrence of EMT, but it was reported that the localization of Vimentin at the nuclear envelope is accompanied by an interaction with Lamin B to set contacts between the karyoskeleton and the plasma membrane skeleton (Georgatos & Blobel 1987). Additionally, it was shown that nuclear localized Vimentin can induce DNA-mediated events and that it can act as a regulator of transcription (Traub & Shoeman 1994; Mergui et al. 2010). Other studies described an interaction of Vimentin with cytoplasmic proteins, such as ERK, AKT1, and Scrib and that Vimentin localized at the plasma membrane can be regulated by TGFβ (Perlson et al. 2006; Phua et al. 2009; Yin et al. 2006). The influence of MMP3 and Rac1b overexpression to localization of Vimentin in S2-007 and MiaPaCa cells, the relationship to EMT occurrence, as well as the influence of MMP3 and Rac1b on other EMT-associated molecules should be investigated in more detail in further *in vitro* experiments. Then it would be advising to adjust the experimental settings of this very complex system for its dependency to kind and pulse of stimulation even more.

In a study similar to the present one, it was shown that the co-expression of MMP3 and KRas in transgenic mice lead to alterations in acinar cells and the recruitment of immune cells, which primes a stromal microenvironment (Mehner et al. 2014). In the context of these findings I used a related mouse model and induced chronic pancreatitis to investigate whether the co-expression of MMP3 and mutated KRas is also sufficient to cause pancreatic cancer on the background of already existing inflammation. We found that after 5 months of treatment the alterations of acinar cells arose to ADM, but neither PanINs nor PDAC were detectable. In some other studies, mouse models expressing activated mutants of KRas at endogenous levels, develop precursor lesions, such as higher grade PanINs, which either did not progress to PDAC or even within 1-2 years (Hingorani et al. 2003; Ji et al. 2009). If LSL-KRas/Ela-CreERT mice were crossed with a conditional p53 deletion mice, most of the offspring develop PDAC within 6 month (Ji et al. 2009). Similar observations were made by Guerra et al. where mice develop moderately to poorly differentiated PDACs only, when they carry both $KRas^{G12V}$ and mutant p53. They summarize from several experiments that mutated KRas alone has just a few consequences

for adult acinar cells (Guerra et al. 2007). Mutated KRas needs various stimuli, such as TGFα to mediate inflammation (Siveke et al. 2007) without external stimuli, such as Caerulein, which we were using to promote chronic pancreatitis. Also, further genetic alterations beyond KRas mutation are required for development of pancreatic lesions and PDAC (Guerra et al. 2007; Logsdon & Ji 2009). Not having used additional p53 or other deletions, might explain why the CP of my transgenic mice did not develop into PanINs or PDAC. Additionally, we made our investigations after a comparatively short period of 5 months, which could explain the lack of PanINs and PDAC development in MMP3 mouse models. Also, for my Rac1b expressing mouse model, it might be better to investigate over an extended time period, as it was described by Stallings-Mann et al. in 2012 that the development of lung cancer in transgenic mice under Rac1b overexpression occurs after 60 weeks.

The next step in studying the influence of MMP3 and Rac1b during development and progression of pancreatic cancer was the investigation of EMT markers after transgene activation. The results from immunohistochemistry and RT-qPCR suggest that MMP3 did not have an influence on the EMT machinery in vivo. Complicating, the activation of HA-MMP3 was not clearly detectable. That means, a missing EMT effect could be caused by a missing transgene activation and has no molecular reasons. But why did the activation of Rac1b expression show evidence for EMT in immunohistochemistry, but not in RT-qPCR? Since EMT is a transient event and is reversible, we suggest that EMT mainly occurs in transforming tissue, such as PanINs or in tumor cells, neither of which did I detected.

In summary, my results suggest that the direct influence of MMP3 is not as high as expected and seems to depend on some other factors, which were not investigated here. For further *in vitro* studies, it might be necessary to focus on the TGFβ and NFκB signaling pathways and their relationship to MMP3 and Rac1b. Especially for Rac1b, it is controversial whether or not it is an activator for NFκB (Matos et al. 2003; Matos & Jordan 2005; Singh et al. 2004). Also, Rac1b was shown to interact with TGFβ itself or components of the TGFβ-induced EMT pathway, such as SMAD3 in different ways (Ungefroren et al. 2014). A mouse model containing tetracycline controlled TGFβ might be helpful for similar investigations performed *in vivo*. Additionally, it will be required to investigate the reciprocal effect of KRas on MMP3/Rac1b-mediated EMT on the background of chronic pancreatitis for a longer period.

References

Agnihotri, R. et al., 2001. Osteopontin, a Novel Substrate for Matrix Metalloproteinase-3 (Stromelysin-1) and Matrix Metalloproteinase-7 (Matrilysin). *Journal of Biological Chemistry*, 276(30), pp.28261–28267.

Alexander, C.M. et al., 1996. Expression and function of matrix metalloproteinases and their inhibitors at the maternal-embryonic boundary during mouse embryo implantation. *Development*, 1736, pp.1723–1736.

Almoguera, C. et al., 1988. Most human carcinomas of the exocrine pancreas contain mutant c-K-ras genes. *Cell*, 53(4), pp.549–54. Available at: http://www.ncbi.nlm.nih.gov/pubmed/2453289 [Accessed April 6, 2016].

American Cancer Society, 2013. Cancer Facts & Figures 2013. *Cancer Facts & Figures*, pp.1–9.

American Cancer Society, 2016. Cancer Facts & Figures 2016. *Cancer Facts & Figures*, pp.1–9.

Aune, D. et al., 2012. Body mass index, abdominal fatness and pancreatic cancer risk: a systematic review and non-linear dose-response meta-analysis of prospective studies. *Annals of oncology*, 23(4), pp.843–52. Available at: http://www.ncbi.nlm.nih.gov/pubmed/21890910 [Accessed March 20, 2014].

Balkwill, F. & Mantovani, A., 2001. Inflammation and cancer: back to Virchow? *Lancet*, 357(9255), pp.539–45. Available at: http://www.ncbi.nlm.nih.gov/pubmed/11229684 [Accessed February 12, 2015].

Barrallo-Gimeno, A. & Nieto, A.M., 2005. The Snail genes as inducers of cell movement and survival: implications in development and cancer. *Development*, 132(14), pp.3151–3161.

Bartsch, D.K. et al., 2002. CDKN2A germline mutations in familial pancreatic cancer. *Annals of surgery*, 236(6), pp.730–7. Available at: http://www.pubmedcentral.nih.gov/articlerender.fcgi?artid=1422639&tool=pmcentrez&rendertype=abstract.

Berrington de Gonzalez, A., Sweetland, S. & Spencer, E., 2003. A meta-analysis of obesity and the risk of pancreatic cancer. *British Journal of Cancer*, 89(3), pp.519–23. Available at: http://www.pubmedcentral.nih.gov/articlerender.fcgi?artid=2394383&tool=pmcentrez&rendertype=abstract [Accessed March 26, 2014].

Berx, G. & van Roy, F., 2009. Involvement of members of the cadherin superfamily in cancer.

Cold Spring Harbor Perspectives in Biology, 1(6).

Bierie, B. & Moses, H.L., 2006. Tumour microenvironment: TGFbeta: the molecular Jekyll and Hyde of cancer. *Nature Reviews Cancer*, 6(7), pp.506–20. Available at: http://www.ncbi.nlm.nih.gov/pubmed/16794634 [Accessed March 13, 2016].

Blackford, A. et al., 2009. SMAD4 gene mutations are associated with poor prognosis in pancreatic cancer. *Clinical Cancer Research*, 15(14), pp.4674–4679.

Boettner, B. & Van Aelst, L., 2002. The role of Rho GTPases in disease development. *Gene*, 286(2), pp.155–174.

Bramhall, S.R. et al., 1996. Expression of collagenase (MMP2), stromelysin (MMP3) and tissue inhibitor of the metalloproteinases (TIMP1) in pancreatic and ampullary disease. *British Journal of Cancer*, 73(8), pp.972–8. Available at: http://www.pubmedcentral.nih.gov/articlerender.fcgi?artid=2075817&tool=pmcentrez&rendertype=abstract.

Brentnall, T.A. et al., 1995. Microsatellite instability and K-ras mutations associated with pancreatic adenocarcinoma and pancreatitis. *Cancer Research*, 55(19), pp.4264–7. Available at: http://cancerres.aacrjournals.org/content/55/19/4264.short%5Cnhttp://www.ncbi.nlm.nih.gov/pubmed/7671233.

Chen, Q.K. et al., 2013. Extracellular matrix proteins regulate epithelial-mesenchymal transition in mammary epithelial cells. *Differentiation; research in biological diversity*, 86(3), pp.126–32. Available at: http://www.pubmedcentral.nih.gov/articlerender.fcgi?artid=3762919&tool=pmcentrez&rendertype=abstract.

Couch, F.J. et al., 2007. The prevalence of BRCA2 mutations in familial pancreatic cancer. *Cancer Epidemiology, Biomarkers & Prevention*, 16(2), pp.342–6. Available at: http://www.ncbi.nlm.nih.gov/pubmed/17301269.

Deramaudt, T. & Rustgi, A.K., 2005. Mutant KRAS in the initiation of pancreatic cancer. *Biochimica et biophysica acta*, 1756(2), pp.97–101. Available at: http://www.ncbi.nlm.nih.gov/pubmed/16169155 [Accessed August 6, 2016].

Egeblad, M. & Werb, Z., 2002. New functions for the matrix metalloproteinases in cancer progression. *Nature Reviews Cancer*, 2(3), pp.161–74. Available at:

http://www.ncbi.nlm.nih.gov/pubmed/11990853 [Accessed August 24, 2016].

Ekbom, A. et al., 1994. Pancreatitis and pancreatic cancer: a population-based study. *Journal of the National Cancer Institute*, 86(8), pp.625–7. Available at: http://www.ncbi.nlm.nih.gov/pubmed/8145277 [Accessed August 6, 2016].

El-Serag, H.B. et al., 2009. Risk of hepatobiliary and pancreatic cancers after hepatitis C virus infection: A population-based study of U.S. veterans. *Hepatology*, 49(1), pp.116–23. Available at: http://www.pubmedcentral.nih.gov/articlerender.fcgi?artid=2719902&tool=pmcentrez&rendertype=abstract [Accessed April 8, 2014].

Ellenrieder, V. et al., 2001. Transforming Growth Factor β1 Treatment Leads to an Epithelial-Mesenchymal Transdifferentiation of Pancreatic Cancer Cells Requiring Extracellular Signal-regulated Kinase 2 Activation. *Cancer Research*, pp.1–8.

Ferreras, M. et al., 2000. Generation and degradation of human endostatin proteins by various proteinases. *FEBS Letters*, 486(3), pp.247–251.

Fiegen, D. et al., 2004. Alternative Splicing of Rac1 Generates Rac1b, a Self-activating GTPase. *Journal of Biological Chemistry*, 279(6), pp.4743–4749.

Fujioka, S. et al., 2003. Function of nuclear factor kappaB in pancreatic cancer metastasis. *Clinical Cancer Research*, 9(1078–0432 (Print)), pp.346–354.

Georgatos, S.D. & Blobel, G., 1987. Lamin B constitutes an intermediate filament attachment site at the nuclear envelope. *Journal of Cell Biology*, 105(1), pp.117–125.

Gerdes, J. et al., 1983. Production of a mouse monoclonal antibody reactive with a human nuclear antigen associated with cell proliferation. *International journal of cancer*, 31(1), pp.13–20. Available at: http://www.ncbi.nlm.nih.gov/pubmed/6339421 [Accessed December 1, 2016].

Giehl, K. et al., 2000. TGFbeta1 represses proliferation of pancreatic carcinoma cells which correlates with Smad4-independent inhibition of ERK activation. *Oncogene*, 19(39), pp.4531–41. Available at: http://www.ncbi.nlm.nih.gov/pubmed/11002426.

Guerra, C. et al., 2007. Chronic Pancreatitis Is Essential for Induction of Pancreatic Ductal Adenocarcinoma by K-Ras Oncogenes in Adult Mice. *Cancer Cell*, 11(3), pp.291–302. Available at: http://www.ncbi.nlm.nih.gov/pubmed/17349585 [Accessed January 20,

2014].

Hahn, S.A. et al., 2003. BRCA2 germline mutations in familial pancreatic carcinoma. *Journal of the National Cancer Institute*, 95(3), pp.214–21. Available at: http://www.ncbi.nlm.nih.gov/pubmed/12569143.

Hanahan, D. & Weinberg, R.A., 2011. Hallmarks of cancer: The next generation. *Cell*, 144(5), pp.646–674.

Hashimoto, G. et al., 2002. Matrix metalloproteinases cleave connective tissue growth factor and reactivate angiogenic activity of vascular endothelial growth factor 165. *Journal of Biological Chemistry*, 277(39), pp.36288–36295.

Hassan, M.M. et al., 2008. Association between hepatitis B virus and pancreatic cancer. *Journal of Clinical Oncology*, 26(28), pp.4557–62. Available at: http://www.pubmedcentral.nih.gov/articlerender.fcgi?artid=2562875&tool=pmcentrez&rendertype=abstract [Accessed April 8, 2014].

Heuberger, J. & Birchmeier, W., 2010. Interplay of cadherin-mediated cell adhesion and canonical Wnt signaling. *Cold Spring Harbor Perspectives in Biology*, 2(2), pp.1–24.

Hingorani, S.R. et al., 2003. Preinvasive and invasive ductal pancreatic cancer and its early detection in the mouse. *Cancer Cell*, 4(6), pp.437–450.

Hordijk, P.L., 2006. Regulation of NADPH Oxidases: The Role of Rac proteins. *Circulation Research*, 98(4), pp.453–462.

Huber, M.A., Kraut, N. & Beug, H., 2005. Molecular requirements for epithelial-mesenchymal transition during tumor progression. *Current Opinion in Cell Biology*, 17(5), pp.548–58. Available at: http://www.ncbi.nlm.nih.gov/pubmed/16098727 [Accessed May 12, 2016].

Huth, J. et al., 2011. TimeLapseAnalyzer: Multi-target analysis for live-cell imaging and time-lapse microscopy. *Computer Methods and Programs in Biomedicine*, 104(2), pp.227–234.

Ikushima, H. & Miyazono, K., 2010. TGFbeta signalling: a complex web in cancer progression. *Nature Reviews Cancer*, 10(6), pp.415–24. Available at: http://www.ncbi.nlm.nih.gov/pubmed/20495575 [Accessed October 29, 2015].

Imai, K. et al., 1997. Degradation of decorin by matrix metalloproteinases: identification of the cleavage sites, kinetic analyses and transforming growth factor-beta1 release. *The Biochemical Journal*, 322 (Pt 3, pp.809–814.

Ito, A. et al., 1996. Degradation of interleukin 1beta by matrix metalloproteinases. *The Journal of Biological Chemistry*, 271(25), pp.14657–14660.

Janda, E. et al., 2002. Ras and TGFβ cooperatively regulate epithelial cell plasticity and metastasis: Dissection of Ras signaling pathways. *Journal of Cell Biology*, 156(2), pp.299–313.

Ji, B. et al., 2009. Ras Activity Levels Control the Development of Pancreatic Diseases. *Gastroenterology*, 137(3), pp.1072–1082.

Kalluri, R. & Weinberg, R. a, 2009. The basics of epithelial-mesenchymal transition. *Journal of Clinical Investigation*, 119(6), pp.1420–1428.

Kataoka, H. et al., 1999. Enhanced Tumor Growth and Invasiveness in Vivo by a Carboxyl-Terminal Fragment of ␣ 1-Proteinase Inhibitor Generated by Matrix Metalloproteinases. *American Journal of Pathology*, 154(2), pp.457–468.

Kheradmand, F. et al., 1998. Role of Rac1 and oxygen radicals in collagenase-1 expression induced by cell shape change. *Science*, 280(5365), pp.898–902. Available at: http://www.ncbi.nlm.nih.gov/pubmed/9572733 [Accessed August 26, 2016].

Koorstra, J.-B.M. et al., 2008. Pancreatic carcinogenesis. *Pancreatology*, 8(2), pp.110–25. Available at: http://www.pubmedcentral.nih.gov/articlerender.fcgi?artid=2663569&tool=pmcentrez&rendertype=abstract [Accessed February 16, 2014].

Lee, K. et al., 2012. Matrix compliance regulates Rac1b localization, NADPH oxidase assembly, and epithelial-mesenchymal transition. *Molecular Biology of the Cell*, 23(20), pp.4097–108. Available at: http://www.pubmedcentral.nih.gov/articlerender.fcgi?artid=3469523&tool=pmcentrez&rendertype=abstract.

Lee, S. et al., 2005. Processing of VEGF-A by matrix metalloproteinases regulates bioavailability and vascular patterning in tumors. *Journal of Cell Biology*, 169(4), pp.681–691.

Liu, F. et al., 2010. Feedback amplification of fibrosis through matrix stiffening and COX-2 suppression. *Journal of Cell Biology*, 190(4), pp.693–706.

Liu, P. et al., 1999. Requirement for Wnt3 in vertebrate axis formation. *Nature Genetics*, 22(4), pp.361–5. Available at: http://www.ncbi.nlm.nih.gov/pubmed/10431240 [Accessed May

22, 2016].

Lochter, A. et al., 1997. Matrix Metalloproteinase Stromelysin-1 Triggers a Cascade of Molecular Alterations That Leads to Stable Epithelial-to-Mesenchymal Conversion and a Premalignant Phenotype in Mammary Epithelial Cells. *The Journal of Cell Biology*, 139(7), pp.1861–1872.

Logsdon, C.D. & Ji, B., 2009. Ras activity in acinar cells links chronic pancreatitis and pancreatic cancer. *Clinical Gastroenterology and Hepatology*, 7, pp.40–43.

Löhr, M. et al., 2005. Frequency of K-ras mutations in pancreatic intraductal neoplasias associated with pancreatic ductal adenocarcinoma and chronic pancreatitis: a meta-analysis. *Neoplasia*, 7(1), pp.17–23. Available at: /pmc/articles/PMC1490318/?report=abstract.

Lowenfels, A.B. et al., 1993. Pancreatitis and the risk of pancreatic cancer. *New England Journal of Medicine*, 328(20), pp.1753–1759.

Lynch, H.T. et al., 2002. Phenotypic variation in eight extended CDKN2A germline mutation familial atypical multiple mole melanoma-pancreatic carcinoma-prone families: The familial atypical multiple mole melanoma-pancreatic carcinoma syndrome. *Cancer*, 94(1), pp.84–96.

MacCallum, D.E. & Hall, P.A., 1999. Biochemical characterization of pKi67 with the identification of a mitotic-specific form associated with hyperphosphorylation and altered DNA binding. *Experimental cell research*, 252(1), pp.186–98. Available at: http://www.ncbi.nlm.nih.gov/pubmed/10502411 [Accessed December 1, 2016].

Maeda, S. et al., 2002. The first stage of transforming growth factor beta1 activation is release of the large latent complex from the extracellular matrix of growth plate chondrocytes by matrix vesicle stromelysin-1 (MMP-3). *Calcified Tissue International*, 70(1), pp.54–65. Available at: http://www.ncbi.nlm.nih.gov/pubmed/11907708 [Accessed August 24, 2016].

Maier, H.J., Schmidt-Strassburger, U., et al., 2010. NF-kappaB promotes epithelial-mesenchymal transition, migration and invasion of pancreatic carcinoma cells. *Cancer Letters*, 295(2), pp.214–28. Available at: http://www.ncbi.nlm.nih.gov/pubmed/20350779 [Accessed August 8, 2016].

Maier, H.J., Wirth, T. & Beug, H., 2010. Epithelial-mesenchymal transition in pancreatic

carcinoma. *Cancers*, 2(4), pp.2058–83. Available at: http://www.pubmedcentral.nih.gov/articlerender.fcgi?artid=3840444&tool=pmcentrez&rendertype=abstract [Accessed May 13, 2015].

Maitra, A. et al., 2003. Multicomponent Analysis of the Pancreatic Adenocarcinoma Progression Model Using a Pancreatic Intraepithelial Neoplasia Tissue Microarray. *Modern Pathology*, 16(9), pp.902–912.

Maitra, A. & Hruban, R.H., 2008. Pancreatic Cancer. *Annual Review of Pathology*, 3, pp.157–188.

Matos, P., Collard, J.G. & Jordan, P., 2003. Tumor-related Alternatively Spliced Rac1b Is Not Regulated by Rho-GDP Dissociation Inhibitors and Exhibits Selective Downstream Signaling. *Journal of Biological Chemistry*, 278(50), pp.50442–50448.

Matos, P. & Jordan, P., 2005. Expression of Rac1b stimulates NF-kappaB-mediated cell survival and G1/S progression. *Experimental Cell Research*, 305(2), pp.292–9. Available at: http://www.ncbi.nlm.nih.gov/pubmed/15817154 [Accessed August 18, 2016].

McQuibban, G.A. et al., 2002. Matrix metalloproteinase processing of monocyte chemoattractant proteins generates CC chemokine receptor antagonists with anti-inflammatory properties in vivo. *Blood*, 100(4), pp.1160–7. Available at: http://www.ncbi.nlm.nih.gov/pubmed/12149192.

Mehner, C. et al., 2014. Tumor Cell-derived MMP-3 Orchestrates Rac1b and Tissue Alterations that Promote Pancreatic Adenocarcinoma. *Molecular Cancer Research*, 12(10), pp.1430–1439.

Mehner, C. et al., 2015. Tumor cell expression of MMP3 as a prognostic factor for poor survival in pancreatic, pulmonary, and mammary carcinoma. *Genes & Cancer*, 6(11–12), pp.480–489.

Mergui, X. et al., 2010. p21Waf1 expression is regulated by nuclear intermediate filament vimentin in neuroblastoma. *BMC cancer*, 10, p.473.

Nagase, H. & Woessner, F.J.J., 1999. Matrix metalloproteinases. *The Journal of Biological Chemistry*, 1803(1), pp.1–2. Available at: http://www.ncbi.nlm.nih.gov/pubmed/20159302.

Nelson, C.M. et al., 2008. Change in CellShape Is Required for Matrix Metalloproteinase-

induced Epithelia-Mesenchymal transition of Mammary Epithelial Cells. *Journal of Cell Biochemistry*, 105(1), pp.25–33.

Nieto, A.M., 2011. The ins and outs of the epithelial to mesenchymal transition in health and disease. *Annual Review of Cell and Developmental Biology*, 27, pp.347–76. Available at: http://www.ncbi.nlm.nih.gov/pubmed/21740232 [Accessed August 8, 2016].

Orlichenko, L.S. & Radisky, D.C., 2008. Matrix metalloproteinases stimulate epithelial-mesenchymal transition during tumor development. *Clinical & Experimental Metastasis*, 25(6), pp.593–600. Available at: http://www.ncbi.nlm.nih.gov/pubmed/18286378 [Accessed August 11, 2016].

Overall, C.M., 2002. Molecular determinants of metalloproteinase substrate specificity: matrix metalloproteinase substrate binding domains, modules, and exosites. *Molecular Biotechnology*, 22(1), pp.51–86. Available at: http://www.ncbi.nlm.nih.gov/pubmed/12353914 [Accessed August 24, 2016].

Peinado, H., Olmeda, D. & Cano, A., 2007. Snail, Zeb and bHLH factors in tumour progression: an alliance against the epithelial phenotype? *Nature Reviews Cancer*, 7(6), pp.415–428. Available at: http://www.ncbi.nlm.nih.gov/pubmed/17508028 [Accessed October 6, 2015].

Perlson, E. et al., 2006. Vimentin binding to phosphorylated Erk sterically hinders enzymatic dephosphorylation of the kinase. *Journal of molecular biology*, 364(5), pp.938–44. Available at: http://www.ncbi.nlm.nih.gov/pubmed/17046786 [Accessed October 19, 2016].

Phua, D.C., Humbert, P.O. & Hunziker, W., 2009. Vimentin Regulates Scribble Activity by Protecting it from Protesasomal Degradation. *Molecular Biology of the Cell*, 20(4), pp.2841–2855.

Pöpperl, H. et al., 1997. Misexpression of Cwnt8C in the mouse induces an ectopic embryonic axis and causes a truncation of the anterior neuroectoderm. *Development*, 124(15), pp.2997–3005.

Radisky, D.C. et al., 2005. Rac1b and reactive oxygen species mediate MMP3-induced EMT and genomic instability. *Nature*, 436(7047), pp.123–127.

Radisky, D.C. & Bissell, M.J., 2006. Matrix metalloproteinase-induced genomic instability. *Current Opinion in Genetic Development*, 16(1), pp.45–50.

Raimondi, S. et al., 2010. Pancreatic cancer in chronic pancreatitis; aetiology, incidence, and early detection. *Best Practice & Research Clinical Gastroenterology*, 24(3), pp.349–58. Available at: http://www.ncbi.nlm.nih.gov/pubmed/20510834 [Accessed March 23, 2014].

Ridley, A.J., 2001. Rho family proteins: coordinating cell responses. *Trends in Cell Biology*, 11(12), pp.471–7. Available at: http://www.ncbi.nlm.nih.gov/pubmed/11719051 [Accessed August 18, 2016].

Risch, H.A. et al., 2010. ABO blood group, Helicobacter pylori seropositivity, and risk of pancreatic cancer: a case-control study. *Journal of the National Cancer Institute*, 102(7), pp.502–5. Available at: http://www.pubmedcentral.nih.gov/articlerender.fcgi?artid=2902822&tool=pmcentrez&rendertype=abstract [Accessed April 8, 2014].

De Rooij, J. et al., 2005. Integrin-dependent actomyosin contraction regulates epithelial cell scattering. *Journal of Cell Biology*, 171(1), pp.153–164.

Sahai, E. & Marshall, C.J., 2002. RHO-GTPases and cancer. *Nature Reviews Cancer*, 2(2), pp.133–42. Available at: http://www.ncbi.nlm.nih.gov/pubmed/12635176 [Accessed August 18, 2016].

Schnelzer, A. et al., 2000. Rac1 in human breast cancer: overexpression, mutation analysis, and characterization of a new isoform, Rac1b. *Oncogene*, 19(26), pp.3013–3020.

Schonbeck, U., Mach, F. & Libby, P., 1998. Generation of biologically active IL-1 beta by matrix metalloproteinases: a novel caspase-1-independent pathway of IL-1 beta processing. *Journal of Immunology*, 161(7), pp.3340–3346. Available at: http://www.ncbi.nlm.nih.gov/entrez/query.fcgi?cmd=Retrieve&db=PubMed&dopt=Citation&list_uids=9759850.

Singh, A. et al., 2004. Rac1b, a tumor associated, constitutively active Rac1 splice variant, promotes cellular transformation. *Oncogene*, 23(58), pp.9369–80. Available at: http://www.ncbi.nlm.nih.gov/pubmed/15516977 [Accessed March 27, 2014].

Singh, M. & Maitra, A., 2007. Precursor lesions of pancreatic cancer: molecular pathology and clinical implications. *Pancreatology*, 7(1), pp.9–19. Available at: http://www.ncbi.nlm.nih.gov/pubmed/17449961 [Accessed August 6, 2016].

Sipos, B. et al., 2003. A comprehensive characterization of pancreatic ductal carcinoma cell

lines: towards the establishment of an in vitro research platform. *Virchows Archiv : an international journal of pathology*, 442(5), pp.444–52. Available at: http://www.ncbi.nlm.nih.gov/pubmed/12692724 [Accessed April 26, 2017].

Siveke, J.T. et al., 2007. Concomitant Pancreatic Activation of KrasG12D and Tgfa Results in Cystic Papillary Neoplasms Reminiscent of Human IPMN. *Cancer Cell*, 12(3), pp.266–279.

Slater, E.P. et al., 2010. Prevalence of BRCA2 and CDKN2a mutations in German familial pancreatic cancer families. *Familial Cancer*, 9(3), pp.335–343.

Song, J., 2007. EMT or apoptosis: a decision for TGF-β. *Cell Research*, 1725(17), pp.289–290.

Stallings-Mann, M.L. et al., 2012. Matrix Metalloproteinase Induction of Rac1b, a Key Effector of Lung Cancer Progression. *Science Translational Medicine*, 4(142), pp.1–24. Available at: http://www.pubmedcentral.nih.gov/articlerender.fcgi?artid=3733503&tool=pmcentrez&rendertype=abstract [Accessed March 9, 2014].

Sternlicht, M.D. et al., 1999. The Stromal Proteinase MMP3 / Stromelysin-1 Promotes Mammary Carcinogenesis. *Cell*, 98, pp.137–146.

Stetler-Stevenson, W.G., Hewitt, R. & Corcoran, M., 1996. Matrix metalloproteinases and tumor invasion: from correlation and causality to the clinic. *Seminars in Cancer Biology*, 7(3), pp.147–54. Available at: http://www.ncbi.nlm.nih.gov/pubmed/8773300 [Accessed August 16, 2016].

Stocks, T. et al., 2009. Blood glucose and risk of incident and fatal cancer in the metabolic syndrome and cancer project (me-can): analysis of six prospective cohorts. *PLoS medicine*, 6(12), p.e1000201. Available at: http://www.pubmedcentral.nih.gov/articlerender.fcgi?artid=2791167&tool=pmcentrez&rendertype=abstract [Accessed April 8, 2014].

Stolzenberg-Solomon, R.Z. et al., 2005. Insulin, Glucose, Insulin Resistance and Pancreatic Cancer in Male Smokers. *Journal of American Medical Association*, 294(22).

Streff, H. et al., 2016. Cancer Incidence in First- and Second-Degree Relatives of BRCA1 and BRCA2 Mutation Carriers. *The Oncologist*, pp.1–6.

Suzuki, M. et al., 1997. Matrix metalloproteinase-3 releases active heparin-binding EGF-like growth factor by cleavage at a specific juxtamembrane site. *Journal of Biological Chemistry*, 272(50), pp.31730–31737.

Tanaka, M. et al., 1998. Downregulation of Fas ligand by shedding. *Nature Medicine*, 4(1), pp.31–6. Available at: http://www.ncbi.nlm.nih.gov/pubmed/9427603 [Accessed August 24, 2016].

Thiery, J.P. et al., 2009. Epithelial-mesenchymal transitions in development and disease. *Cell*, 139(5), pp.871–90. Available at: http://www.ncbi.nlm.nih.gov/pubmed/19945376 [Accessed July 10, 2014].

Thiery, J.P., 2002. Epithelial-mesenchymal transitions in tumour progression. *Nature Reviews Cancer*, 2(6), pp.442–54. Available at: http://www.ncbi.nlm.nih.gov/pubmed/12189386 [Accessed October 19, 2016].

Thompson, D. & Easton, D.F., 2002. Cancer Incidence in BRCA1 mutation carriers. *Journal of the National Cancer Institute*, 94(18), pp.1358–1365.

Thun, M.J., Henley, S.J. & Gansler, T., 2004. Inflammation and cancer: an epidemiological perspective. *Novartis Foundation Symposium*, 256, pp.6-21–8, 49–52, 266–9. Available at: http://www.ncbi.nlm.nih.gov/pubmed/15027481 [Accessed August 6, 2016].

Tjomsland, V. et al., 2016. Profile of MMP and TIMP Expression in Human Pancreatic Stellate Cells: Regulation by IL-1α and TGFβ and Implications for Migration of Pancreatic Cancer Cells. *Neoplasia (United States)*, 18(7), pp.447–456. Available at: http://dx.doi.org/10.1016/j.neo.2016.06.003.

Traub, P. & Shoeman, R.L., 1994. Intermediate filament proteins: cytoskeletal elements with gene-regulatory function? *International review of cytology*, 154, pp.1–103. Available at: http://www.ncbi.nlm.nih.gov/pubmed/8083030 [Accessed October 19, 2016].

Ungefroren, H. et al., 2014. Rac1b negatively regulates TGF-β1-induced cell motility in pancreatic ductal epithelial cells by suppressing Smad signalling. *Oncotarget*, 5(1), pp.1–28. Available at: http://www.ncbi.nlm.nih.gov/pmc/articles/PMC3960208/.

Vetter, I.R. & Wittinghofer, A., 2001. The guanine nucleotide-binding switch in three dimensions. *Science*, 294(5545), pp.1299–304. Available at: http://www.ncbi.nlm.nih.gov/pubmed/11701921 [Accessed August 18, 2016].

Volkholz, H., Stolte, M. & Becker, V., 1982. Epithelial dysplasias in chronic pancreatitis. *Virchows Archiv. A, Pathological anatomy and histology*, 396(3), pp.331–49. Available at: http://www.ncbi.nlm.nih.gov/pubmed/7135827 [Accessed August 6, 2016].

Vu, T.H. & Werb, Z., 2000. Matrix metalloproteinases: Effectors of development and normal physiology. *Genes and Development*, 14(17), pp.2123–2133.

Waldmann, J. et al., Rac1b and MMP-3 can induce Epithelial-to-Mesenchymal-Transition (EMT) in alveolar epihelilal type 2 cells and provoke lungfibrosis upon adenoviral endotracheal delivery. , pp.1–15.

Whitelock, J.M. et al., 1996. The Degradation of Human Endothelial Cell-derived Perlecan and Release of Bound Basic Fibroblast Growth Factor by Stromelysin , Collagenase , Plasmin , and Heparanases *. *The Journal of Biological Chemistry*, 271(17), pp.10079–10086.

Witty, J.P., Wright, J.H. & Matrisian, L.M., 1995. Matrix metalloproteinases are expressed during ductal and alveolar mammary morphogenesis, and misregulation of stromelysin-1 in transgenic mice induces unscheduled alveolar development. *Molecular Biology of the Cell*, 6(10), pp.1287–1303.

Yang, J. & Weinberg, R.A., 2008. Epithelial-Mesenchymal Transition: At the Crossroads of Development and Tumor Metastasis. *Developmental Cell*, 14(6), pp.818–829.

Yin, T. et al., 2006. Implication of EMT induced by TGF-beta1 in pancreatic cancer. *Journal of Huazhong University of Science and Technology. Medical sciences = Hua zhong ke ji da xue xue bao. Yi xue Ying De wen ban = Huazhong keji daxue xuebao. Yixue Yingdewen ban*, 26(6), pp.700–2. Available at: http://www.ncbi.nlm.nih.gov/pubmed/17357493 [Accessed October 19, 2016].

Zeisberg, M., Shah, A.A. & Kalluri, R., 2005. Bone morphogenic protein-7 induces mesenchymal to epithelial transition in adult renal fibroblasts and facilitates regeneration of injured kidney. *Journal of Biological Chemistry*, 280(9), pp.8094–8100.

Zhao, S. et al., 2008. Inhibition of STAT3Tyr705 phosphorylation by Smad4 suppresses transforming growth factor beta-mediated invasion and metastasis in pancreatic cancer cells. *Cancer Research*, 68(11), pp.4221–4228.

Tabellarischer Lebenslauf

PERSÖNLICHE ANGABEN

Juliane Förster

Wohnort: Schützenstr. 11
08499 Mylau

Telefon: 0172/9864796

E-Mail: juliane_foerster@outlook.de

Geboren am: 07. November 1987 in Greiz

Familienstatus: Lebenspartner und Kind

SCHULE, AUSBILDUNG, STUDIUM

09/1998 – 07/2006	Goethe Gymnasium, Reichenbach Abschluss: Allgemeine Hochschulreife
09/2006 – 07/2008	Bildungsinstitut Pscherer Abschluss: Staatlich geprüfte technische Assistentin für chemische und biologische Laboratorien
10/2008 – 04/2009	Universität Konstanz Studium der *biological science*
04/2009 – 09/2011	Universität des Saarlandes Studium der Human- und Molekularbiologie Abschluss: Bachelor of Science
10/2011 – 09/2013	Universität Marburg Studium der Humanbiologie, Schwerpunkt Tumorbiologie Abschluss: Master of Science

PRAKTIKA, ABSCHLUSSARBEITEN

05/2007 – 07/2008	Institut für Humangenetik und Institut für Tumorbiologie des Helmholtz Zentrums München
02/2009 – 04/2009	Institut für Zellbiologie der Universität Konstanz AG Prof. Christof Hauck
06/2010 – 06/2011	José-Carreras-Zentrum Homburg AG Prof. Klaus Römer Bachelorarbeit: *„Subzelluläre Lokalisation der neuen Interaktionspartner MDM2 und NIR“*
10/2011 – 06/2012	Institut für Molekular- und Tumorbiologie der Universität Marburg AG Prof. Thorsten Stiewe und AG Dr. Elena Pucetti
10/2012 – 09/2013	Institut für Molekular- und Tumorbiologie der Universität Marburg AG Prof. Uta-Maria Bauer Masterarbeit: *“The effect of protein arginine methylation on p14Arf and NPM”*
10/2013 – 12/2016	Labor der Visceral-, Thorax- und Gefäßchirurgie des Universitätsklinikums Marburg Beginn der Doktorarbeit: *„The role of MMP3 and Rac1b during development and progression of pancreatic cancer“*
01/2017 – 06/2017	Fertigstellung der Doktorarbeit und berufliche Neuorientierung
Ab 07/2017	Pharmareferentin bei Bristol-Myers Squibb über Ashfield Healthcare GmbH

LEHRE

2011 – 2013	Betreuung des humangenetischen und biochemischen Praktikums für Mediziner des 1. und 4. Semesters
2012 – 2013	Betreuung molekularbiologischer Praktika für Humanbiologen des 3. und 5. Semesters
2013 – 2014	Betreuung von medizinischen Doktoranden im Rahmen des MMP3/Rac1b-Projektes

SPRACHEN, KENNTNISSE

Fremdsprachen:

Englisch	fließend
Französisch	Grundkenntnisse

IT-Kenntnisse:

MS Office-Paket	Sehr gut
Umgang mit biologischen Datenbanken (z.B. NCBI; Integrated DNA Technologies)	Sehr gut

Sonstiges:

Zertifikat für Teilnahme an EMF Weiterbildung von der Idee zum Projekt

Versuchstierkundezertifikat nach FELASA B – Richtlinien

Mitglied im Organisationsteam des Molekulare Medizinsymposium 2013 in Marburg; Design der Website

VERÖFFENTLICHUNGEN

Heyne K, Förster J, Schüle R, Roemer K.
Transcriptional repressor NIR interacts with the p53-inhibiting ubiquitin ligase MDM2; Nucleic Acids Res. 2014; 42(6):3565–79

Verzeichnis akademischer Lehrer

Bachelor Studium - Konstanz

Prof. Hartig – Allgemeine Chemie

Prof. Boneberg – Experimentalphysik I

Prof. Beran – Mathematik für Biologen

Prof. Mayer – Genetik I

Prof. Hauck – Zellbiologie I, Histologie

Dr. Kleineidamm – Organisationsformen des Tierreichs

Prof. Bürkle – Molekulare Medizin

Bachelorstudium – Saarbrücken

Prof. Müller – Zoologie, Tierphysiologie, Biostatistik

Prof. Bauer – Botanik, Pflanzenphysiologie

Dr. Paulsen – Genetik

Prof. Veith – Anorganische Chemie

Prof. Deicher – Physik

Mathematik

Prof. Katzmaier – Organische Chemie

Prof. Heinzle – Bioinformatik

Prof. Walldorf – Entwicklungsbiologie

Prof. Lancaster – Biophysik

Prof. Römisch – Mikrobiologie, Immunologie

Prof. Freichel – Pharmakologie, Toxikologie

Prof. Meese – Humangenetik

Prof. Schmitt – Zellbiologie

Prof. Bernhardt - Biochemie

Robert Chamberlain – Englisch für Naturwissenschaftler

Jun Prof. Rother - Pathobiochemie

Masterstudium - Marburg

Prof. Müller – Biostatistik

Prof. Thorsten Stiewe – Molekulare Tumor-Zellbiologie, Aktuelle Themen der Tumorbiologie

Dr. Pucetti – Biochemie onkogener Signalwege

Prof. Ocker – Hallmarks of Cancer, Scientific Writing

Dr. Buchholz – Modellerkrankungen II, Life cell imaging

Dr. Müller-Brüsselbach – Aktuelle Themen der Tumorbiologie

Dr. Exner – Tierversuchskunde

Prof. Bauer – Betreuung der Masterarbeit

Danksagung

Es wäre nicht möglich gewesen ohne die Hilfe und Unterstützung einiger wichtiger Menschen diese Arbeit zu erstellen.

Zu nächst möchte ich mich bei Herrn Prof. Jens Waldmann dafür bedanken, dass er mich in seine Arbeitsgruppe aufgenommen und mir nicht nur die Durchführung dieses Projektes, sondern auch die stellvertretende Leitung im Labor überlassen hat.

Ich möchte mich bei Dr. Malte Buchholz bedanken, der es mir, durch die Übernahme der Position als Doktorvater, ermöglicht hat den *Dr. rer. nat.* Titel anzustreben.

Ich bin überaus dankbar für die Hilfe von Dr. Emily P. Slater. Sie hat keine Kosten und Mühen gescheut mich und unsere Arbeitsgruppe während aller Phasen des Projektes zu unterstützen. Ihre Hilfe und ihr Engagement sind unbeschreiblich.

Ein herzlicher Dank geht ebenso an meine Arbeitskollegen, sie haben das Labor zu einem Ort gemacht an den man gerne arbeiten. Danke, nicht nur für die lehrreichen Anleitungen und die Unterstützung bei der Durchführung verschiedener Experimente, sondern auch für die gemeinsame Zeit zwischen und nach dem Laboralltag.

Mehr als ich beschreiben kann, möchte ich meiner Familie und meinem Lebenspartner danken. Ihr habt mir nicht nur ein liebevolles Umfeld gegeben, sondern mich auch in jeder noch so schwierigen Situation unterstützt. Ohne euch wäre es nicht möglich gewesen, meine Arbeit fortzusetzten.

Ein ganz besonderer Dank geht an Paul. Du bist der beste Grund niemals aufzugeben!

Acknowledgement

This thesis had not been possible without the help and support of several people.

I would first like to express my gratitude to Prof. Jens Waldmann for giving me not only the opportunity to perform my PhD in his lab, but for also providing me this interesting topic.

I would like to thank Dr. Malte Buchholz who adopted the position as my advisor, which gives me the opportunity to graduate as *Dr. rer. nat*.

I am absolutely thankful to Dr. Emily P. Slater who spared no efforts supporting me throughout this project. Her help, patience, and encouragement during my thesis time was indescribably.

My warmest thanks go to my lab colleagues and friends for making the lab a very nice place to stay in. I want to thank you for guiding and teaching me all the necessary skills. Thanks to all of you for an enjoyable time.

More than words can say, I am thankful for the support of my parents and my companion in life. You are not only providing me a loving environment, but also support me in every struggling situation. Thank you for having faith in me and for encouraging me.

A special thank goes to Paul. You have been the inducement to never give up.

Ehrenwörtliche Erklärung

Hiermit erkläre ich, Juliane Förster, geboren am 07.11.1987 in Greiz, ehrenwörtlich, dass ich die dem Fachbereich Medizin Marburg zur Promotionsprüfung eingereichte Doktorarbeit mit dem Titel “The role of MMP3 and Rac1b during the development and progression of pancreatic cancer” in der Klinik für Visceral-, Thorax- und Gefäßchirurgie unter der Leitung von Jens Waldmann und PD Dr. Malte Buchholz mit Unterstützung durch Antonia Spieß, Anna Martin und Nina Voss ohne sonstige Hilfe selbst durchgeführt und bei der Abfassung der Arbeit keine anderen als die in der Dissertation aufgeführten Hilfsmittel benutzt habe. Ich habe bisher an keinem inner- oder ausländischem Fachbereich ein Gesuch um Zulassung zur Promotion eingereicht, noch die vorliegende oder eine andere Arbeit als Dissertation vorgelegt.
Bisher wurden keine Bemühungen angestrebt, die vorliegende Arbeit in einem Publikationsorgan zu veröffentlich.

Marburg,

_____

Juliane Förster